Solvent Dependence of Organic Exciplex Fluorescence Studied by Magnetic Effect on Reaction Yield (M.A.R.Y) Spectroscopy

Dissertation

zur Erlangung des akademischen Grades des Doktors der Technischen Wissenschaften

von

Kunal Pal M.Sc.

vorgelegt bei

O.Univ.-Prof.Dipl.Chem.Dr.Günter Grampp

Institut für Physikalische und Theoretische Chemie

Der Technischen Universität Graz

Graz, im May 2011

To my family and my best friend

Acknowledgements

Right from the days in India when I was doing my Masters and received the offer of the Ph.D position in Graz until now when I am at the verge of finishing my doctoral studies, I owe in my highest esteem the contribution of my supervisor Prof. Dr. Günter Grampp. He has provided me with the platform to do science for the sake of science, provided me all the logistic support that we as foreigners need in Graz, allowed me the freedom of working and endured all my follies. I owe my sincere regards for him. Along with Prof. Grampp, his wife Jutta too has provided me with all the warmth, support and love even in times of difficulties, just like my own mother would have perhaps done. I owe my sincere thanks to her also for everything she has done for me.

The MARY instrument with which I worked with four long years would not have run the same way and perhaps would have been completely grounded had not Prof. Dr. Stephan Landgraf came along with his expertise whenever required and thought of ways to solve the problem, be it insulating the sample holder or giving finishing touches to the new set-up of the instrument we have at the institute at present. My sincere thanks to him.

Thanks and regards also goes my colleague Dr. Daniel Kattnig who helped me with programming, analyzing data and helping me with fixing a direction of my work. Thanks and regards to my former colleague Arnulf Rosspeintner, with whom I was sharing office along with Dr. Kattning in the first two years of my stay in Graz. Ulf, as we call him lovingly also helped me a lot with a lot a enlightening discussions.

Among my other colleagues, regards and thanks to Dr. Kenneth Rasmussen, with whom I share office since we shifted to the new chemistry building. I share a very good rapport with him, not only in professional front but also on a personal level. His unwavering support and help to other people is worth appreciating. Colleagues like Faiza, Noureen, Rasheeda who are no more in the instititute but has done a lot for me during the time they were here. My sincere regards to Asim, Sadia, Zahid, Tahir. My special regards to my

“coffee friend” Tim, with whom I go for coffee almost everyday in the afternoon break. Thanks everybody for making my stay at the institute meaningful.

Among the other people in the Institute I would like to thank are Mrs. Hilde Freissmuth for her support (and also endurance of our follies) in the lab, Mrs. Marion Hofmeister for all the administrative support she has given, Mr. Helmut Eisenkölbl for his ever-ready help in computer related matter, Mr. Herbert Lang for his support in building parts and components for the machine. Special thank goes to Dr. Brigitte Bitschnau for her help in translating to German the abstract of my work in such a short notice.

I owe my sincere gratitude to all my teachers in India starting from school to the university who have provided me with knowledge in chemistry. I owe gratitude to my parents who have devoted their life to give meaning to our life, my dear brother and also Gita. Last but not the least, to my best friend, who continues to support and stay with me, *hic et ubique*.

Abstract

This work aims at understanding the various facets of one of the elementary reactions in nature, the electron transfer reaction using MARY (MAgnetic effect on Reaction Yield) spectroscopy as a tool. The prime focus of study by the use this technique was the solvent dependence of organic exciplex fluorescence. Apart from that temperature dependent measurements using MARY spectroscopy have been performed to extract the activation energy parameters of electron transfer reaction. The discovery of magnetic field effect on new system was also a part of our study.

The study of solvent dependence of organic exciplex fluorescence using MARY spectroscopy was carried out on the system of 9,10-dimethylanthracene (as the fluorophore) and N,N'-dimethylaniline and 4,4'-Bis(dimethylamino) diphenylmethane (as quenchers) in binary solvent mixtures of toluene/dimethylsulfoxide, benzylacetate/dimethylsulfoxide, toluene/propylenecarbonate and propylacetate/ butyronitrile. The work focuses on the use of solvent mixtures rather than pure solvents. The solvent mixtures, tailored to simulate different microenvironemets, were employed to find out the effect of preferential solvation on electron transfer reaction. The contrast in the absolute field effect and linewidth values of the MARY spectra obtained in the four system as a function of dielectric constant scan suggest the imperative effect of concentration fluctuation on the electron transfer reaction.

Temperature dependent measurements were performed on the system of N,N,N',N'-tetramethylparaphenylendiamin, photo-ionizing in a mixture of toluene/ dimethylsulfoxide. However the sluggish response of the system to temperature changes does not really permit us to extract fruitful results. The magnetic field effect on the much studied system of Perylene/ N,N'-dimethylaniline was discovered for the first time.

.

Zusammenfassung

Ziel der vorliegenden Arbeit ist es, eine weitere Facette zum Verständnis einer der elementaren Reaktionen in der Natur, der Elektronenübertragungsreaktion, unter Verwendung der MARY Spektroskopie (MAgnetic effect on Reaction Yield) beizutragen. Der Schwerpunkt der Untersuchungen bei der Anwendung dieser Technik lag auf der Lösungsmittelabhängigkeit von organischer Exciplex- Fluoreszenz. Zusätzlich wurden mittels MARY Spektroskopie temperaturabhängige Messungen zur Bestimmung der Aktivierungsenergieparameter der Elektronenübergangsreaktion durchgeführt. Die Entdeckung eines magnetischen Feldeffektes auf einen neues System war ebenso Teil dieser Arbeit.

Die Untersuchung der Lösungsmittelabhängigkeit von organischer Exciplex-Fluoreszenz unter Verwendung der MARY Spektroskopie wurde am System 9,10 Dimethylanthrazen (als Fluorophor) und N,N'-Dimethylanilin und 4,4'-Bis(dimethylamino)diphenylmethan (als Quencher) in binären Lösungsmittelmischungen von Toluol/Dimethylsulfoxid, Benzylazetat/Dimethylsulfoxid, Toluol/Propylencarbonat und Propylazetat/Butyronitril.
Die Arbeit war speziell auf Lösungsmittelmischungen und nicht auf reine Lösungsmittel fokussiert.Die Lösungsmittelmischungen, speziell zur Simulation unterschiedlicher Mikroumgebungen gewählt, wurden eingesetzt zur Untersuchung der Effekt der begünstigten Solvatation auf die Elektronenübertragungsreaktion. Der Unterschied in den absoluten Feldeffekten und den Linienbreiten der MARY Spektren als Funktion der Dielektrizitätskonstanten der vier untersuchten Systeme geben Hinweis auf den zwingenden Effekt der Konzentrationsschwankungen auf die Elektronenübergangsreaktion.Temperaturabhängige Messungen wurden am System N,N,N',N'-tetramethyl-p-phenyldiamin, photoionisierend in einer Mischung aus Toluol/Dimethylsulfoxid, durchgeführt.Allerdings führte die sehr träge Reaktion des Systems auf Temperaturänderungen nicht zu aussagekräftigen Ergebnissen. Der magnetische Feldeffekt im gut untersuchten System Perylen /N,N'-dimethylanilin wurde erstmals festgestellt.

Contents

List Of Figures

List of Tables

1 Introduction

Parallel to the other important branches of physical chemistry that evolved since the birth of quantum mechanics in the mid twenties, grew and developed in its own might the field of spin chemistry. The term “spin”, and its convoluted connotation find direct application in NMR and ESR spectroscopy, “spin chemistry” however is a broad term which stands at the cross-roads of chemical kinetics, photochemistry, magnetic resonance and free-radical chemistry and phenomenon that might include the ubiquitous spin in its recipe and most importantly, manifesting itself in modulating rates and/or product yield of the reaction. The immediate and direct effect of spin chemistry phenomenon is obvious in the CIDNP (*Chemically Induced Dynamic Nuclear Polarization*), CIDEP (*Chemically Induced Dynamic Electron Polarization*) and of course magnetokinetic effects. It is the field of the magnetokinetic phenomenon, the modulation of rates and/or product yield of chemical reactions driven by spin-magnetic events by an external magnetic field that will form the platform of our study and the techniques involving such probes our “modus operandi”.

The area of magnetic fields perturbing chemical systems is relatively new addition to the area of physical chemistry in general. The topic is diverse and includes a multitude of substances (a large part of which include solid state materials, the reports of magnetic field effect phenomenon on which is practically innumerable and pouring from almost all parts of the world) which might show magnetic field dependent behavior in reaction, but from a photochemists point of view, we are concerned with magnetic field effect on photo-initiated reactions in condensed media. The phenomenon of magnetic field effect in condensed media involving electron-spin-nonconserving processes such as radical pair recombination has been bestowed with scholarly reviews[1-8] in the past years.

Among the prominent application of magnetic field effect in the area of photochemistry is the recent years include its use in the identification of intermediate species such as exciplex and triplex in photochemical reaction[9], determination of spin states of chemical species involved in photo-induced electron transfer reactions[10], studying the distance dependence of the electron-transfer reactions in freely diffusing systems[11], extracting out the values of self-exchange rate constants[12], experimental detection of quantum coherence and quantum beats among others. In industrial avenues too, the phenomenon of magnetic field effect has been put to succinct use by studying the magnetic-field affected photoluminescence in poly-para-phenylene (PPP) films to study the structure-property relationship in conjugated polymers. In the areas of biological interests, path breaking research has been done using magnetic field effect phenomenon to understand the phenomenon of magnetoreception in birds and how these species use the weak earth magnetic fields to traverse long distances during migration. The scientific literature is brimming with reports of magnetic field effect in various condensed systems including biological ones and the theoretical studies in this field are also numerous.

Although all systems are not susceptible to magnetic field effects, one of the elementary reaction in nature, i.e. the photo-induced electron transfer reaction are responsive to magnetic field effect by the virtue of a unique mechanism operating in them. One of the established techniques to probe the magnetic field effect phenomenon in these systems is by the use of MARY (*MAgnetic effect on Reaction Yield*) spectroscopy, a technique based on the magnetic field modulated detection of the exciplex luminescence. Our work aims at using this technique of magnetic field effect detection in the areas of studying the electron transfer on a newer perspective and more importantly understanding the preferential solvation effect brought in by mixed solvent medium rather than a pure one. It might be referred at this point that MARY spectroscopy, like EPR can yield a spectrum characterized with a certain linewidth (in the modulated mode) and with the information about the absolute magnetic field effects in the unmodulated mode. Both these spectral parameters are a function of the external perturbations and/or certain physical phenomenon. The linewidth and the absolute magnetic field effect values therefore could be used as a probe for the physicochemical effect under consideration. We have tried to

use the linewidth data from a MARY spectrum to investigate basically two effects, first the extraction of the activation energies of the electron-transfer process by studying the temperature dependent magnetic field effect on the self-exchange reaction which takes place under zero driving force ($\Delta G^0 = 0$) and hence using MARY spectroscopy as a tool to gain new insights into electron transfer reaction and secondly, to study the effect of binary solvation using the MARY linewidth data. In both the areas we have attempted to take an approach to understand some physicochemical effect, something which has not been done in past. Although temperature dependent measurements are common to extract activation parameters, the linewidth data of MARY spectroscopy has hardly been used (although EPR linewidth data has been used widely). In the area of the binary solvent effects, while the reports of absolute magnetic field effect as a function of the solvent polarity is widespread, the effect of solvent polarity on the line-width has been studied for the first time. Devising novel solvent mixtures, some of which allow scan of polarity keeping the other solvent macroscopic properties constant, we have found out that some systems are capable of showing large changes in the linewidth and $B_{1/2}$ values contrary to the common notion that these parameters are rather insensensitive to the polarity changes in binary solvent mixtures. The experimental results although call for detailed theoretical interpretation of the effect, a study which we plan to do in the near future.

Equation Chapter 2 Section 1

2 THEORY & FUNDAMENTALS

2.1 Introduction

As early as 1929, when quantum mechanics was just booming, a report[13] whether a magnetic field is really capable of altering the product yield of a chemical reaction perhaps marked the onset of this diverse field of Spin Chemistry of today. The arguments were based purely on thermodynamic criterion, i.e. whether a magnetic field is capable of having any effect on the activation energy of a reaction and thereby if could alter the course of the reaction. But energetic calculations show that even a very strong magnetic of the order of 10 T (which can only be obtained by use of superconducting magnets), can have an effect as high as only about 0.13 kJ/mol. The relation $\Delta G = 0.5\Delta\chi_M B^2$, relating ΔG to the molar susceptibility χ_M, which has very low values justifies the negligible dependence of the Gibbs free energy changes to external magnetic fields. If the common order of activation energies is considered, which is as high as 40 kJ/mol, then the effect of the magnetic field even with such high fields is almost negligible on the reaction! However alternate mechanisms might exist for a magnetic field effect, the most common being the susceptibility of the frequency factor 'A' of the Arrhenius equation to external forces like electric and magnetic field. Since it is known that the frequency factor is a convoluted term comprising many factors including the entropy factor (degrees of freedom), the magnetic field, if capable of altering the degrees of freedom in some way (i.e. shut off or enhance selected reaction channels), might alter the course and/or the product yield of the reaction. But which reactions are the candidates for visualizing such effects? Not all of course, but one of the fundamental reactions in nature i.e. the Electron Transfer (could also be photoinduced), is responsive to such kind of effect. We would thereby develop the ensuing discussion basing on the detailed treatment of the Photoinduced Electron Transfer (PET) reaction, how such reactions are susceptible to external magnetic fields, quantum mechanical aspects involved in such an interaction, and thereafter the subjects and topics pertinent to our research.

2.2 Photo-induced Electron Transfer Reactions (PET)

2.2.1 General Description of the Process

A photo-induced electron transfer reaction (PET) can be schematically represented as follows [14]:

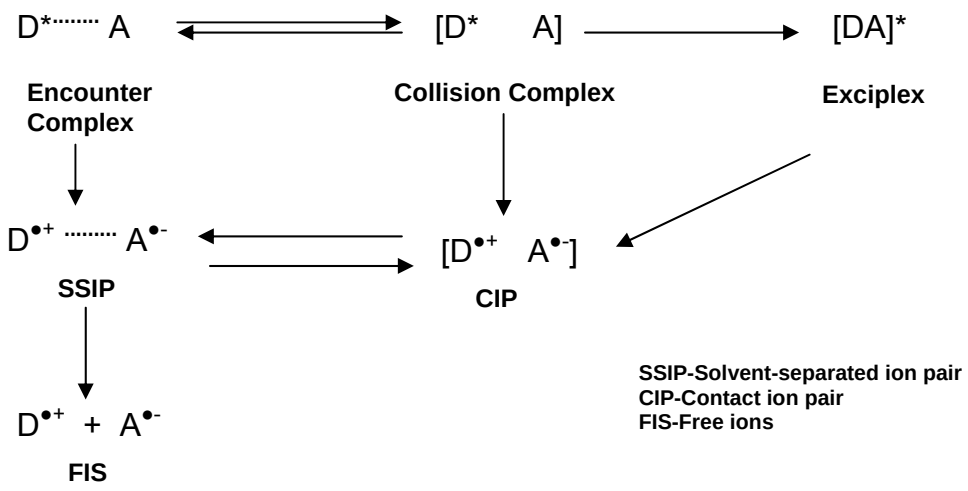

Figure 2.1 General description of Photoinduced Electron Transfer reaction

The scheme shown above is discussed below in brief to understand origin of magnetic field effects in PET reactions. Discussed are the events and fate of the PET reactions, definition of terms like "Contact Ion Pair (CIP)" and "Radical Ion pair (RIP)", which are vital to the understanding of MFE in condensed media. The sequence of the events is as follows:

i) After a photoexcited species (D*) is formed, it can undergo spontaneous decay (fluorescence or phosphorescence), unimolecular rearrangement or participate in bimolecular reaction with another ground state molecule during its lifetime. This type of bimolecular reaction which leads to the quenching the electronic energy of the former, might include a direct electron transfer

reaction leading to the formation of a charged-transfer state (in reality a radical pair, as discussed later). However in a condensed medium, there are multiple steps leading to the actual electron transfer. First, the two reacting partners must approach each other through diffusive interaction till they are close enough for the transfer of electron. Hence the stages of approach start with "encounter" (and the formation of an Encounter complex) till they start approaching each other even closer for optical collisions (Collision complex). In the duration of the collisions during the lifetime of the excited state, the actual electron transfer takes place to give a charge transfer state or Radical Ion-pair (RIP). As can be seen from the Molecular-Orbital representation of PET reaction, it leads to the formation of a species (D^+ A^-) with an unpaired electron on each counter-ion. Radical Ion-pairs can also be formed by the homolytic cleavage or thermal cleavage of a molecule, but these cases are of less importance from our viewpoint of discussion.

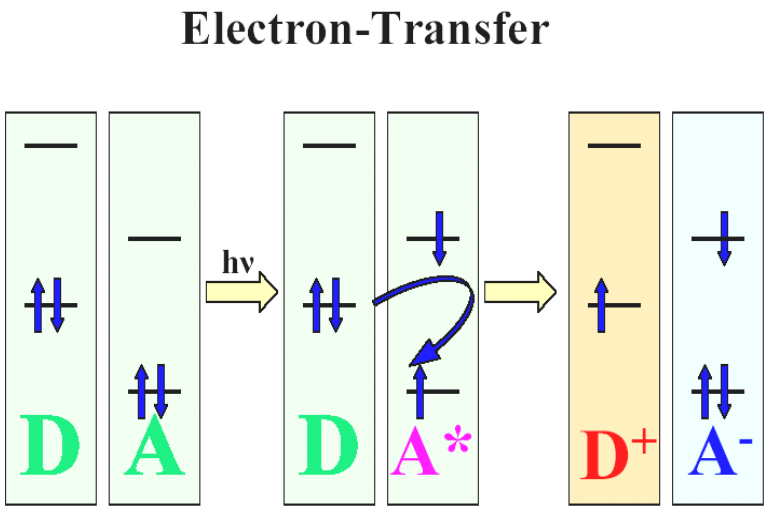

Figure 2.2: Molecular orbital representation of RIP formation

ii) The dynamics of the process which starts with encounter of the reacting moieties do not stop by the formation of the radical-pair. On the contrary, it becomes more complex from here-on. We must take into account the fact that we are probing the process in condensed media with dielectric and

polarization effects, and the effect of these factors are imperative on the dynamics of the exciplex. The actual dynamics are so complex that it is best treated by the stochastic Louivelle equation, but for practical purposes a semi-analytical process also suffices.

iii) From here on now, we will discuss the process therefore taking the well-known "cage-effect" into account. The "**cage-effect**" implies that, in a solvent, while describing the electron transfer process of a Donor/Acceptor moiety, we can no longer treat the moiety as independent, but rather as an ensemble where the interacting species are "hemmed in" by solvent dipoles. Hence the RIP so formed although has no physical bond, but in reality should be regarded as a single entity owing to the cage effect, which impedes any immediate diffusion away from each other.

iv) Coming back, the RIP formed in the nascent stage, is referred to as the *geminate-pair* (the Latin *geminus* means "twin-born") and is of-course surrounded by solvent molecules. (Synonymous name for the geminate-pair is also a Contact-Ion Pair (CIP)). It now depends on the properties of the solvent structure around the exciplex, as to what fate the CIP will meet with. (Hence the dependence of Luminescence and MFE phenomenon on the nature of the solvent, to be taken up in detail later on). If the solvent cage is non-polar in nature (like Toluene), then no further charge separation in the CIP is possible, the ions might recombine back to form the *exciplex*, and eventually decays to its structureless ground state, which might be radiative in nature. The following reaction shows this phenomenon:

$$^{1}\left[{}^{2}A^{-} + {}^{2}D^{+} \right] \longrightarrow {}^{1}\left(A^{-}D^{+} \right)^{*}$$

v) If the solvent cage is polar, or even slightly polar, then the CIP starts getting dissociated into a further charge-separated form, with each counter-ion drifting away from each other. This "prying-apart" of the charge transfer states by the surrounding solvent molecules marks the onset of "diffusional excursion" of the state, where as indicated, the counter-ion are falling away from each other.

vi) The onset of the diffusional excursion is very important as far the MFE is concerned. Because after a certain extent of diffusional dynamics, starts the Spin dynamics simultaneously which is actually responsive to the Magnetic field. Since the events of the spin-dynamical process will be our prime focus, we will defer it for a while, so that we can see the next stages in the diffusion dynamical process. The CIP could further get completely "pried-apart" by the solvent dipoles, such that solvent molecules occupy the space between these two ion, to give a solvent-separated ion pair (SSIP). On further passage of time, two independent solvent encapsulated free ions (FIS) can freely diffuse to the bulk solvent. This ends the events of a charge-transfer phenomenon in solution. The following figure illustrates how the solvent shell reorganizes itself around various intermediate stages as a PET reaction proceeds.

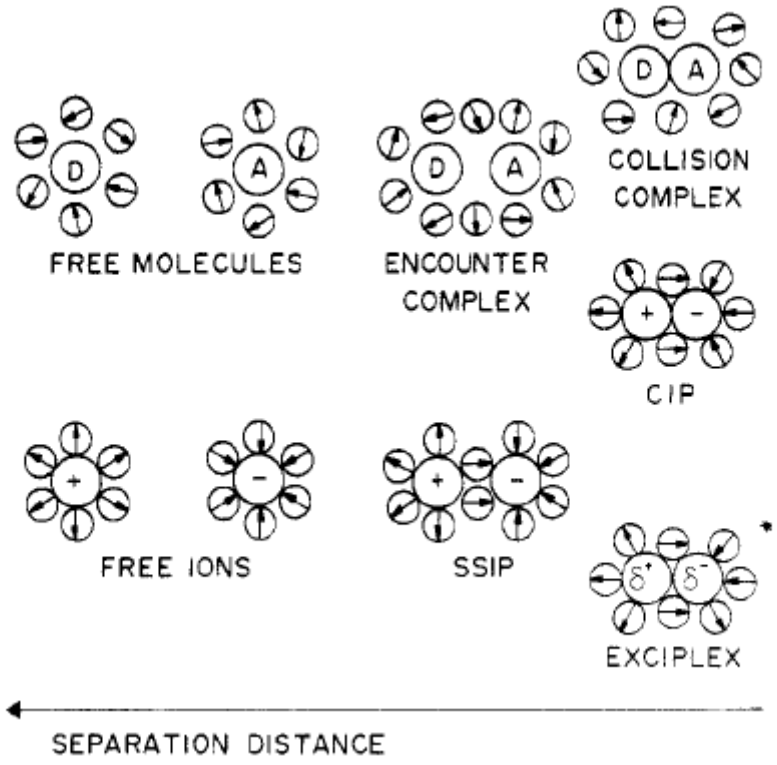

Figure 2.3: Schematic representation of donor and acceptor partners in solution at various separation distances preceding and following electron transfer. Surrounding solvent molecules (smaller circles) comprise the solvent cage. Adapted from : Kavarnos, G. J.; Turro, N. J. *Chem.Rev* 1986, *86*, 401.)

2.2.2 Radical Pair Recombination

The PET reaction has so far in the above section been viewed under the light of "cage-effect", an effect pertinent to the condensed media, something which allows a complex dynamics within the charge separated moiety and something which impedes the immediate separation of the charge separated species after its formation. But more interestingly, the condensed medium enhances another effect, which must be taken into account while analyzing the MFE effect in solution, namely- the increased chance of re-encounter from radical diffusion. As we have talked in the preceding section, that the events of the PET reaction starts with the formation of the encounter complex, but all

encounters are not effective encounters. If the surrounding condition provides chances for multiple encounters in the lifetime of the reacting species and before the radical ions diffuse into the bulk, then it is certainly modifies the events and fate of the reaction.

2.2.3 Spin-Correlation in Radical Ion-Pairs

As has been pointed out earlier, the RIP's are the species of interest in MFE phenomenon in condensed medium (although there are also other established mechanisms which do not invoke the formation of a RIP, but we will restrict our discussion by assuming the RIP mechanism to be the most commonplace and suited to our purpose). Radical Pairs can be formed as a reactive intermediate in many types of reaction including homolytic bond cleavage, by random encounter of free radical (the termination step of many free radical induced chain reaction) and of course by electron transfer reaction (ref. section *2.2.1*). The radical pair so formed can either be a correlated or an un-correlated pair. In reality, formation of RIP (either by cleavage or electron transfer) is such a fast process, that at the instant of its formation, its overall spin can be correlated with the spin of the parent molecule from which it is formed.

The spin of a RIP so formed is always correlated because the time taken for the rupture of a bond to give a RIP is much faster than any mechanism which might convert it to any other spin-state. Spin-correlated pairs are also called Geminate pairs. But it might also happen so that two independent spin radicals (singlet radicals which diffuse out of the geminate cage or triplet which eventually get converted to singlet by some mechanism) might encounter each other in the bulk solvent and pair-up to form a radical pair. This is a random encounter, and the spin-state of the radical pair is not correlated. They are non-correlated or F-pair. It might be noted for subsequent discussion that while the evolution of the Geminate-pair is magnetosensitive, the evolution of F-pairs are not.

2.3 Quantum Mechanical Treatment of Spin-Evolution and Magnetic Field Effect

Having laid out all the initial and prerequisite conditions, criterion, factors and fate of PET reaction, we will take detailed look into the reaction scheme from a quantum mechanical point of view. Our general plan of discussion will be to see how the RIP, a coupled spin system, is represented (vector and wave-function), the construction of the spin Hamiltonian and how the spin-state evolves under the influence of the Spin-Hamiltonian.

2.3.1 Representation of Radical Pair (Coupled Systems)

Radical Pairs are coupled spin systems, much to the likeness of coupled systems encountered in NMR. But before we see how a coupled spin system is represented in theory, we will first consider the case of an isolated spin and later extend the parameters to the coupled system. Hence we start by asking the simple, yet complex question, what is spin?

2.3.1.1 Spin Magnetic Moment

Spin in quantum mechanics is a fundamental property of elementary particles (electron, protons, nucleus etc) that associates an angular momentum to them apart from orbital angular momentum, but at the same time with no classical analogue to the particle spinning about its own axis. The quantum mechanical spin which can take non-integer values also satisfies all the commutation relations obeyed by the orbital angular momentum and for many purposes therefore the spin angular momentum is loosely termed as spin. Although spin is quantum mechanically not represented by vectors, but rather spinors, we will still represent spin with vectors for convenience of

understanding. Having said so, the property of the spin under the effect of a magnetic field will be examined, which is pertinent to the understanding to evolution of RIP will be discussed.

An electron with spin quantum number 's', $m_S = \pm 1/2$, has $2s$+1 orientations and an angular momentum of magnitude $S = \sqrt{s(s+1)}\hbar$. But the fact that spin of a particle can be used for spectroscopic purpose lies in the fundamental fact that, *charged particles with non-zero spin possess a magnetic dipole moment* , just like a rotating electrically charged particle in classical physics. But unlike classical physics, the magnetic moment of such particles with non-zero spin is also quantized, and is given by:

$$\mu_e = -g\mu_B \boldsymbol{S} \tag{2.1}$$

2.3.1.2 Spins in a Magnetic Field

The spin (magnetic) substates represented by the quantum number $m_S = \pm 1/2$ are degenerate in the absence of a magnetic field. But under the influence of a laboratory magnetic filed B_z (defining the z-axis of the system), the magnetic moment interacts with the field, the degeneracy gets lifted, the spin-substates adopt two orientations with respect to the field [α-state ($m_s = +1/2$,spin up, with $+1/2\hbar$ units of angular momentum along the z-axis] and β-state [$m_s = -1/2$,spin down and $-1/2\hbar$ units of angular momentum along the z-axis)]. Further by the principles of Uncertainty principle it also follows that spin vector also has a component that is perpendicular to the z-axis and that it precesses about the field direction. This interaction of the electron spin with the applied magnetic field results in an energy difference between the parallel and antiparallel spin-states given as

$$\Delta E = g\mu_B B \tag{2.2}$$

However there are further (sometimes quite complex) pattern of splitting of these energy levels due to hyperfine interaction with the neighboring nuclei. The following figure shows the alignment of the spin with respect to the laboratory magnetic field.

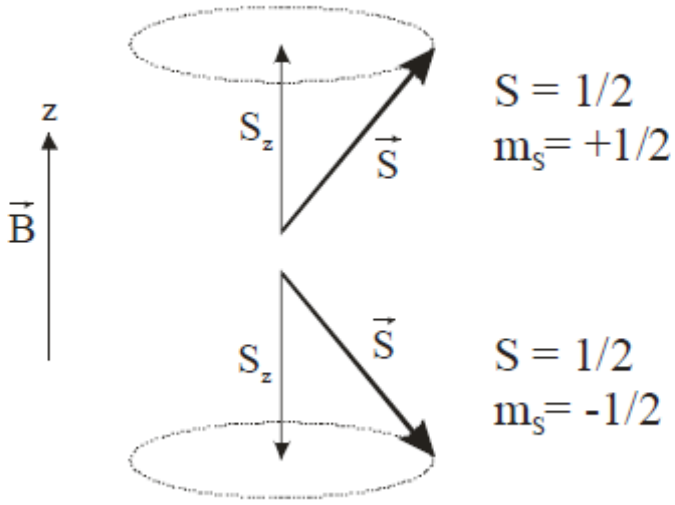

Figure 2.4: Orientation of the electron spin under the effect of a laboratory magnetic field.

2.3.1.3 Vectorial Representation of Radical Ion-pairs

We have already defined a RIP and also that it constitutes a coupled system. But in spite of being a coupled system, the vectors corresponding to the spin of each electron exhibit the same behavior as those of a single electron. The possible orientations of RIP according to the vector model are as follows. The two spins in a RIP can exist in a singlet state, the spin vectors on the electrons 1 and 2 must be aligned so that one spin is α, one spin is β, ($M_S = 0$) and their components perpendicular to the field are 180^0 out of phase, which thereby forms a state with total zero units of angular momentum. An alternative triplet state can be formed from the two spins, with three substates. The possible orientation include a) with both moments aligned parallel to the field, with spin angular momentum $+\hbar$ along the field axis ($M_S = 1$) and termed

as the $T_+(\alpha\alpha)$ state, b) both spin anti-parallel with spin angular momentum $-\hbar$ along the field axis ($M_S = -1$) termed as the $T_-(\beta\beta)$ state, c) one spin parallel (α) and one spin anti-parallel (β)with $M_S = 0$ along the field axis (but the spins are not 180^0 out of phase) and termed as the $T_0(\alpha\beta)$ state. The states are pictorially represented in the figure below.

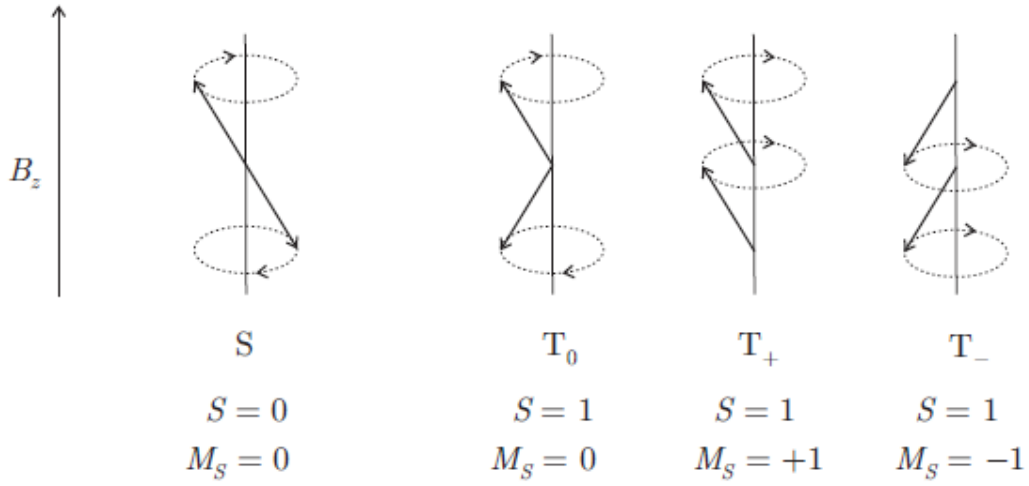

Figure 2.5: Vector model of the spin states of the RIP. While the singlet remains with the two spin 180^0 out-of phase, the triplet states are with their spins aligned mutually in three ways to match their M_S=+1, 0, -1 values.

2.3.1.4 Wave-function of the RIP Spin States

Having seen the vectorial representation of the RIP's, we will take look at the wavefunctions representing these coupled states. These states can be represented via the product of their individual electron and nuclear spin wavefunctions as follows:

$$
\begin{aligned}
|S\rangle &= \left(|\alpha_1\beta_2\rangle - |\beta_1\alpha_2\rangle\right)/\sqrt{2} \\
|T_0\rangle &= \left(|\alpha_1\beta_2\rangle + |\beta_1\alpha_2\rangle\right)/\sqrt{2} \\
|T_{+1}\rangle &= |\alpha_1\alpha_2\rangle \\
|T_{-1}\rangle &= |\beta_1\beta_2\rangle
\end{aligned}
\tag{2.3}
$$

Here α and β refer to the parallel (spin up state with $m_s = +1/2$) and anti-parallel (spin-down with $m_s = -1/2$) magnetic substates of the electron in the presence of an external magnetic field, B_z, respectively. The nuclear spin wavefunction accordingly is represented as follows

$$
|\chi_N\rangle = \prod_i^a |m_{I,i}\rangle \prod_j^b |m_{I,j}\rangle = |m_{I,i}, m_{I,j}\rangle \tag{2.4}
$$

where $m_{I,i}$ and $m_{I,j}$ denote the magnetic spin quantum numbers on atom *i* of radical 1 and atom *j* of radical 2, respectively.

2.3.2 The RIP Spin Hamiltonian

Having discussed the basic quantum mechanical aspects of the radical ion pair, we will now take a look at the energy interactions present therein, which ultimately (section *2.3.5*) pushes it to evolve under the effect of a magnetic field. A radical pair consists of two weakly coupled radicals and its total Hamiltonian can be thought to comprise of the magnetic and the exchange terms. The total Hamiltonian is therefore given as (equation *2.5*) and the origin of each Hamiltonian is explained below.

$$
\widehat{\boldsymbol{H}}_{RP} = \widehat{\boldsymbol{H}}_{ex} + \widehat{\boldsymbol{H}}_{mag} \tag{2.5}
$$

2.3.3 Interaction between Electron Spins ($\widehat{H}_{ex}$)

2.3.3.1 The Exchange Interaction

The exchange interaction is given by the following equation, with J as the value the exchange integral between two electron spin $\hat{\mathbf{S}}_1$ and $\hat{\mathbf{S}}_2$

$$\widehat{\boldsymbol{H}}_{ex} = -J(r)\left(2\widehat{\boldsymbol{S}}_1\widehat{\boldsymbol{S}}_2 + 1/2\right) \tag{2.6}$$

where $\widehat{\boldsymbol{S}}_i$ denotes the operator of the electron spin *i* and $J(r)$ is the distance dependent exchange interaction between the two electron spins. The origin of the exchange integral is traced to the basic quantum mechanical effect that, when the electronic wavefunctions of two unpaired electrons overlap and their spins exchange, the distinguishability of the spins are lost. The quantum mechanical exchange interaction is given by

$$J(r) = 2\int \psi_1^*(r_1)\psi_2^*(r_2)\frac{1}{|r_1 - r_2|}\psi_2(r_1)\psi_1(r_2)dr_1dr_2 \tag{2.7}$$

where $\psi_i(r_j)$ represents the wavefunction of electron i at position r_j. The exchange integral being a function of the wavefunction overlap, it can of course be assumed to be distant dependent. Experiment[15] has further proven this fact, and the distance dependence of this parameter is given by

$$J(r) = J_0 \exp(-\xi r) \tag{2.8}$$

The exponential dependence of the exchange interaction on the distance between the two spins reflect the fact that the exchange interaction falls off rapidly with increasing separation between the counter-ions and might at some optimal distance fall-off to zero.

In fact at typical reaction distances of tens of angstroms, the exchange interaction falls of practically to zero.

2.3.3.2 The Dipolar Interaction

The dipolar interaction refers to the interaction via the magnetic dipoles. But for all practical reasons and isotropic situations (for non-rigid molecules in condensed media where molecules are rapidly tumbling), these interactions are averaged out to zero.

2.3.4 The Magnetic Interactions ($\widehat{H}_{mag}$)

The magnetic interactions in the radical ion-pair refer either to the interaction of the electron/nuclear spins with the applied magnetic field (Zeeman effect) or between the mutual interaction of the electron spins with the weak nuclear spins (Hyperfine interaction). It should be noted that the order of the magnitude of the electron Zeeman interaction is of much higher order of magnitude than the hyperfine interactions and under the influence of a strong magnetic field the hyperfine interactions ceases to exist. The interactions are elucidated below.

2.3.4.1 The Zeeman Interaction

The Zeeman Interaction refers to the interaction between the electron spins of the RIP and the applied magnetic field. Much to the likeness of the EPR phenomenon the contribution to the total energy will be an addition of like contribution from the individual spins (the spins being independent).The Hamiltonian is given as

$$\widehat{\boldsymbol{H}}_{zeeman} = g_1\mu_B B\widehat{\boldsymbol{S}}_{1z} + g_2\mu_B B\widehat{\boldsymbol{S}}_{2z} \tag{2.9}$$

with g_i denoting the isotropic electron g-factor of the radical i, μ_B being the Bohr magneton, $\hat{\boldsymbol{S}}_{iz}$ being the z-component of the *i*th electron spin operator, $\hat{\boldsymbol{S}}_i$

Similar to the electron Zeeman term, there is also contribution from the nuclear Zeeman term, which is the interaction of the nuclear spin with magnetic field. The nuclear Zeeman Hamiltonian assumes a similar form like equation *2.9* except that the Bohr magneton is replaced by the nuclear magneton, electron g-factor is replaced by the nuclear g-factor (g_n) and the electron spin $\hat{\boldsymbol{S}}_i$ replaced by the nuclear spin $\hat{\boldsymbol{I}}_i$. However the order of magnitude of the nuclear Zeeman interaction is so low compared to the other energies, that its contribution can be easily neglected.

2.3.4.2 Hyperfine Interaction

Unpaired electron spin(s) of the RIP can interact with those of the magnetic nuclei, for which the nuclear spin quantum number $I \neq 0$**.** Analogous also to the EPR phenomenon, the hyperfine interaction is expressed for coupled system of the RIP as an addition of two hyperfine terms arising out of the individual electron spins and is expressed in isotropic media of low viscosity in terms of hyperfine coupling constant a. The Hamiltonian denoting the hyperfine interaction is denoted as:

$$\hat{\boldsymbol{H}}_{hyp} = \sum_i a_{1i} \hat{\boldsymbol{S}}_1 \cdot \hat{\boldsymbol{I}}_{1i} + \sum_j a_{2j} \hat{\boldsymbol{S}}_2 \cdot \hat{\boldsymbol{I}}_{2j} \qquad (2.10)$$

where $\hat{\boldsymbol{I}}_{ij}$ denotes the the *j*th nuclear spin operator for the *i*th electron spin with its corresponding hyperfine coupling constant a_{ij}

2.3.4.3 The Total Hamiltonian

The Hamiltonian under which the spin-evolution phenomenon are operative should therefore be a sum of all the energy terms derived above, i.e. neglecting all the minor contributions and the contributions which average out in isotropic conditions like the dipolar interactions, the total Hamiltonian should be given as

$$\widehat{\boldsymbol{H}}_{total} = \widehat{\boldsymbol{H}}_{ex} + \widehat{\boldsymbol{H}}_{zeeman} + \widehat{\boldsymbol{H}}_{hyp} \tag{2.11}$$

But in reality the actual Hamiltonian is a "redundant Hamiltonian", given the fact that one or more of the contributing terms might cease to exist under the given conditions of experiment. The terms whose contribution is most likely to be cancelled is the one due to exchange, as described earlier, whose value falls off to zero at distances where actual magnetic field dependent phenomenon start operating. The Zeeman and the hyperfine terms work simultaneously until the system is under very high values of magnetic field, when only the Zeeman interaction is the dominating force.

2.3.5 Spin-State Evolution under the Spin-Hamiltonian

Having made a long survey of the PET reaction and having seen the quantum mechanical parameters governing the effect of the magnetic field on PET reactions, now lets turn to the most important section of how these parameters can translate into giving a perceptible magnetic field effect on photochemical reactions.

We have see before how the spatially separated, spin-correlated RIP generates a new set of magnetic substates of a singlet state $|S\rangle$ and three degenerate triplet states $|T_0\rangle, |T_{\pm}\rangle$ (the corresponding wavefunctions are given through equation *2.3*. Given this information, we will see how these magnetic substates behave in the absence of a magnetic field and what changes are brought about by the introduction of a magnetic field and the concomitant changes in the spectral parameters.

2.3.5.1 Spin-substates in the absence of magnetic field

The reader is now reminded of section *2.3.1.3***,** where the RIP coupled systems were vectorially represented. To recapitulate, we had seen the singlet state with the two spins 180^0 out-of-phase and the triplet state with three spin substates. Before we see any interaction between the given states, first we have to see how the individual states are placed in the energy scale. We do that by calculating the diagonal elements with the exchange interaction Hamiltonian as the only operating force. The results are given by the following equation.

$$E(S) = \langle S, \chi_N \,|\, \widehat{\boldsymbol{H}}_{ex} \,|\, S, \chi_N \rangle = J(r) \tag{2.12}$$

$$E(T_n) = \langle T_n, \chi_N \,|\, \widehat{\boldsymbol{H}}_{ex} \,|\, T_n, \chi_N \rangle = -J(r) \tag{2.13}$$

with n=-1,0,+1 for the three triplet states $|T_-\rangle, |T_0\rangle$ and $|T_{+1}\rangle$ respectively. As has been referred to earlier, we see a singlet state and three degenerate triplet states. The singlet and triplet states are separated by an energy $2J(r)$ and the distance dependence of the exchange parameter makes in-turn the singlet and triplet energies also distance dependent. The figure below (Fig. *2.6*) depicts this fact. However as has been indicated earlier, in spite of the separation in energy between the singlet and the triplet states, in almost all cases the singlet and triplet states become mutually degenerate at typical separation distances of tens of angstroms where the exchange integral virtually falls off to zero. So *in the absence of any magnetic field, the singlet and triplet states dwells in mutually degenerate condition.* However, the question that arises now is that is there any possibility and mechanism of interconversion (Inter-system crossing) under these circumstances even in the absence of magnetic fields? Yes, of course, as will be discussed in the next subsection.

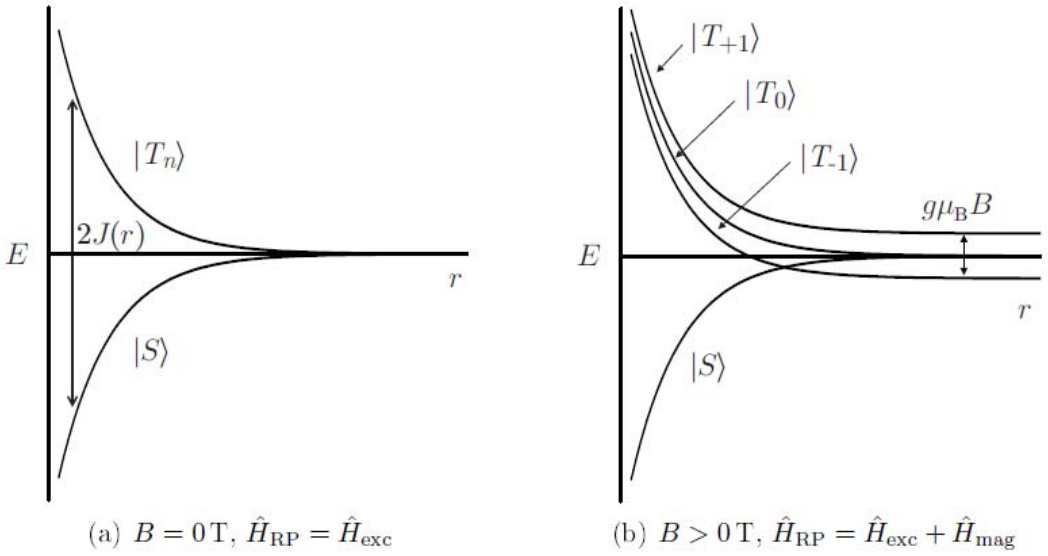

Figure 2.6: Distance dependence of the radical ion pair in the a) absence and b) presence of an external magnetic field, with the radical ion pair having a negative exchange integral J.

2.3.5.2 ISC phenomenon at *J=0, B=0*

Before making any calculation of the matrix elements, by speculation we can infer that in an initially formed singlet pair will continue to remain in that state if the precessional frequencies remain same for the two electron in the RIP. In other words, the difference in precessional rate ($\Delta\omega$) remains zero. In this case the magnetic fields experienced by the two electrons are the same. However, if these magnetic field should differ, then the precessional rates may become different ($\Delta\omega \neq 0$), the electron will lose its singlet phasing and with the passage of time will slowly convert to the $|T_0\rangle$ state. Of course this might be one mechanism of transition. But for the other two triplet states, requires a change in the z-component of electronic spin-angular momentum from $+\hbar$ or $-\hbar$ to zero and a spin-flip is necessary. However the law of conservation of momentum forbids such change and these flips can only be achieved by a simultaneous change in nuclear spin-angular momentum along with electron spin-angular momentum conserving thereby the

total spin angular momentum. We will now see these mechanisms which induces these changes.

Hyperfine-induced ISC mechanism.

The most pronounced driving force for inducing inter-system crossing phenomenon is the hyperfine coupling between the electron and the nucleus. The hyperfine induced phenomenon has the ability to covert the singlet state into all the three triplet states in the absence of any magnetic field. The qualitative justification might be given by the fact that the presence of the local nuclear magnetic field as transmitted to the electron via the hyperfine coupling provides the torque required for both the spin-rephasing and the spin-flip phenomenon[16] just like the Zeeman effect, only differing in the fact that its size is almost always much smaller than the Zeeman term.This comes from the fact that the hyperfine coupling term $\boldsymbol{I}.\boldsymbol{S}$ will have three components $\boldsymbol{I_zS_z}$, $\boldsymbol{I_xS_x}$, $\boldsymbol{I_yS_y}$ with respect to the laboratory field. This will cause not only S-T_0 transition but also $S-T_{\pm}$ transitions. The flip-flop motion which causes the $S-T_{\pm}$ transition in the zero field could be pictorially represented as follows, where the electron (S) and nuclear (I) spins of a one-nucleus radical precess about the total spin, making a flip-flop motion. The electron spin configuration corresponding to the triplet state S state is seen to turn into configuration corresponding to the T_+ state.

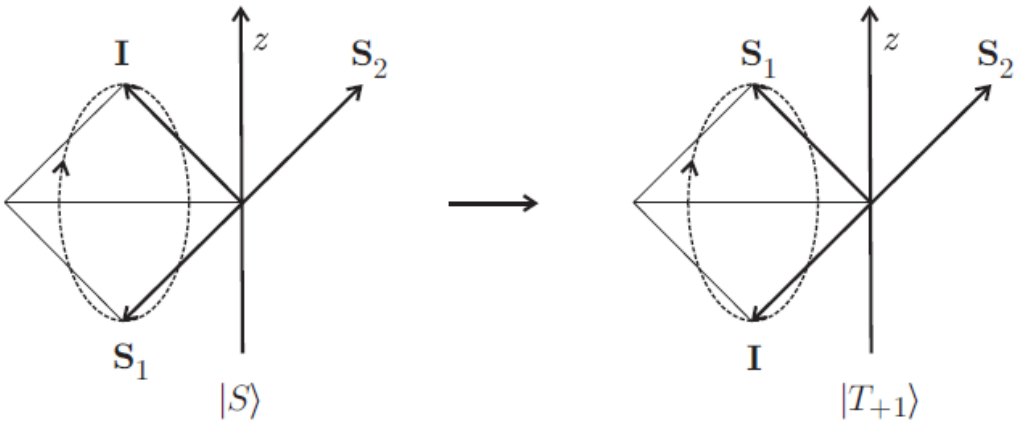

Figure 2.7: Vector model depicting the transformation of the singlet state into T_+ state by spin-flip mechanism. The electron spin (S_1) and the total nuclear spin (I) precessing about their resultant and ultimately foraying into another spin state by flip-mechanism.

Hence at zero magnetic field, there exists mechanism to interconvert the given spin states and there exists a dynamic equilibrium between the singlet state to all the three triplet substates.

2.3.5.3 ISC phenomenon at *J=0, B≠0*

We will now take a look to what happens to the dynamic equilibrium between the spin-substates in the presence of the magnetic field. We will assume that the exchange interaction forces have fallen to zero and the system is under the influence of $\widehat{\boldsymbol{H}}_{mag}$. The diagonal matrix elements are first calculated to see the relative positioning of the energy of the spin-substates. Calculation gives

$$E(S) = \langle S, \chi_N \,|\, \widehat{\boldsymbol{H}}_{mag} \,|\, S, \chi_N \rangle = J \tag{2.14}$$

$$E(T_n) = \langle T_n, \chi_N \,|\, \widehat{\boldsymbol{H}}_{mag} \,|\, T_n, \chi_N \rangle = -J + ng\mu_B B + \frac{n}{2}\left(\sum_i^a a_i m_i + \sum_k^b a_k m_k\right) \tag{2.15}$$

As can be see from the results that the $|S\rangle$ and $|T_0\rangle$ (with n=0) still manages to remain degenerate w.r.t each other provided the interactions take place at zero exchange energy. But for the $|T_{\pm}\rangle$ state with n=-1,+1 the picture is different. The two states, which have non-zero projection of their spin momenta along the axis of the field, are either raised in energy ($|T_{+1}\rangle$ state , $M_S = 1$) or lowered in energy ($|T_{-}\rangle$ state, $M_S = -1$) by an amount $g\mu_B B$ (considering only the Zeeman splitting and neglecting the shift due to hyperfine changes, which are much lower than the Zeeman splitting). So *at large separation distances under the effect of the magnetic field, all three triplet state and the singlet state is reduced to a degeneracy between* $|S\rangle$ *and* $|T_0\rangle$. However even under these conditions, another degeneracy between $|S\rangle$ and $|T_{-}\rangle$ state (vide Fig *2.8*) at some intermediate separation distance, and gives rise to the so called “level-crossing” mechanism, which is

a possible explanation of the low-field feature often observed in MARY spectroscopy (discussion to found in Section *2.4.2*)

Now under the new circumstances of relative energies of the spin-state, is there any mechanism (and how) of intersystem crossing possible? The answer to this is found by calculating the off-diagonal matrix elements connecting the singlet with the other spin-states. These matrix elements are found to be

$$\langle T_0, \chi_N \mid \widehat{\boldsymbol{H}}_{mag} \mid S, \chi_N \rangle = \frac{1}{2}\left[\Delta g \mu_B B + \left(\sum\nolimits_i^a a_i m_i - \sum\nolimits_k^b a_k m_k \right) \right] \tag{2.16}$$

$$\langle T_{\pm 1}, \chi_N{}' \mid \widehat{\boldsymbol{H}}_{mag} \mid S, \chi_N \rangle = \frac{\mp a_i}{2\sqrt{2}} \left[I_i \left(I_i + 1 \right) - m_i \left(m_i \mp 1 \right) \right]^{1/2} \tag{2.17}$$

The terms in the above two equations have usual implications.

Inspection of the above equation (*2.16* and *2.17*) brings out some important features of the interconversion process, i.e. the $|S\rangle$ and $|T_0\rangle$ states, which are degenerate even in the presence of the magnetic field can now interconvert into two ways:

- Δg mechanism: when $\Delta g \neq 0; J = 0; a_i = a_j = 0$
- Hyperfine mechanism when $\Delta g = 0; J = 0; a_i \neq a_j \neq 0$

The conversion of the $|T_{+1}\rangle$ is now forbidden as these two states are shifted in energy.

The splitting up of the triplet substates and the relative positioning of the energies are explained by the following figure (Fig *2.8*)

In the next section, a brief discussion of the Δg mechanism will be taken up. The details of the Hyperfine mechanism has already been discussed above (Section *2.3.5.2*)

Before we move on to the next section, we would like to leave some brief note on other possible mechanisms of intersystem crossing, which are although not relevant to our case of study, but relevant in the other branches of spectroscopy. These include the relaxation mechanism and spin-orbit coupling. These mechanisms are excluded from our discussion that owing to the fact that in our systems of freely diffusing radicals, with no heavy atom effect, they are generally not operative.

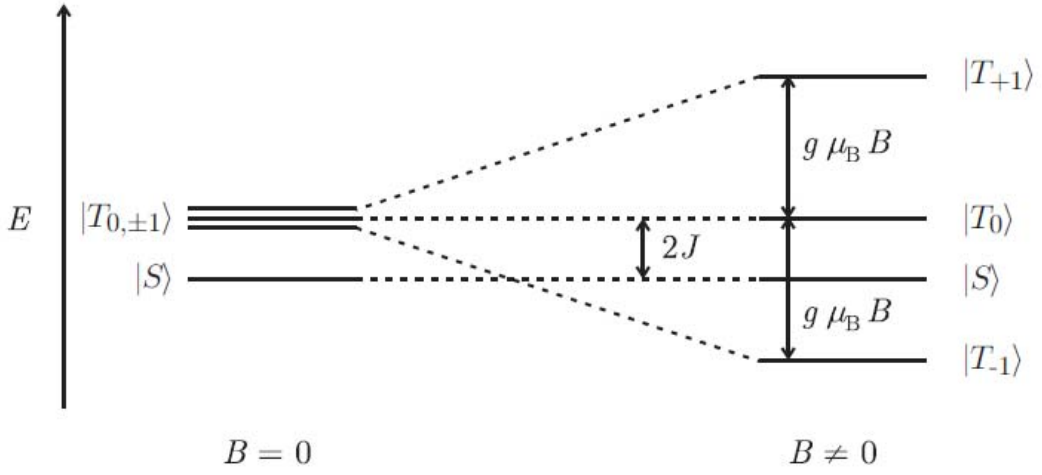

Figure 2.8: The splitting of the triplet levels in the presence of the magnetic field.

Δg Mechanism

We had earlier indicated that Δg mechanism comes to play when the when the spins on the RIP posses different g-values. The interpretation is given as follows. Each spin precess around the axis of magnetization with a frequency given by the Larmor frequency $\omega_i = g_i \mu_B \hbar^{-1} B$. Evidently when the g-values of the two spin differ, in the course of precession will come into play the gradual dephasing of each spin with respect to each other. This will cause the $|S\rangle$ to slowly convert to $|T_0\rangle$ and vice-versa and the two states will keep oscillating between one-another. This phenomenon can be best understood from

the following figure. Implicit is the fact that the phenomenon is operative only under the presence of the magnetic field.

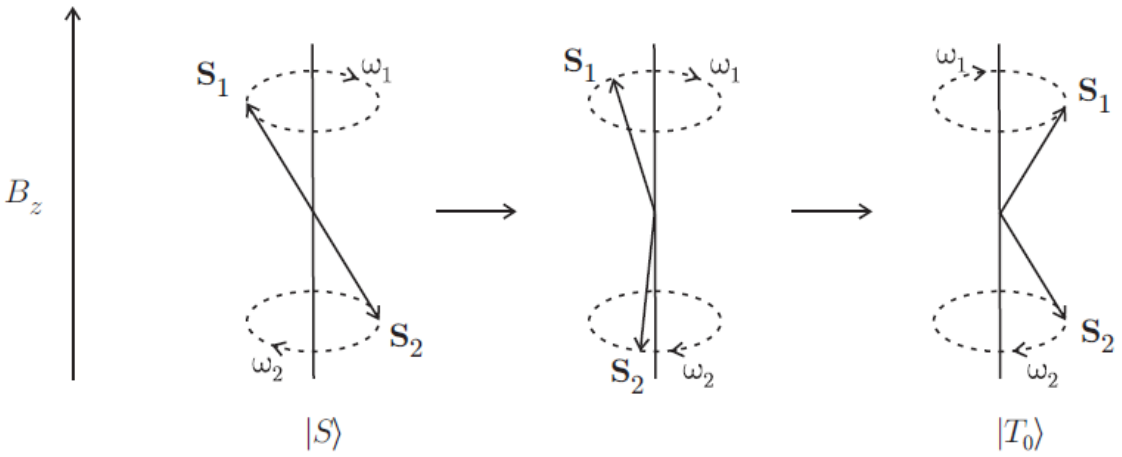

Figure 2.9: The spin-dephasing phenomenon leading to the Δg mechanism. The vector model shown above shows how a difference in Δg between the two RIP spins could result to a gradual change from S to T_0 and vice-versa leading to oscillatory S-T_0 interaction.

Of course the Δg mechanism rules out the conversion to the $|T_{+1}\rangle$ and the $|T_{-}\rangle$ state, as these states are energetically removed in the presence of the magnetic field. However, even for the conversion to the $|T_0\rangle$ state, the Δg mechanism may not the always be the most sought after. This is due to the fact that for common organic radicals with no heavy atom, the Δg values typically range around 0.001. Hence for typical radicals whose lifetimes are in the range of tens of nanoseconds, magnetic fields of the order of 1T are required to bring about an effective S-T_0 mixing.

2.4 The MARY Effect & MARY Spectroscopy

Having discussed the mechanism by which a magnetic field can affect the degrees of freedom of a reaction, we are now ready to see how these effects are translated for a PET reaction into a spectroscopic realm. The basic features and forms of MARY Spectroscopy will also be discussed.

2.4.1 MARY (*MA*gnetic effect on *R*eaction *Y*ield)

As has been highlighted in the caption, MARY stands for *MAgnetic effect on Reaction Yield* and is a powerful tool to observe the magnetic field effects on photochemical reactions. To further elucidate the connotation of this term and see how a MARY spectrum is derived, we will take a look as follows.

The Principle

As we have seen through the discussion of the preceding sections, that an electron transfer reaction, whether initiated by light or any other source culminates in the production of spin-correlated RIP which might eventually form a recombination product in the geminate cage or disproportionate. The spin-conservation laws further restrict this recombination to a spin-selective mode, i.e. only singlet spin states can form a bond back and that the triplet re-encounters will be unproductive and the latter is likely to be thrown out of the geminate cage in the course of the reaction (as F-pairs). Now given the fact that, there exists mechanism which might transform singlet RIP's to triplet within the geminate reaction cage and vice-versa, and that this transformation can be modulated by the application of an external magnetic field, the principle of magnetic field effect thus can be stated as[5] : *The crucial condition for observation of magnetic field is the competition between these geminate recombination and F-pair formation, and that one of these process should be magnetic field independent.* The reader is reminded of section

2.2.3, where it was referred that while the evolution of G-pairs are magnetic field dependent, the F-pair on the other hand is not.

The Technique

In order to understand the exact technique of realizing this effect we start by looking at the following simplified scheme of the reaction.

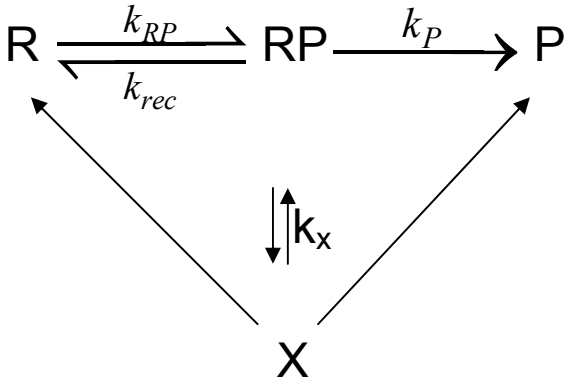

Figure 2.10: Simplified scheme of reaction pathway leading to MARY effect

As is already known by now, R and P are the reactant(s) and the product(s), X is an intermediate other than the geminate radical pair (RP) . The formation of the RP is brought about by either of the common processes like thermal, photochemical or enzymatic with a rate constant k_{RP} and decays by the recombination rate constant k_{rec} (both magnetic field dependent), forms diamagnetic product with a rate constant k_P (magnetic field independent) and sometimes might revert back to the reactant in spin-selective mode by through an intermediate X. Here lies the catch of MARY Spectroscopy, that given under normal modulation conditions and even with cw-laser excitation, the concentration of the RIP in general can be shown around 10^{-10} (M), a concentration which is not profitable to detect. In the other case, if there exists a possibility that the RP reverts back to the product via X, which might be a luminescent exciplex, excited free radical or a diamagnetic molecule, an indirect and relatively easier monitoring of X (at relatively the same concentration as the RIP) should give an indirect

measure of the RIP concentration. So in MARY spectroscopy, it is almost customary to measure the *delayed exciplex luminescence* of the photo-excited species.

2.4.2 MARY Spectral Features

While more details are discussed in the section where instrumentation is discussed, the preliminary details of obtaining a MARY spectrum and its features are discussed here. MARY spectroscopy can either be acquired in a time-resolved mode (using a pulsed laser for instance with recording of the decay-profile at various values of the magnetic field) or in the steady-state mode (using a continuous source of irradiation and recording the luminescence intensity across a scan of the magnetic field). The method used for our work is the steady-state mode. Although the time-resolved mode is suited for monitoring the temporal behavior of the MFE after it is initiated and thus allowing details of the spin-dynamical process but on the other hand the continuous mode gives a much better S/N ratio, sans the temporal behavior.

The MARY spectrum is thus recorded by the monitoring of the exciplex luminescence intensity as a function of the magnetic field, which is swept in the course of the probe. As indicated in the previous section, the concentration of the RIP, which in turn dependent on the luminescent species, the latter in turn being dependent on the luminescence intensity, the following relation formulates the interdependence

$$\frac{\phi_B - \phi_0}{\phi_0} = \frac{I_B - I_0}{I_0} = \frac{I_B}{I_0} - 1 \tag{2.18}$$

The factor $\left(I_B / I_0 - 1\right)$ which is the reduced luminescence intensity difference is plotted against the magnetic field. (ref Figure *2.11*)

The important features of the spectrum and an alternative mode of recording the spectrum are discussed below:

1. The spectrum always shows mirror symmetry about zero field. (The details of offset correction are discussed in the experimental section)
2. The $\left(I_B/I_0 - 1\right)$ value shows a saturation limit at higher fields. The rationalization of this feature is done using the fact that, in systems where hyperfine interactions only regulate the intersystem crossing, after a certain value of the magnetic field, the Zeeman interaction takes over the modulation of the singlet-triplet levels by the magnetic field, and $S \rightleftharpoons T_{\pm}$ transitions get completely cut-off from thereon. Any further increase in magnetic field value can no longer bring any difference to the singlet-triplet interconversion, until perhaps at very high value of the field Δg mechanism might cause any changes.
3. In many spectrum a low-field feature, as shown in the diagram is observable. Discussion about the low-field feature can be found in the next sub-section.
4. Although it might theoretically sound that, in principle all information can be extracted out of the absolute field effect as discussed above, but for effects (which are frequently as low as 0.2%), the resolution and S/N ratio of such a spectrum might prove challenging to extract information. In such cases the S/N ratio may be increased by sinusoidally varying the magnetic field produced in a Helmholtz coil and phase-locking the luminescence detector with it. In practice, instead of modulating the whole field a small modulating field is superimposed on it (more details in the experimental section). This allows one to record the spectra in derivative mode, like the standard ESR practice. This further reduces the noise.

The figure below shows a typical MARY spectrum both in the modulated (derivative) and un-modulated mode. The parameters depicting the spectrum are shown in the figure itself. The modulated spectrum however yields only the peak-to.peak line width given by ΔB_{pp}. The peak position could be derived thereof from $B_p = \Delta B_{pp}/2$. And the crucial $B_{1/2}$ value can be derived assuming a Lorentian lineshape from the following relation

$$B_{1/2} = \frac{\sqrt{3}}{2}\Delta B_{pp} \tag{2.19}$$

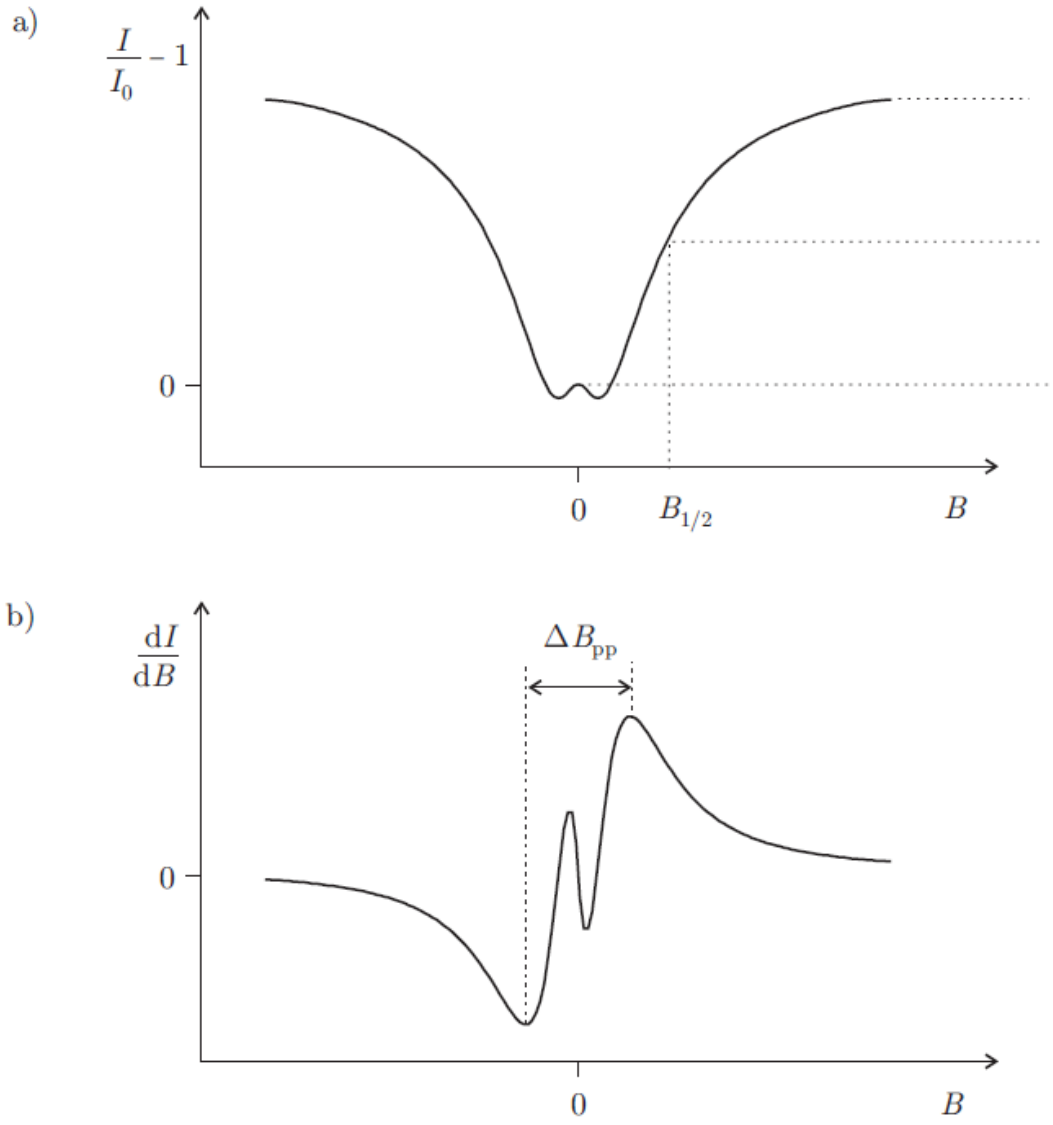

Figure 2.11: Schematic representation of a MARY spectrum a) un-modulated mode and b) modulated (first derivative mode) with characteristic parameters $B_{1/2}$ and ΔB_{pp}

$B_{1/2}$ values obtained from the MARY spectrum can also be obtained from hyperfine coupling constants of the atoms in the radical pair. This could be done step-wise by calculating an average hyperfine coupling constant A_i in quasi-classical fashion by from the root-mean square value of the following expression

$$A_i = \sqrt{\sum_k a_{ik}^2 I_{ik}\left(I_{ik}+1\right)} \tag{2.20}$$

where a_{ik} and I_{ik} are the individual isotropic HF coupling constants and nuclear spin quantum numbers of radical *'i'* , respectively[17] . Now from the average HF coupling of the radicals, the $B_{1/2}$ values could be estimated according to

$$B_{1/2} = \frac{2\left(A_1^2 + A_2^2\right)}{A_1 + A_2} \tag{2.21}$$

2.4.3 Low-field Feature

Often in the MARY spectrum, under the conditions of good S/N ratio and a low modulation amplitude, a phase-inverted region is obtained around very low fields (ref fig *2.11*). The field involved in this case is almost always lesser that 1mT, a window where electron-nuclear hyperfine effect dominates the Zeeman effect. The inversion in phase is attributed to the escape of the singlet born radical to the triplet domain.

The mechanism by which the singlet born radicals escape to the triplet surface under the effect of a very low field is explained in two ways[16]. First, the distorting effect of a small magnetic field (especially with modulation) on the spacing of the spin eigenlevels might be more than at higher fields. The effect might stem from the fact that at small fields the direction of the applied field and the hyperfine induced local field coincides. Under these circumstances, a short $T \rightarrow S \rightarrow T$ recurrence time might be favoured which in turn makes the singlet correlation to remain only for shorter time. The effect is a momentary escape of the singlet born pairs to the triplet manifold. Secondly, there are chances of level-crossing of the S and T_{-1} levels at a certain distance of the counter-ions in the RIP when the magnetic interaction equals the exchange interaction *J(r)* between the radicals in the pair, resulting in further mixing.

The low field effect is charaterised generally by two parameters:

- The strength of the magnetic field at which the yield of the product formed from the S state of the radical pair is at minimum- the "low-field position" (B_{LFE})
- The change in singlet yield between the zero field and the LFE minimum- the "low-field depth" ($\Delta\Phi_S$)

2.5 MARY Spectroscopy and the Fields of Study

Here we start discussing the topics pertinent to our research. Our focus is on the study of the different aspects of Electron-Transfer theory using MARY Spectroscopy as a tool. We begin our discussion by brief introduction to Electron-Transfer theory and the condition of self exchange. The next section introduces the vital feature of line-width effect and their origin in MARY Spectroscopy including the effect of concentration and temperature in particular on line-width. The last section *(2.6)* deals with studying binary solvent effects using MARY Spectroscopy.

2.5.1 Electron Transfer Theory

The essential features of the Electron Transfer in the framework of common theories like the Transition State Theory (TST) and Marcus Theory[18] of are central to the understanding the applications of MARY spectroscopy to extract out information at the molecular level. This includes the extraction of solvent dynamical effects on rate constant and determination of activation parameter[19] rate constants of mixed redox reactions using Marcus cross relation[20] etc.

The Basic Theory

The overall homogenous electron transfer between a donor D and acceptor A is generally given by the following multistep scheme (s2.1)

$$D + A \underset{}{\overset{K_A}{\rightleftharpoons}} \left[D \cdots A\right] \underset{}{\overset{k_{et}^0}{\rightleftharpoons}} \left[D^+ \cdots A^-\right] \rightleftharpoons D^+ + A^- \quad \text{....(s2.1)}$$

Step 1

The electron transfer occurs by the formation of the outer-sphere precursor complex $\left[D \cdots A\right]$, the pre-equilibrium being determined by the association constant K_A given as,

$$K_A = \frac{[D \cdots A]}{[D][A]} = K_0 \exp\left(-w(d)/RT\right) \tag{2.22}$$

where $w(d)$ is the electrostatic energy of the reactants , depending on the distance d .

Step2

The actual electron-transfer occurs takes place from the reorganization of the precursor complex towards a transition state by a first-order unimolecular process characterized by k_{et}^0 to give the successor complex $\left[D^+ \cdots A^-\right]$.

Step 3

Finally the successor complex dissociates to form the product ions D^+ and A^-

The overall rate of the bimolecular quenching reaction depicted above in the limit of diffusion control can be derived from a steady-state approximation of the scheme above using various approximation (omitted here) as

$$k_{et} = K_A k_{et}^0 \tag{2.23}$$

The task remains now is to theoretically calculate K_A and k_{et}^0 , which is done as follows.

Since K_A is directly related to K_0, the first task is to devise a theoretical model for the calculation of K_0. Two model in vogue are one from Eigen[21] and Fuoss[22], both of them applying to spherical molecules with a center-to-center reaction distance given by d , as

$$K_0 = \frac{4\pi}{3} N_A d^3 \tag{2.24}$$

with N_A being the Avogadro's constant.

The other one from Sutin[23] considers a reaction zone of width δd on a sphere of with radius d, which equals to the sum of the radii of the spherical donor and acceptor, $d = a_D + a_A$.

The K_0 from this model is given by

$$K_0 = 4\pi N_A d^2 \delta d \tag{2.25}$$

Next, the unimolecular rate constant of electron transfer is calculated using the classical Transition State Theory as

$$k_{et}^0 = \kappa_{el} \nu_n \exp\left(-\Delta G^* / RT\right) \tag{2.26}$$

where κ_{el} is the electronic transmission coefficient (in classicl treatment usually taken as unity), ν_n is the nuclear frequency factor and ΔG^* is the free energy of activation. The Marcus model[24] calculates theoretically the free energy of activation as a quadratic function of driving force and incorporating the important parameter of re-organization energy within as

$$\Delta G^* = \frac{\lambda}{4}\left(1 + \frac{\Delta G^0}{\lambda}\right)^2 \tag{2.27}$$

with ΔG^0 denoting the driving force of the reaction (can be calculated from cyclic-voltametric studies[25] and λ giving the *reorganization energy*. The re-organization energy is a composite term comprising the changes of energies in the solvent shell on electron transfer (denoted by the outer-sphere reorganization energy λ_0) and the bond-geometrical changes in the reactants and products (denoted by the inner-sphere reorganization energy λ_i). The total reorganization energy appearing in the Marcus relation is a sum of these

two individual contributions given by $\lambda = \lambda_i + \lambda_o$ .The tricky part of the calculation lies in determining the elusive quantity of the re-organization energy λ. The solvent-independent term λ_i arises from structural differences between equilibrium configurations of the reactant and the product states. When treated using a Harmonic model is generally given as.

$$\lambda_i = \frac{1}{2}\sum_i \overline{f_i}\ \left(r_R^{eq} - r_P^{eq}\right)^2 \tag{2.28}$$

where r_R^{eq} and r_P^{eq} are the equilibrium bond lengths in the reactant and the product states, respectively; $\overline{f_i}$ is a reduced force constant for the *i*th vibration, and the sum is taken over all significant intramolecular vibrations.

Using a dielectric continuum model, it can be shown that the outer-sphere reorganization energy λ_0, also known as the solvent reorganization energy can be given as follows[26-27] . The origin of this re-organization energy is the differences between the orientation and polarization of solvent molecules around the successor complex and the final product. The term is given by, using a spherical reagent model is

$$\lambda_0 = \frac{(\Delta e)^2}{4\pi\varepsilon_0}\left(\frac{1}{2r_D} + \frac{1}{2r_A} - \frac{1}{r_{AD}}\right)\left(\frac{1}{\varepsilon_{op}} - \frac{1}{\varepsilon_s}\right) \tag{2.29}$$

where Δe is the charge transferred in the reaction, r_D and r_A are the radii of the donor and the acceptor respectively; r_{AD} is the center-to-center distance between the donor and the acceptor. ε_{op} and ε_s are the optical and static dielectric constants, respectively of the surrounding solvent medium.

Electron-Self Exchange Reaction

A redundant condition arises, when the driving force of the reaction becomes zero. This type of reaction is very important from our point of research. One of the reaction having zero driving force are the homogenous **electron self-exchange** reaction between a molecule Q and its radical anion/cation as represented below.

$$Q^{\bullet\pm} + Q \underset{}{\overset{k_{ex}}{\rightleftharpoons}} Q + Q^{\bullet\pm}$$

Clearly for this type of reaction has free energy change of the reaction $\Delta G^0 = 0$, and the thermodynamic equilibrium constant K=1. Consequently the re-organization energy of this type of reaction (a quantity which is obviously not zero as the driving force due to the change in the nuclear configuration from going from one side to the other) of the reaction (vide equation *2.27*) becomes a lone function of the free energy of the activation as, i.e. $\lambda/4 = \Delta G^*$. The use of this important relation will be examined in the next section.

2.5.2 Linewidth effects in MARY Spectroscopy vis-á-vis EPR

Spectral data in almost all type of spectroscopy is analyzed generally on the basis of peak position(s) or linewidthb/bandwidth (FWHm in spectroscopic term) and these parameters are the indicator of the energy gaps or some physicochemical effect under consideration. But one often encounters situation where the spectra is often not resolved in the way it should be in an ideal case. For example, in fluorescence or absorption spectroscopy while one is supposed to get a spectra resolved in vibrational structure as well, one has to almost always contend himself with a broad band unresolved spectra. On the flop side while one misses the vital molecular-vibrational information, on the flip side the appearance of the broad band on the spectra might suggest of other important physical effects in play which have contributed to the distortion of the spectra.

In this light, we will discuss the line-width information and information thereof in MARY spectroscopy , which has close resemblance with the phenomenon in ESR spectroscopy. We therefore, like before discuss the appearance and factors influencing linewidth effects and its implication in ESR and then extend the concept to MARY spectroscopy.

Spin-exchange[20,28] reactions, which are similar to the self-exchange reaction often encountered in MARY are one the widely studied reactions in ESR. Linewidth as indicated earlier, in ESR spectroscopy indicate the resonance frequency of transition, could however be affected severely by dynamical processes which might change/bring uncertainty in the resonant states. While physical process like rotational diffusion, anisotropic interactions (g-tensor or dipolar hyperfine interactions) can contribute the modulation of linewidth, important chemical processes like isomerizations, ligand exchange and in particular spin-exchange (or self exchange) processes can contribute to this effect. The explanation is simple at least for the case of spin exchange processes, i.e. when an electron is transferred in the spin exchange process, it finds itself in a random nuclear spin configuration and is thereby likely to experience a different hyperfine field

compared to the former. The average time the electron spends in a certain nuclear spin environment, i.e. its lifetime (and hence the lifetime broadening) will add to the broadening of the spectrum. The lifetime referred to above, is inversely related to the exchange frequency, which in turn is dependent on the concentration of the neutral molecule [Q] and the exchange frequency for a bimolecular process as

$$\tau = \frac{1}{k_{ex}[Q]} = \frac{1}{\nu_{el}} \tag{2.30}$$

where ν_{el} is the electron exchange frequency. The effect of the inter-relationship of the above parameters is expressed by the fact that, on increasing [Q], the lifetime will get shortened, and hence the contribution to the line-broadening will be more. When the exchange is very 'fast', i.e. the electron visits all possible nuclear spin environment is a short span of time, all the hyperfine effects gets washed out and the spectrum collapses to a single narrowed line (in fact a broadened spectrum). As one ascends up the stairs of decreasing exchange rate, the merging due to becomes less dominating and the spectrum is in the hyperfine-resolved form (in fact the narrowed spectrum). So the broadening and narrowing of the spectrum is used as an indicator of the kinetics of the exchange process, an effect which can be quantified also[29-31] (The treatment is omitted here).

2.5.2.1 Origin of Linewidth Effect in MARY Spectroscopy

In MARY spectroscopy however, an analogous self-exchange is observed, but here not between a molecule and its neutral free radical, but rather between a radical as a part of spin-correlated RIP and its diamagnetic parent molecule. The scheme below illustrates this exchange effect

$$^{1,3}\left[D^{\bullet+}\cdots A^{\bullet-}\right]+D \underset{}{\overset{k_{ex}}{\rightleftharpoons}} D+{}^{1,3}\left[D^{\bullet+}\cdots A^{\bullet-}\right]$$

$$^{1,3}\left[D^{\bullet+}\cdots A^{\bullet-}\right]+A \underset{}{\overset{k_{ex}}{\rightleftharpoons}} A+{}^{1,3}\left[D^{\bullet+}\cdots A^{\bullet-}\right]$$

As is evident, the effect of lifetime broadening functions analogous to the ESR scenario, where the exchange shortens the residence time at a given nuclear spin configuration, thereby perturbing the coherent spin-evolution process and bringing about changes in the linewidth of the spectrum. The change in linewidth is reflected in the spectral parameter $B_{1/2}$.

As was discussed in the case of ESR spectroscopy, the effect of the concentration of the neutral molecule being exchanged is imperative to the process. In case of MARY spectrum, the general trend of the linebroadening (with respect to $B_{1/2}$) is an initial increase, followed by a platue-like maxima and then subsequent decrease (ref fig below) with the concentration of one of the donor/acceptor kept constant and varying the other.

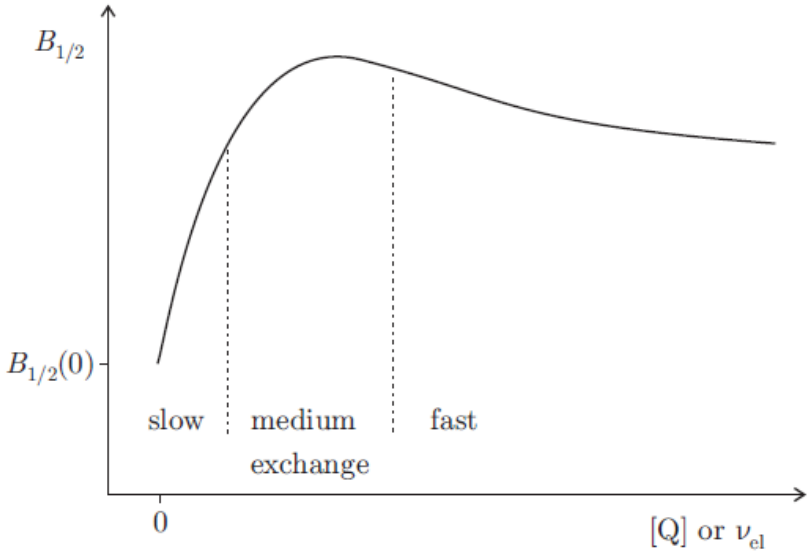

Figure 2.12: Schematic representation of the dependence of $B_{1/2}$ on the self-exchange rate or the concentration or of the neutral donor/acceptor molecule**.**

While a detailed theoretical analysis and prediction of this effect in given in [32-33] a simplified illustration of the effect is given as follows. The explanation, which can be based on the Heisenberg's uncertainty principle, calls for a broadening of the spin-energy levels with decreasing lifetime (or increasing concentration of the neutral molecule). As a consequence larger magnetic fields are required for the modulation of the S or T recombination yield and the saturation value of the MFE is reached more slowly. In the spectroscopic realm, $B_{1/2}$ gets shifted to the higher magnetic fields when the spin levels are broadened.

An analytical expression connecting $B_{1/2}$ as a function of [Q] can be derived basing on the uncertainty relation $\Delta E \geq \hbar/\tau$ and expressing ΔE as

$$\Delta E = m_S g \mu_B \left(B_{1/2}[Q] - B_{1/2}\left([Q] \to 0\right)\right) \tag{2.31}$$

we arrive at the following expression

$$B_{1/2}([Q]) = B_{1/2}([Q]_0) + \frac{\hbar}{g\mu_B} k_{ex}[Q] \tag{2.32}$$

The above equation, derived by converting the inequality in the Heisenberg's relation as an equality in limiting cases, gives an approximate method to determine k_{ex} from the slope of the $B_{1/2}$ vs [Q] plot in the linear region in the limit of slow exchange.

2.5.2.2 Temperature Dependent MARY Spectrum

A plot of $B_{1/2}$ vs. [Q] gives the as per equation *2.32* above gives an estimate of the crucial exchange rate constant k_{ex} from concentration dependent measurement. However other interesting parameters could be extracted from a temperature-dependent measurement as follows.

One can conversely holds [Q] constant, and takes $B_{1/2}$ measurements at different temperatures (i.e at different k_{ex} values), and then a subsequent plot of the k_{ex} values v. 1/T is supposed to give the activation energies of the self-exchange reaction. This approach has been utilized in our work and the temperature dependent MARY spectroscopy of different donor/acceptor compounds in various solvents has been done. The results have been compared with those obtained from cw-ESR spectroscopy.

2.6 Binary Solvent Effect in MARY Spectroscopy

The pith and marrow of MFE perhaps lies in its perturbation by a plethora of external factors like solvents polarity, viscosity, conformational effects, exterplexes, organized assemblies etc[8]. Although all the external properties mentioned above deserve importance as topics of research, the effect of solvent properties (like polarity, viscosity) has perhaps by far got the lion's share. The intrinsic dependence of the mechanism of MFE on solvent properties and the availability of a large number of solvents (either pure or mixtures) with a myriad of properties which are often tunable, has led to an enormous contribution from this field. Our discussion of this section starts with a brief description of how solvent properties can modulate so strongly the magnetic field effect phenomenon in solution and thereafter the topic of MFE in binary solvent mixtures.

2.6.1 Effect of Solvent Properties (Dielectric Constant & Viscosity) on MFE

Having seen the mechanism of MFE, throughout the discussion above it is not so difficult to understand the effect of solvent properties on MFE. We will still invoke yet another equation at this point in order to understand the effect from a mathematical point of view. MFE or MARY spectroscopy is directly related to the product yield $\phi(B)$ of the luminescent species at a given magnetic field B (ref. equation *2.18*). The luminescent species under consideration constitutes the exciplex in its precursor (formed directly from the excited fluorophore and the quencher) and recombined (delayed) form. But the formation of the exciplex in its precursor form is magnetic field independent while the recombination (delayed) product is magnetic field dependent. Hence we can say that the MFE is a sole function of the singlet recombination yield ϕ_S, although in practice we are monitoring the total exciplex luminescence, the luminescence from the precursor form just getting added as a constant additive term. This effect just scales the MARY spectrum by a certain factor, and has no real influence.

The singlet probability yield, ϕ_S is dependent on two factors, first the probability $p_S(t)$ of finding the RIP in the singlet state at time t, and the probability of the RIP recombination at that time given by the recombination function $f(t)$. The singlet yield then is given by

$$\phi_S(B) = \int_0^\infty p_S(B,t) f(t) dt \tag{2.33}$$

Evidently now, considering the interplay of spin-dynamics and diffusion-dynamics that modulate the magnetic field effect in solution, the role of the solvent on the singlet recombination yield will be registered through the recombination function $f(t)$. If the dielectric constant of the solvent is too high, then the radical pair will be "pried apart" in the geminate cage to give a solvent-separated ion pair (SSIP) which might be eventually thrown out of the geminate cage as F-pairs. In this case the probability of recombination is virtually fall to zero and the decreasing yield of the singlet recombination product will vanish the MFE. On the other hand if the dielectric constant of the medium is too low, then the diffusional excursion (and hence the Spin Evolution) of the incipient RIP will not start at all, the RIP will remain as close Contact-Ion pair (CIP), might eventually decay back to ground state. In this case too there is no recombination product, and the MFE will cease to exist. The MFE in the optimal case would be in the window of a moderate dielectric constant range, where a compromise of recombination and escape from the geminate cage is reached. The MFE is also dependent on the solvent viscosity in the sense that, a too viscous (or even moderately viscous medium) may impede the initial formation of the RIP and might hinder with the diffusional excursion of the RIP too. We therefore try to always stay in the "low-viscosity" approximation.

2.6.2 Binary Solvent mixtures and Magnetic Field Effect

Having seen the effect of the solvent parameters on the MFE phenomenon, we are now ready to take an advanced look into the matter from a structural point of view of the solvent and the solvation shell, especially for the solvent mixtures. To put the matter in another way, we have seen that solvents can modify the geminate reaction, but here we will see how the geminate cage, which is actually bringing about the change, gets structurally modified in the course.

Any solvent, for the matter of fact covers the solute with a sheath of its own, in which each molecule of the covering sheath is held in the vicinity of the encapsulated solute by non-covalent bonds, the process being known as solvation. But when the solvent used is a blend of two or more solvents, then new interesting features start appearing. Solvent blend in this respect are quite interesting entities, because due to some specific interaction between the molecules of different components culminate in the appearance of new useful properties. An added advantage with solvent mixture- the reaction medium can be tuned (e.g. with respect to mole fraction of a certain component) to suit a given task.

The appearance of new useful features in binary solvent mixtures is generally attributed to the phenomenon of **preferential solvation** or dielectric enrichment in these blends. The phenomenon of preferential solvation stems from the fact that in solvent mixtures, the micro-composition around the solute (i.e the composition of the solvent shell) is generally not same as the bulk composition. While in thermodynamic jargon, this phenomenon manifests itself in the form of “excess functions” (e.g. Gibbs energy of mixing, excess volume, excess temperature) , in spectroscopic realm, especially from a photochemist’s point of view, the preferential solvation phenomenon has marked influence on fluorescence and magnetic field detected fluorescence phenomenon (MARY) effects. In the next section we briefly discuss some model to understand preferential solvation, the parameters which characterize it and its influence on MFE phenomenon. In particular, when the dielectric constants of the two components in the mixture differ widely (e.g. Toluene /DMSO), the effect is more prominent.

2.6.3 Binary Solvent Mixtures:: Models

A model to theorize and quantify the effect of dielectric enrichment in binary solvent mixture is surely a complex one and work in this field remains improvising till date[34-35]. The basic idea and aim of each model is to provide a physical picture of the interaction and to provide a quantitative/semi-quantitative measure of the extent of this type of heterogeneous concentration fluctuation known as "preferential solvation"

Probably the first attempt to provide useful information in this respect was done by Suppan[36] who studied the solvatochromic shifts in binary solvent mixtures and concluded that the polar microdomain , i.e. the dielectric enriched region around the solute is produced via the preferential dielectric interaction of the of the solute intermediates with the polar component of the binary mixture, something resulting from the effect of increased solvent stabilization energy as a result of dipole-dipole forces which increase with increasing polarity. The dimension of the polar microdomain as per this model is of the characteristic length of the ion-dipole interaction, i.e. where $e\vec{\mu}/\varepsilon r^2 \approx k_B T$, where e is the electron charge, $\vec{\mu}$ is the dipole moment, ε is the relative permittivity, k_B is the Boltzmann constant and T is the absolute temperature. Under the conditions of thermodynamic equilibrium, when this increase in stabilization energy is compensated by the loss in entropy of mixing, and one can show that the index of preferential solvation is related to the molar ratio of the components in bulk ($X = x_{N,bulk}/x_{P,bulk}$) and the molar ratio of the components in the solvation shell ($Y = y_{N,solvation}/y_{P,solvation}$) by the following relation

$$Y = Xe^{-Z} \tag{2.34}$$

where Z is the 'index of preferential solvation' given as

$$Z = CM\mu_M^2 \Delta f\left(D\right)_{N,P}/2\delta Ra^6 \tag{2.35}$$

where M and δ are the solvents mean molecular weight and density respectively. $\Delta f(D)_{N,P} = f(D)_P - f(D)_N$, μ_M is the solute molecules dipole moment, and a is the molecular radius. C is a constant. However, the model from Suppan, although perfectly plausible from theoretical view could not explain properly some of the effects of MFE observed, and improvisation to the model continued.

One can also modify the Onsager theory for the use in the case of binary solvent mixtures. As per Onsager's general theory of dielectric interaction, he assumed a point electric dipole $\vec{\mu}$ in spherical cavity of radius a in a uniform dielectric with permittivity ε.The effect of the dipole polarizing the dielectric gives rise to the reaction field R, which in turn acts on the dipole. Modifying the scenario to fit the case of binary solvents, we now assume that owing to preferential solvation in the binary solvent with bulk permittivity ε_2, a spherical layer of polar molecules with permittivity ε_1 is formed around a molecular dipole. The figure represents the scenario

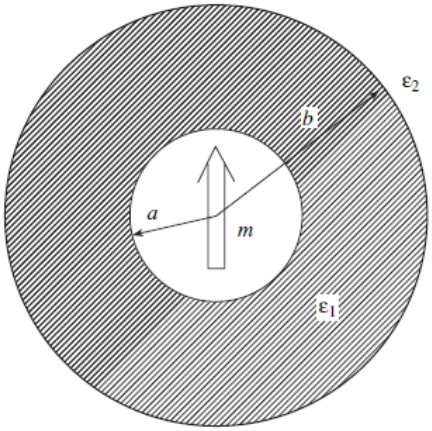

Figure 2.13: Schematic representation of the solvation shell for preferential solvation

Solving the Laplace equation [37-38], one obtains the value of the reactive electric field in this case as

$$R \approx \frac{2\vec{\mu}}{a^3}\frac{(\varepsilon_1 - 1)}{(2\varepsilon_1 + 1)} \times \left[1 + \frac{(\varepsilon_2 - \varepsilon_1)}{\varepsilon_2 + 2\varepsilon_1}\frac{9\varepsilon_1}{(\varepsilon_1 - 1)(1 + 2\varepsilon_1)}\left(\frac{a}{b}\right)^3\right] \tag{2.36}$$

One can see the effect the polar microcluster on the value of the reactive field, which in case of solvation in pure liquid is given by $R = \frac{2\vec{\mu}}{a^3}\frac{(\varepsilon - 1)}{(2\varepsilon + 1)}$. The effect of the polar microcluster is given as correction term to the reactive field in normal case. Equation *2.36* can be simplified by putting $\varepsilon_1 \approx 50$ and $\varepsilon_2 \approx 5$, such that R is simplified to[39]

$$R \approx \frac{\vec{\mu}}{a^3}\left[1 - \frac{9}{2\varepsilon_1}\left(\frac{a}{b}\right)^3\right] \tag{2.37}$$

From the above equations one can calculate then the maximum change in the dipole energy upon preferential solvation to be approximately as $(9/2\varepsilon_1)/(m^2/a^3)$.

Qualitative explanation of the preferential solvation effects was given by Frenkel now on the basis of a new concept of the appearance if preferential solvation effects as a result of the interaction of the solvation shell around a excited fluorophore with the concentration fluctuations of the solvent. Frenkel formulated a hypothesis that under these conditions heterophase fluctuations can result from the formation of small unstable nuclei of a new phase (in a state of the system far from phase transition) in nano-sized clusters. Confirmation was obtained from light scattering experiments in binary liquid mixtures[40] which indicated at the formation of these dynamic aggregates of alcohol molecules. In solution of polar sulfoxides, the possibility of formation of these clusters was indicated through these experiments.

Now modeling on the basis of the concentration fluctuations, we proceed as follows[41]. The concentration fluctuation can be described rigorously as

$$\left(\Delta x_P\right)^2 = R^0 T \Big/ \left(\partial \mu_P / \partial x_P\right)_{V,T} \tag{2.38}$$

where x_P is the mole fraction of the polar component of the binary mixture, $\left(\Delta x_P\right)^2$ is its dispersion (concentration fluctuation) in a certain given volume, R^0 is the gas constant and μ_P is the chemical potential of the polar component.

But according to the Hildebrandt theory, the chemical potential of the polar component is given as

$$\mu_P \approx \mu^0 + R^0 T \ln x_P + \phi_N^2 V_{mP} \left(\delta_P - \delta_N\right)^2 \tag{2.39}$$

Here ϕ_N is the volume fraction of the non-polar component and can be given as $\phi_N = \left[1 + \left(V_{mP}/V_{mN}\right) x_P\right]^{-1}$, δ is the empirical parameter of solubility given as $\delta = \sqrt{E/V_m}$, where E is the molar energy of cohesion and V_m is the molar volume playing an important role in the Hildebrandt theory. Substituting all these expressions in eqn (****), one obtains for a mixture where the molar volumes of the components do not differ significantly, that

$$\left(\Delta x_P\right)^2 \approx \frac{x_P}{1 - 2V_{mP}\left(\delta_P - \delta_N\right)^2 \dfrac{x_P}{R^0 T}} \tag{2.40}$$

One can easily see that when $2V_{mP}\left(\delta_P - \delta_N\right)^2 \to 0$, leads to $\left(\Delta x_P\right)^2 = x_P$, a condition when fluctuations are not perceptible. But when the above parameter tends to unity, the value of $\left(\Delta x_P\right)^2$ may exceed statistical levels of a perfect mixture.

2.6.4 Preferential Solvation and MFE

Literature reports on unusually high values of MFE [39,42] in binary solvent mixtures whose components differed substantially on dielectric properties are found. The field effect is much higher compared to pure solvents with comparable dielectric properties. Therefore we can assume that the effect of preferential solvation might be contributing in enhancing the cage effect and thereof geminate recombination in some way. One might think that the dynamic supramolecular structures arising out of concentration fluctuations could in fact as a bridge or covalent bond between the donor and the acceptor, thereby enhancing the time they spend beside each other and in turn increasing the recombination probabilities. One of the primary aim our study is to examine the effect the effect of preferential solvation, by designing solvent mixtures which are a)very close in the dielectric property , b) moderately separated in dielectric properties, c)widely separated in dielectric properties.

3 Experimental

3.1 Instrumentation of the MARY Equipment

As has already been explained, MARY spectroscopy is the magnetic field modulated detection of exciplex luminescence from a donor(D)/acceptor(A) pair in a certain solvent (or mixture of solvents). A conventional fluorimeter is also capable of generating the emission spectrum which might include emissive exciplex luminescence if the system permits so. So if we can adapt a conventional fluorimeter set-up to allow for the magnetic field effects on the exciplex luminescence, we have instrumented a MARY spectrometer. Therefore we discuss the instrumentation of a MARY spectrometer in the light that it is like a modified version of a *conventional fluorimeter with the provision of modulated magnetic field affected detection.* We break down the instrumental set-up into various modules, examine each module and then see how the modules are integrated to one another yielding a MARY spectrum.

Module 1: Light source and the associated parts

A schematic representation of the spectrum is shown in Fig 3.2. As all reactions under study are initiated by light, a light source is an indispensable part of the spectrometer. The light source we use for the steady-state measurement is a Xe-arc lamp (150 W, Oriel instruments, model 66056) with an AMKO type 02-LPS 0210-U power supply . The spectral range of the emitted light is from around 250 nm to near infrared. The light is a versatile source for a steady-state spectrometer, with the lamps providing relatively continuous output from 250-700 nm, although a number of sharp lines occur near 450nm and above 800 nm[43]. A schematic diagram[44] of the spectral output is given in Fig 3.1

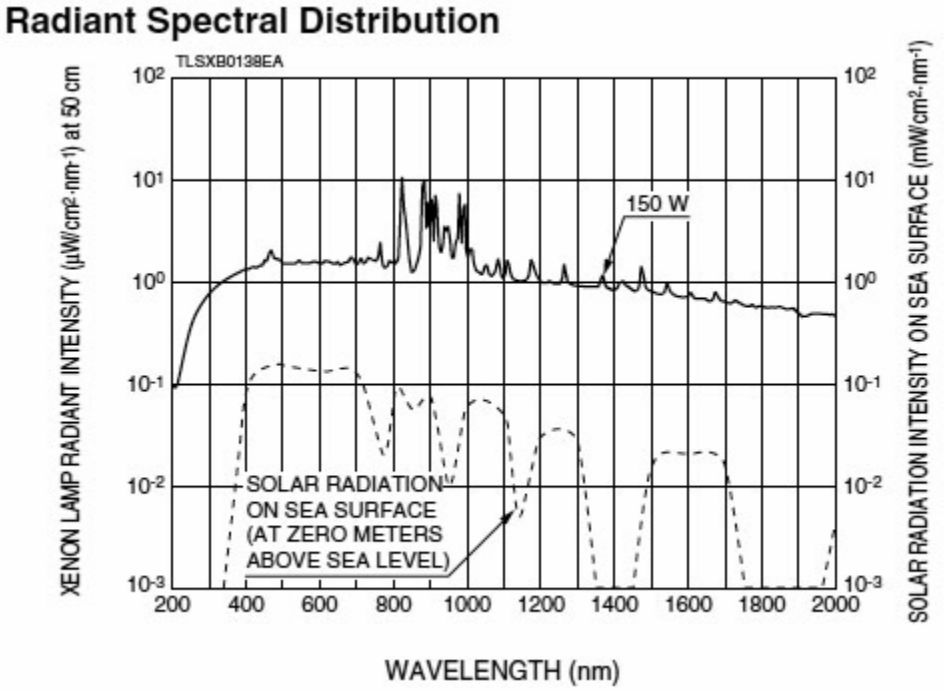

Figure 3.1 Spectral output of a high-pressure Xe-arc lamp

To protect the other components in the optical path from excessive heating, the emitted radiation is passed through a water-cooled water filled cylinder (path length 8 cm), which absorbs the infrared rays generated from the light source. In order to ensure constant lamp output, a beam splitter is used to feed a fraction of the light into an optical stabilization unit (Photon Technology International, type 02-LPS 002). The light next enters a grating monochromator (Photon Technology International model 101, 1200 lines/mm , 500nm blaze). The grating monochromator is also equipped with variable entrance and exit slits (band pass 0-20 nm), in order to control the amount of light entering and leaving the component (it is often required to adjust the amount of light falling on the sample by adjusting the monochromator slits as all systems do not fluoresce to the equal extent). Care has to taken that the entire set up, which is mounted on a horizontal scale allows an unhindered rectilinear propagation of the light, and such that all the entrance and exit slits are collinear and adjusted to the same height. The Xe-arc lamp can be focused using various knobs to allow for the maximum intensity of the light. The light thus generated is fed to the sample from the monochromator using a liquid light guide (Lumatec, series 300, transmission ranging from 50-80% in the range 260-700 nm).

Alternative source of light:

The above elaborate arrangement of the light can be bypassed by using a LED as the light source. We have constructed home-built set up of LED light source available at various wavelengths and with the provision of an iris to control the intensity of the incident light. In almost all cases the intensity of the light obtained with the LED source was more compared to the Xe-arc lamp source.

Module 2: The Magnet and the ancillary units

The magnetic field is applied to the sample held in a chamber (details of the sample holder to be discussed in the next module) between the poles of an electromagnet . The electromagnet in use (Bruker, Model B E-15) is driven by power supply (Bruker) can generate a static magnetic field upto 3 kG. With an adjustable field scan rate (0-1000 G/min), the power supply produces in the electromagnet temporally increasing magnetic field up to a specified limit, in the duration of which the spectrum is recorded. But the magnetic field so produced is static, what is required is a sinusoidally modulated field, which can eliminate noise upto a large extent. For this homebuilt Helmholtz coils (diameter 80mm) are fitted in between the recessed sample holder walls and the poles of the magnet, the Helmholtz coils in turn being connected with correct polarity to a DC-offset unit and a function generator (model Voltcraft , type FG 506) in conjunction with an amplifier. While the function generator in conjunction with the amplifier provides the modulation signal, usually sinusoidally modulating the field component with frequencies upto 1000 Hz (or even more) and modulation amplitude upto 50 G , the DC-offset generates a constant negative field offset, serving a dual purpose of generation of a negative field and allowing us to obtain zero field, which otherwise would have been impossible due the remanence of the electromagnet. A Hall effect devise placed close to the sample chamber and connected to the Gaussmeter (model FW Bell 9200) allows one to measure (and record) the static (DC-mode) as well as the modulated field (AC-mode) values.

Module 3: The Cuvette and sample holder

The sample is contained in a quartz cuvette (all faces transparent) with the provision of closing the mouth with a septum, thus allowing air-tight environment for the sample inside. For housing the cuvette, temperature controlled holder is built. While the top part of the holder can be detached like a lid to insert the sample, there is a hole on the bottom of the holder, just below the cuvette where a light guide collects the emitted light, and further two holes on two faces at right angles to the bottom face for making passage for the light guide with the exciting light and the Hall probe (diametrically opposite) respectively. The arrangement allows for temperature controlled measurement as well, with fluid water being used as the circulating liquid by the use of a pump and a thermostat (Haake, model F3 in combination with model C), the range of temperature obtainable is from 15^0C to 80^0C.

Alternative model of the sample holder: Alternatively for most of our measurements, which could be performed at room temperature, a plastic bodied sample holder was used. The other settings were same as the above although. This sample holder has the advantage of providing a uniform magnetic field due to its low susceptibility. The problem of overheating of the sample from the modulation coils is taken care by air cooling using small pipes.

Module 4: Detection, Registration and Recording Units

As indicated in the above module, the emitted light is collected from the sample holder using liquid light guides. The first step in the detection process is to feed the emitted light to a Photo-multiplier tube (PMT) via a long pass or a short pass filter (the observation wavelength). The filter is chosen to roughly match the exciplex maxima, such that only the exciplex emission is detected and the spontaneous fluorescence emission is cut off. In this context it is worthwhile to say that the choice of a longpass or shortpass filter depends on the type of investigation undertaken, while a longpass filter allows better light

intensities and thereby better S/N ratio, much of the vital mechanistic information might be lost, which otherwise could have been detected with a shortpass filter at the cost of S/N ratio. For some of our studies an interference filter is also used, for example to detect the effect of the magnetic field on the fluorophore. The PMT output is analyzed using a an amplifier, and the output is then fed to a **Lock-in amplifier** (ITHACO DYNATRAC 391-A). The lock-in amplifier assumes a crucial role in the whole process by cutting down noise to a large extent. The lock in amplifier works on the principle of the orthogonality of sinusoidal functions, i.e. when a sinusoidal function of frequency v is multiplied by another sinusoidal function of frequency μ ($\mu \neq v$), integrated over a time much longer than the period of the two functions, the result is zero. In the case when μ is equal to v, *and* the two functions are in phase, the average value is equal to half of the product of the amplitudes. A lock-in amplifier takes the input signal, multiplies it by the reference signal (either provided from the internal oscillator or an external source, the external function generator in our case), and integrates it over a specified time, usually on the order of milliseconds to a few seconds. The resulting signal is an essentially DC signal, where the contribution from any signal that is not at the same frequency as the reference signal is attenuated essentially to zero, as well as the out-of-phase component of the signal that has the same frequency as the reference signal (because sine functions are orthogonal to the cosine functions of the same frequency), and this is also why a lock-in is a phase sensitive detector. Additionally an oscilloscope (Model Tektronix 2440) is used to feed the reference signal from the function generator to the Lock-in-amplifier, a signal used by the Lock-in device to compare it with the output signal and thereby attenuate the noise. Another important feature of the output signal from the Lock-in amplifier is that the signal is already converted in the derivative mode, and that's why the MARY spectrum so recorded with the Lock-in-amplifier is a derivative spectrum.

The next part of the detection procedure is accomplished by analogue/digital processes and software to record the data as follows. In order to further enhance sensitivity of the signal and to "smoothen" the signal, analogue filtering is employed. Both the signal from the gaussmeter (x-axis, channel 0) and the lock-in amplifier (y-axis, channel 1) are passed

through an analogue filter. Digital filtering is performed by a sophisticated USB device (USB-1208HS-XXX), the salient features of which include a) 1.2 kS/s to 1 MS/s sampling, b) 8 analog inputs, 16 digital I/O, counters/timers, up to 4 analog outputs etc. The software for recording of the data is provided by this USB device only and is commercially known as the TracerDAQ® software, for acquiring and displaying data and generating signals

Module 5: Integration & Assembly

The monochromated light (either from Xe-lamp or the LED) enters the sample held in a cuvette, the emitted light is collected by another light guide and fed to the photomultiplier tube through a filter. Now, when the emitted light is collected, the sample is under the influence of a magnetic field, and the emitted light so collected has a component of the magnetic field dependent exciplex luminescence which should be analyzed to yield the MARY spectrum. But here is the catch of the entire instrumentation, that henceforth we are given the task of extracting a signal (or an effect) which might be as low as 2%. Hence our task is to cut off all unwanted part of the signal and amplify the signal of interest. The first step is achieved by the filters (either longpass or bandpass) which eliminate the spontaneous fluorophore emission. The reduced exciplex luminescence (the filter also eats away a part of exciplex luminescence as well), is then amplified by the photomultiplier and analyzed by voltmeter device, the amplification which might be increased by a increasing the power of the power supply for the PMT. The signal might be directly fed to the registration systems, but in the way of light amplification by PMT, the noises might have also been amplified. The signal is then fed to the Lock-in amplifier input, the Lock-in amplifier in turn receiving a reference signal from the function generator through an oscilloscope, analyzing the signal with respect to the reference signal with a supplied phase-angle difference (usually zero degrees), and feeding the output to the analogue/digital registration system. The integration and interplay of the different component is evident in the block diagram of the instrument.

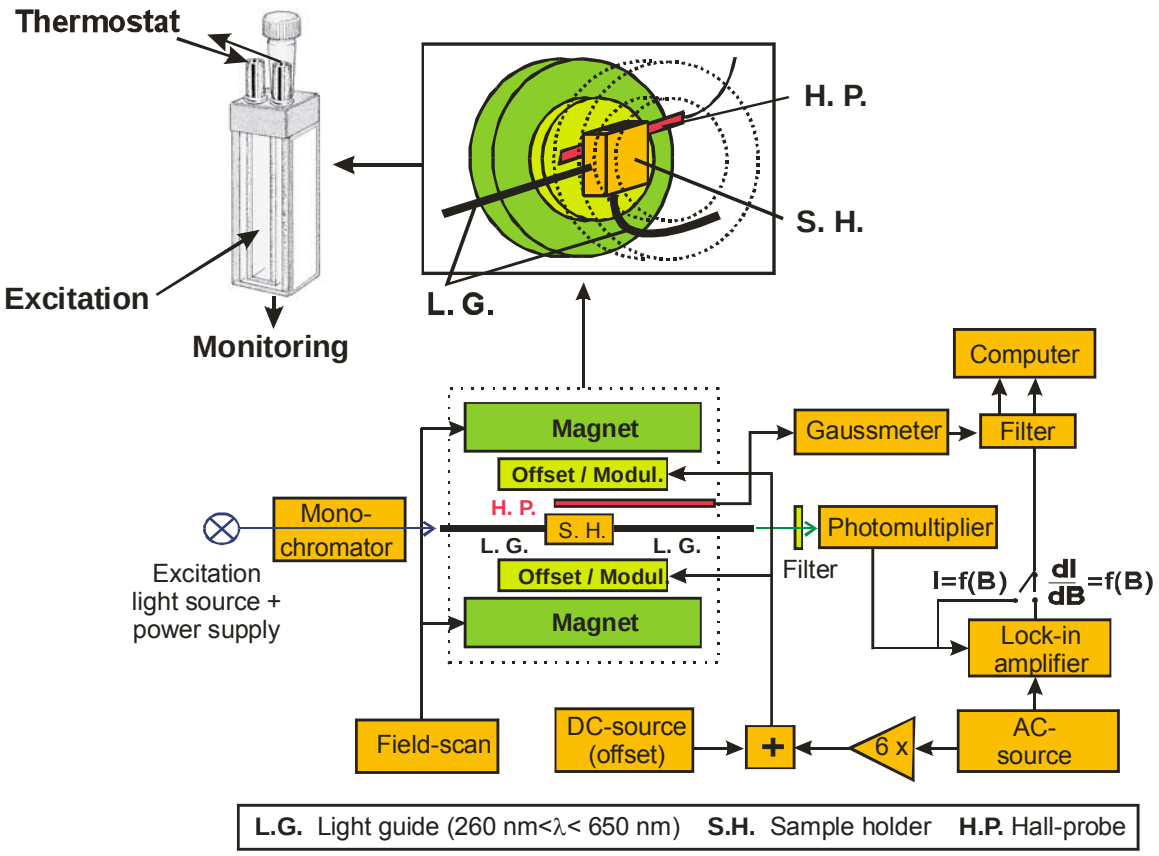

Figure 3.2 Schematic diagram of the MARY apparatus. Abbreviation : B.S. beam splitter, L.G. Light guide, S.H. sample holder, H.P. Hall probe

3.2 Field-Modulated and Unmodulated Mode

A MARY spectra to be recorded with the above arrangement and set-up can be either recorded in modulated or in the un-modulated mode. Typical examples of modulated and un-modulated spectrum are given in the figure 3.3. While the modulated mode with lock-in detection yields a derivative spectrum suitable for line-width effect studies, the un-modulated mode yields the absolute field effect values. In our work both modulated and un-modulated studies were made. In the un-modulated mode, the function generator, oscilloscope and the lock-in amplifier are just switched off, and the output of the PMT which was initially connected to the loc-in input is now detached and fed directly to the analogue filter. Of-course the S/N ratio is better in case of the modulated mode due to phase-sensitive detection, but the modulated mode despite its lower S/N values contains information about the absolute field effects.

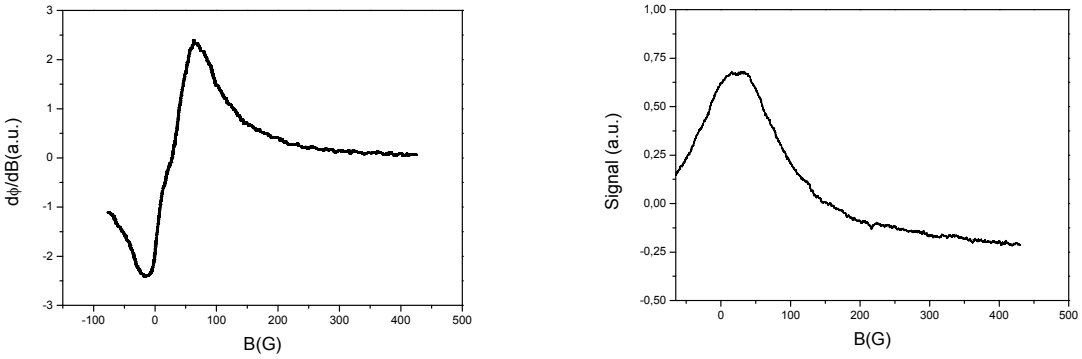

Figure 3.3 Typical example of a modulated MARY spectrum (left) and an un-modulated MARY spectrum (right) obtained from 9,10-dimethylanthracene ($1x10^{-4}$ M) and with N,N'-dimethyaniline ($5x10^{-2}$M) in Toluene/DMSO

3.3 Sensitivity and Instrumental Parameters

As has been highlighted before, the effect on the magnetic field is quite low, even as low as 1-2% of the luminescence. Under these circumstances, we have to set the instrumental parameters to their optimal setting in order to observe a modest spectrum. First we will discuss the issue of the sensitivity of the instrumental components, and then discuss how the instrumental parameters can be optimized to attain a good spectrum. However it should be emphasized here that there is no so called "magic setting" of the instrument parameters and it is often left to the judgment of the experimentalist to set the parameters depending on the system under investigation.

3.3.1 Sensitivity of different components

The delicate and sensitive parts of the instrument comprise especially the Lock-in amplifier and also the Gaussmeter, Oscilloscope, Function Generator and the photodetection units. Care has been taken in the arrangement of the set-up to segregate these sensitive parts from the hazardous lamp and the ignition unit, by using a 2 cm thick aluminium table plate. Each of the sensitive components (as well as the lamp unit) have been grounded or else the power cable is attached to a "Netzfilter". The other sensitive unit in the set-up is also the analog/digital converter connected to the computer unit.

3.3.2 Adjustable Instrumental parameters and their settings:

Following are the tunable instrumental parameters/settings which should be judiciously adjusted to obtain a good spectrum with maximum S/N ratio:

a) Field Scan Rate

The field scan rate can be adjusted from the power supply unit of the magnet. While the choice of setting the field scan rate ranges from a very slow value (0.6 G/min) to very fast (600 G/min), a middle path is generally undertaken to reach a compromise between resolution (lost due to very fast scan but good in slow scan) and photobleaching of the sample (operative in very slow scans). For most of our scan s the field scan rate was fixed at 56G/min.

However the effective field scan rate is determined by two other factors which function in conjunction with the scan rate of the power supply of the magnet, i.e. the time constant of the output filter of the lock-in amplifier (6dB/octave) and the time constant of the analogue filter. Similar to the scan rate of the power supply, a larger time constant of the output filter of the lock-in amplifier reduces the noise level, but increases the scan time (and hence photobleaching). The effect is elucidated in figure *3.4*, in which the spectra are recorded at different pairs of scan rate and the time constant values. The technique used was to start with a fast scan rate and low time-constant and gradually slowering the rate with simultaneous increase of the time constant.

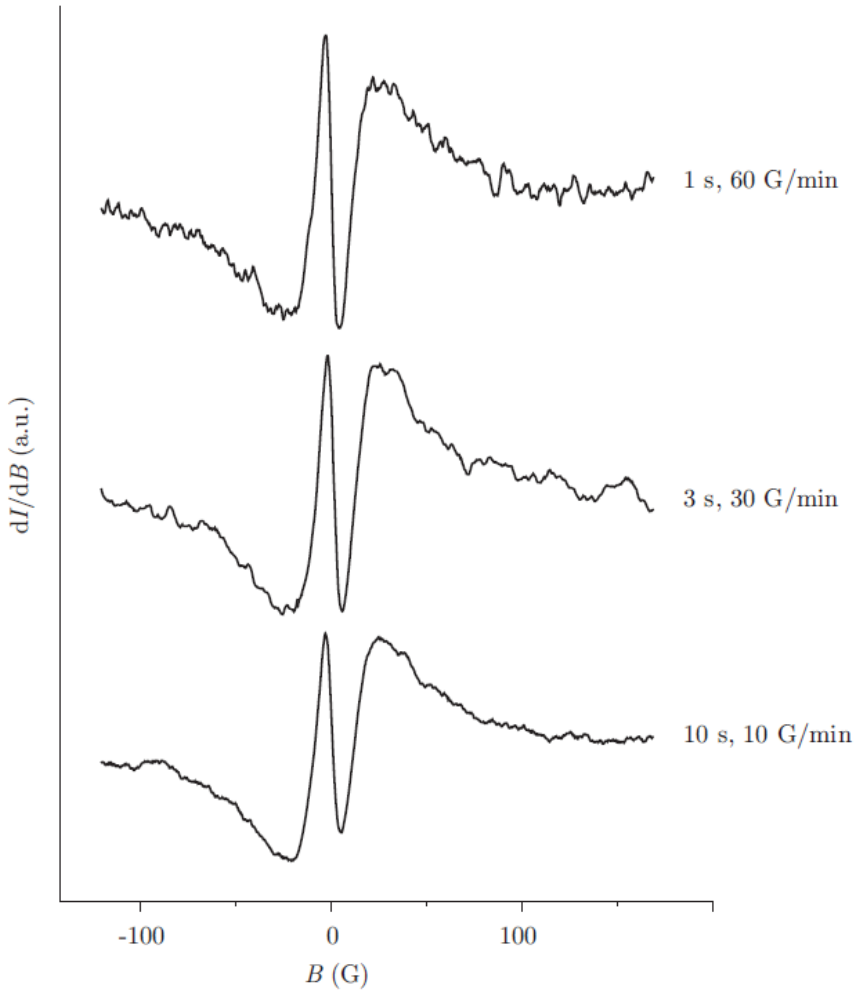

Figure 3.4 :MARY Spectra of 5x10^{-4}M TMPPD in toluene/dimethylsulfoxide (60/40 vol.) recordede with different settings of filter time constant and scan rate. Other parameters: modulation amplitude=5.0 G, modulation frequency=225 Hz. The excitation wavelength was at 295 nm, the observation wavelength >420 nm.

b) Modulation Amplitude

Comparable to the EPR technique, a MARY spectrum is tremendously sensitive to the modulation amplitude. Unfortunately here also, like the effect of the scan rate on the quality of the spectrum, there are also two mutually opposing factors. The increase in the modulation amplitude certainly increases the S/N ratio, but at the cost of the spectral line getting broader, the vital low-field feature getting washed out and even at time distorting the spectrum. So here also a moderate modulation amplitude requires to be chosen in order to balance between the resolution and the S/N ratio of the spectrum. As per the rules of the EPR methods, which also holds good here, smaller the natural linewidth $\Delta B_{pp}(0)$, smaller the modulation field B_{mod} should be chosen. As a general rule of thumb, for a well resolved undistorted spectrum, $B_{\mathrm{mod}} \leq 0.2\Delta B_{pp}(0)$, should be satisfied.

However the choice of the modulation amplitude also lies on the system under investigation and the purpose of the study. If one is interested in studying the low field feature, one should invariably choose very low modulation amplitude around 1 G, or even lower if the spectrum has still permissible values of the S/N ratio. But for the studies of the linewidth effect, where the washing out of the low field feature is not so important and one is interested in the peak-to-peak linewidth, which is generally reproducible under higher modulation amplitudes, one should of course choose higher modulation amplitudes. For our studies, a modulation amplitude of 8G was chosen universally for all linewidth studies. It also depends on the system under investigation as to which linewidth should be chosen, while some system produce good S/N ratio with modulation amplitudes around 3 G, some system might require 10 G or even more. The effect of the modulation is illustrated from the following plot for the system (figure *3.5*).

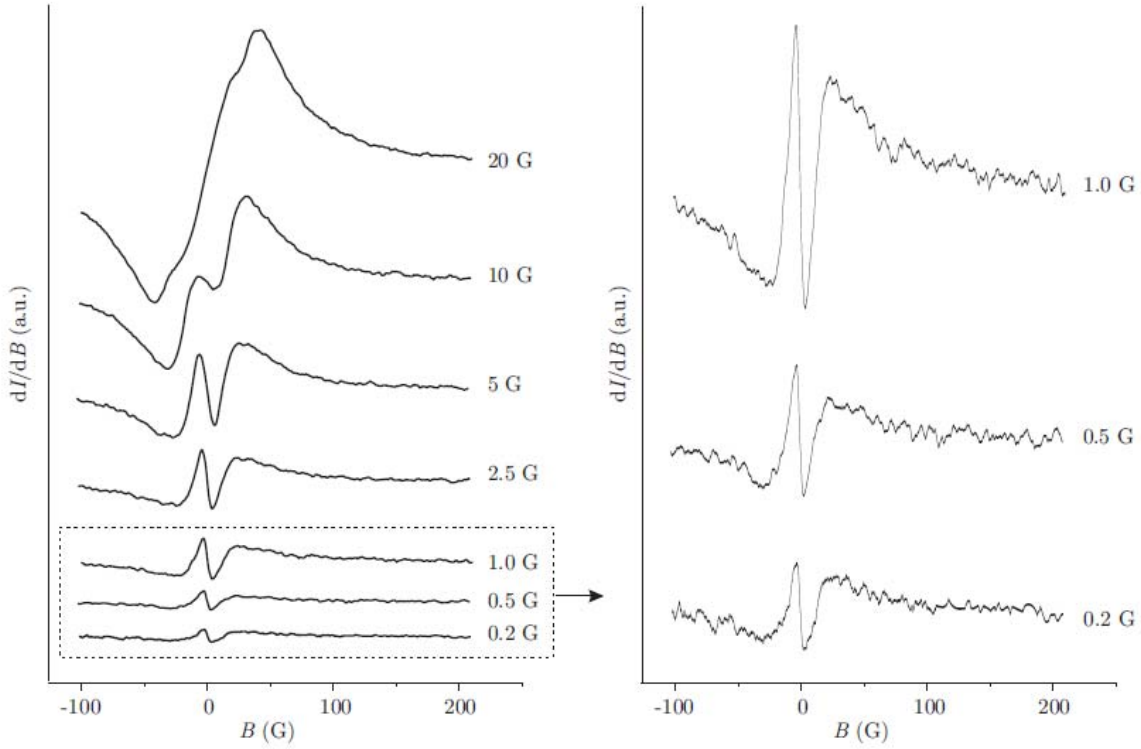

Figure 3.5: MARY Spectra of 5x10^{-4}M TMPPD in toluene/dimethylsulfoxide (60/40 vol.) recordede with different settings of modulation amplitude. Other parameters: modulation frequency=225 Hz, scan rate at 30 G/min. The excitation wavelength was at 295 nm, the observation wavelength >420 nm

c) Modulation Frequency

The effect of the modulation frequency on the MARY signal is not really clear. As per our tests and experiments, the modulation frequency does not bear a great effect on the signal. Although in instruction manuals it is suggested to keep the modulation frequency relatively high, but keeping it too high might just distort the modulating field as relatively large amount of energy is required to drive the modulating coils at higher values of the modulating frequency. Our set-up is capable of generating modulation frequency from as low as 10Hz-1000Hz or even more, but for almost all the measurements the values were set around 200 Hz.

3.4 Working with the MARY Spectrum

3.4.1 Offset correction

Although a MARY spectrum in principle should have mirror symmetry around zero field, but in reality the MARY spectrum, so recorded shows a constant offset both in intensity and field value. The reason of this constant offset value is generally attributed to the signal processing electronics and the exact position of the Hall probe, but the offset generally varies between 10-15 G. The offset is further attributed to the homogeneity of the field produced by the main magnet and the modulation coils, and in reality the field is never really spatially homogenous. The issue of the homogeneity of the field was addressed in our set up by using plastic sample holders which have very low values of magnetic susceptibility. Although the reason for this offset is quite complex and convoluted with many factors that are hard to be taken into account while doing actual measurements, the offset correction is nonetheless an easy task and something which donot really interfere with the spectral characteristics. An example of raw spectra and a spectra with offset correction is shown in the following figure. All experimental spectra shown in this work is offset corrected. The method for offset correction was to find the center of the spectrum by Lorentzian fit and then following the process described above.

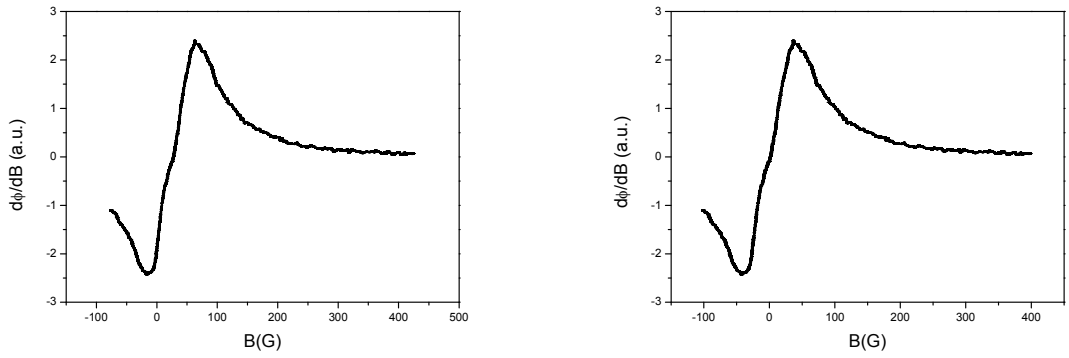

Figure 3.6: A typical MARY spectrum of 9,10-dimethylanthracene ($1x10^{-4}$ M) and with N,N′-dimethyaniline ($5x10^{-2}$M) in Toluene/DMSO without offset correction (left) and with offset correction (right).

3.4.2 Determination of Linewidth and Spectral Simulation

The determination of the linewidth of the spectrum (ΔB_{pp}) or the peak position (B_p) by inspection and so to speak "by hand" is far too imprecise for our purpose, especially when the changes in the linewidth values are only a few gauss in the order of magnitude. Therefore the use of automated fitting programs is indispensable in our analysis of the above parameters. The fitting program used was the Origin 8 software, and the curves were fitted using the user-defined first-derivative Lorentzian functions, whose form is given as:

$$Y' = -Y_{\max} \frac{2\Gamma^2 \left(B - B_0\right)}{\left(\Gamma^2 + \left(B - B_0\right)^2\right)^2} \tag{3.1}$$

where $Y_{\max}$ is the amplitude parameter, B_0 is the centre of the function and Γ is the linewidth parameter, which is related to the peak-to-peak linewidth ΔB_{pp} as follows

$$\Delta B_{pp} = \frac{2}{\sqrt{3}}\Gamma \tag{3.2}$$

The fit in the Origin software, based on the iteration and matrix-inversion methods were done using the built-in commands, and the χ^2 values were noted. The fit could also be done using a first derivative Gaussian function, but the Lorentzian fits seemed to fit the peak position better than the Gaussian ones and moreover the Lorentzian ones are more robust towards the sensitivity to modulation amplitudes. The appearance of the low-field features somehow distorts the ideal Lorentzian shape, but in our measurements the use of relatively higher values of modulation amplitude (8G), made the low-field feature somewhat washed-out.

3.4.3 Absolute Magnetic Field Effect values

A large part of our analysis lies in the absolute magnetic field values as well. Here also the precise determination of the absolute field effect values which could be as low as 1% is also a difficult task. Again this time, using the Origin 8 software, and fitting with the common bell-shaped Gaussian functions, the absolute magnetic effect values were calculated as follows. The MFE on the exciplex, χ_E is given as in equation *3.3*.

$$\chi_E = \frac{I_B - I_0}{I_0} \tag{3.3}$$

But in order to calculate the actual MFE from the plot of the data point in origin, the above quantities are calculated as follows. The plot is first fitted with a Gaussian function of the form [45]

$$Y = Y_{\max} \exp\left[\frac{-(\ln 2)(x - x_r)^2}{\Gamma^2}\right] \tag{3.4}$$

where $Y_{\max}$ is the maximum amplitude parameter, x_r is the center, and Γ is the full-width at half-maxima (FWHM). From a simulation of the curve using the Gaussian functions, the quantity is obtained using the following property of the Gaussian functions

$$y_c = y_0 + \frac{A}{w\sqrt{\pi/2}} \tag{3.5}$$

where y_0 correspond to the y-value at the base line, and y_c, the y-value at the peak of the curve, A is the area under the curve . The dark count Δ_{dark} is noted for each scan, and the absolute field effect is calculated using the formula

$$\chi_E = \frac{y_c - y_0}{\Delta_{dark} - y_0} \tag{3.6}$$

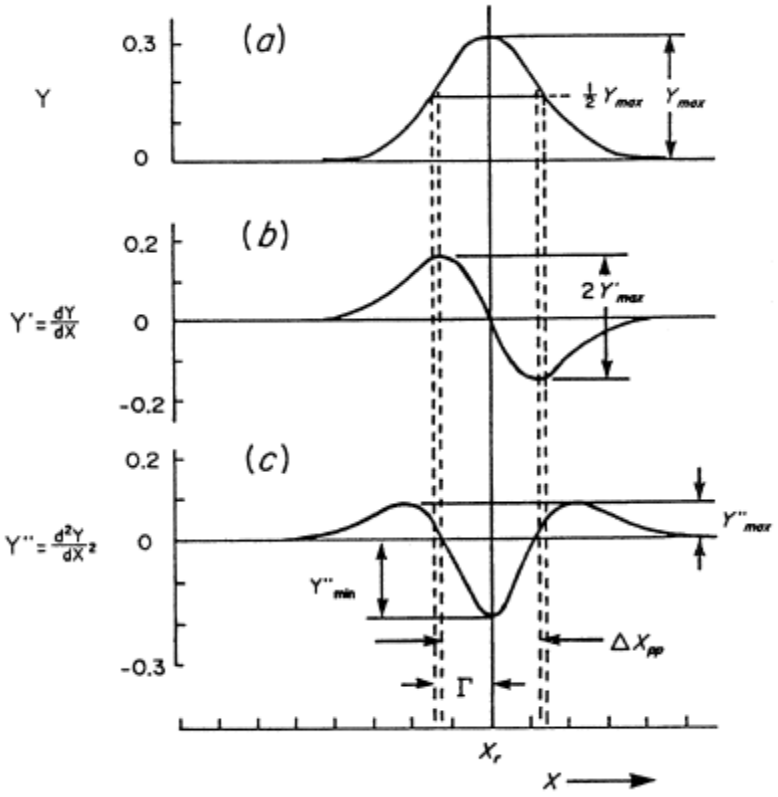

Figure 3.7: Lorentzian lineshapes : a) Absorption Spectrum, b) first-derivative spectrum and c) second-derivative spectrum. The symbols appearing are described above.

3.5 Other Apparatuses

3.5.1 Apparatuses for Solvent Characterization

Since the focus of our studies includes solvent mixtures, the properties of which we want to tune, a precise knowledge of the macroscopic properties of the solvent mixtures in special are an absolute necessity. From electron transfer theory it is known that the properties/parameters which are the main controlling factors in electron transfer and magnetic field effect phenomenon include the a) the static dielectric constant (pure solvent or mixture), ε_s and b) the refractive index n_D, together appearing as the Pekar factor in the outer-sphere reorganization term. However the factors which determine the criterion of the initial approach of the reactants include the dynamical solvent viscosity η, and the free-energy of formation ΔG_{et}^0. But in solvents of mixed composition, these macroscopic parameters of ε_s, n_D and η often show non-linear and far-from ideal behavior. For example, for some solvent mixture composition the overall dielectric constant could be given as $\varepsilon_{s,mix} = v_1\varepsilon_1 + v_2\varepsilon_2$, with '$v_i$' represent the volume fraction of the solvent. Unfortunately for most solvents such a linear relationship does not hold, and one has to experimentally determine the parametric equation explaining the behavior. The following experimental methods for the determination of the macroscopic properties of the solvents were employed.

3.5.1.1 Dielectric Constant

Static dielectric constant of solvent mixtures were determined using a home-built apparatus similar to one described in[46]. The built up of the apparatus consists of an electronic swing-circuit operating at an approximate frequency of 400 kHz. The actual frequency is determined by the intrinsic capacitance of the apparatus , C and the capacitance of the sample cell C', which is in turn determined by the static dielectric

constant of the solvent in the cell. The output of the apparatus is a frequency against each dielectric constant. The method to obtain the dielectric constant of the mixture of solvent is to first calibrate the instrument at a certain temperature (the sample compartment and the electronic circuit can be thermostated by water cooling) to obtain the frequency (*f*/KHz) values against the known static dielectric constants and obtain a fit of the curve. Next, this fitting equation is used to extrapolate the values of the dielectric constant of the mixture at various molefractions of the given components from the frequency readings. Our experiment was performed at 22^0C and the following fit for the calibration curve was obtained. The corresponding fitting equation for the calibration curve is was found to be

$$f = 102.6\exp\left(-\varepsilon/48.3\right) + 304.4 \tag{3.7}$$

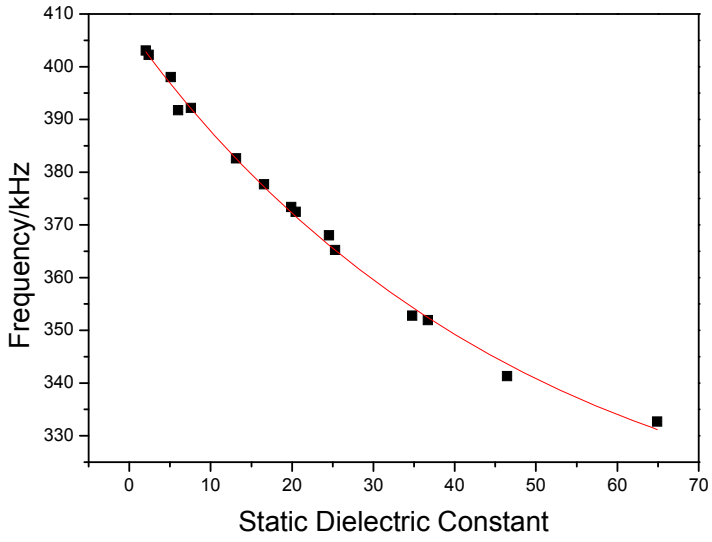

Figure 3.8: Plot of frequency vs. dielectric constant values for the representative solvents.

3.5.1.2 Dynamic Viscosity

Ubbeholde viscometers (SCHOTT) were used to obtain the dynamic viscosities of solvents and solvent mixtures. We have three viscometers at our disposal which provide the possibility of covering a wide range of viscosity. The ranges and instrumental constants available in our laboratory are as follows: $K(0c, 0.5-3cSt) = 0.003164 mm^2/s^2$, $K(Ic, 3-30cSt) = 0.02934 mm^2/s^2$ and $K(IIc, 30-300cSt) = 0.3044 mm^2/s^2$. The dynamic viscosities, $v = K\overline{t}$, were obtained as the mean passage of time of the liquid, $\overline{t}$, taken from the last three repetitions and multiplied by the capillary instrument constant, *K*. The dynamic viscosity η was then calculated as follows.

$$\eta = K\overline{t}\,\rho \tag{3.8}$$

where ρ being the mass density of the solvent. The densities of the solvent mixtures were then evaluated /approximated as $\rho_{mix} = \frac{(m_1 + m_2)\rho_1\rho_2}{m_1\rho_2 + m_2\rho_1}$.

3.5.1.3 Refractive Index

The refractive indices were determined using a temperature-controlled Abbé Refractometer (IT model from Atago)

3.6 Optical Spectroscopy and Sample Preparation

3.6.1 Optical Spectroscopy

Steady state absorption spectra were recorded with a UV-VIS-NIR scanning spectrometer (Shimadzu model UV-3101 PC). Steady-state fluorescence spectra were taken using Jobin Yvon Fluoro-Max 2 spectrometer.

3.6.2 Sample Preparation

The substances under investigation were used either used as received or purified as described under.

3.6.2.1 Fluorophores

9,10 dimethylanthracene used as the focus compound in the majority of binary solvent effect studies was used as received (Aldrich, 99%). Pyrene (Fluka, 99%) was purified by vacuum sublimation and so was TMPPD (Fluka 98%).

3.6.2.2 Quenchers

N,N'-dimethylaniline used in the majority of investigation was either used as received (99.9%, Aldrich) in septum sealed container, with small portions being sucked out with a syringe under anaerobic conditions. Alternatively it was also distilled under vacuum using an elaborate arrangement for maintaining the distillation under anaerobic conditions. The dicyanobenzene isomers (1,2- dicyanobenzene and 1,4- dicyanobenzene) from Aldrich,98% were recrystallized from toluene. DMDPM (4,4'-Bis(dimethylamino)diphenylmethane) was used as received (Aldrich 98%)

3.6.2.3 Solvents

All the solvent used in the investigation were HPLC grade and were either distilled after dynamic drying over molecular sieves or purified by recrystallization by freezing (DMSO).

3.6.2.4 Preparation of Sample for Measurement

Our investigation into MARY effect consists of primarily two types of studies, one on the temperature dependence and the other on the binary solvent effects. Although the basic principle for preparation of sample remains the same for either kind of study, there were subtle differences owing to the physical form(solid/liquid) and sensitivity of the fluorophore/quencher to atmospheric conditions. The temperature dependent measurements performed on pyrene/dicyanobenzene system were performed relatively easier by preparing the stock solution of pyrene and the dicyanobenzenes (which is solid at room temperature) in the respective solvents and then mixing/diluting them in the required amount in volumetric flask before pouring about 2 ml of the fluorophore/quencher mixture in the cuvette, which were septa sealed and proceeding for purging with dry argon for 20 mins. Similarly for the TMPPD systems were also performed relatively easy because the system does not need any "quencher" at all, the photo-ionization process itself produces the RIP. Therefore the stock solution of TMPPD was prepared in Toluene/DMSO mixture and the usual procedure as above was followed.

The sample for the binary solvent effect studies were prepared as follows owing to the extreme sensitivity of DMA to air and light. The sample was prepared by weighing the required amount (using a volume to mass conversion) of the fluorophore solutions in various solvents directly into the cuvette (septa sealed quartz cuvette) in various weight ratios to give a certain bulk permittivity of the sample. The fluorophore solution was then degassed for about 10min, before injecting in pure DMA under argon through Hamilton syringes of 10 μL size. The amount of DMA to be poured was calculated in accordance

with the mass of the fluorophore solution inside the cuvette and the effect of volume change on the addition of the fluorophore was neglected.

Furthermore care was taken during degassing the solution with argon so as to ensure no loss of the solvent by evaporation due to the passage of dry argon. This was done by saturating the argon gas with the solvent in a special arrangement and then passing the argon saturated with the solvent into the cuvette, such that any loss due to evaporation of the solvent is compensated by the saturated argon vapour.

3.7 Solvents

Our work includes both pure solvents and solvent mixtures. Solvent properties as indicated earlier controls to a great extent the events and the fate of the electron transfer reactions. As indicated in the theoretical discussions, the differences in the properties of the solvents make up a lot of difference in determining whether the medium is homogenous, quasi-homogenous or heterogeneous. The nature of the solvent blend from the view-point of the extent of concentration fluctuations might have a pronounced effect on the magnetic field effect phenomenon. Therefore we have devised four solvent mixture primarily to simulate different microenvironments in terms of homogeneity or heterogeneity as follows. The table 3.1 gives a compilation of the macroscopic properties of the solvents in use.

Table 3-1: The solvents used and their respective macroscopic properties (ref) relevant to our purpose including their mass density, ρ, dynamic viscosity, η, dielectric constant, ε_s, the refractive index , n_D and the boiling point of each solvent . Unless otherwise mentioned, the macroscopic properties are given at 25^{0}C and the boiling point at 1 atm. The additional information in the table also includes the supplier of the chemical and also the relevant purification process.

Solvent[a]	Boiling Point (^{0}C)	ρ (g mL^{-1})	ε_s	η (cP)	n_D (25^{0}C)	Supplier/ Purity	Purification/ drying
DMSO	189.0	1.110	50.0	2.20	1.479	ROTI DRY(99.5%)	as received
PA	101.5	0.888	6.0	0.58	1.383	Aldrich (99%)	3Å molecular sieves/distillation
BN	117.6	0.794	24.7	0.58	1.383	Alfa Aesar (99%)	4Åmolecular sieves/distillation

BA	215.5	1.054	5.7	2.18	1.502	Alfa Aesar (99%)	3Å molecular sieves/distillation under reduced pressure
TOL	110.6	0.862	2.4	0.55	1.494	ROTI DRY(99.5%)	3Å molecular sieves/distillation
PC	241.7	1.195	64.9	2.53	1.419	Aldrich (99%	3Å molecular sieves/distillation under reduced pressure
THF	65.96	0.873	7.6	0.46	1.404	Roth HPLC (99.9%)	3Å molecular sieves/distillation

[a] Used acronyms : dimethylsulfoxide (DMSO), propylacetate (PA), butyronitrile (BN), benzylacetate (BA), toluene (TOL), propylenecarbonate (PC), tetrahydrofuran (THF).

.

3.8 Binary Solvent Mixtures

For the purpose of our study the following binary solvent mixture were used.

Propylacetate/Butyronitrile (PA/BN)

Looking at Table 3.1, one can easily figure out the purpose these solvents. This mixture perhaps constitute the most homogenous or pure-solvent like environment, still allowing for variation of the dielectric constant values in relatively smaller range. The two solvents have equal viscosity, equal refractive indices and close densities. The solvent mixture thus allows one to vary the dielectric constant while keeping all other parameters constant. Very few solvent blends allow such a choice. The dependence of the dielectric constant values with weight fraction of BN is given as

$$\varepsilon_s\left(w_1\right) = w_1\varepsilon_1 + \left(1 - w_1\right)\varepsilon_2 \tag{3.9}$$

with w_i and $\varepsilon_{s,i}$ denoting the weight fraction of the component *i.*

Dimethylsulfoxide/Benzylacetate(DMSO/BA)

While the PA/BN gives almost a perfect mixture where the components do not differ greatly in the dielectric constant values, we have devised another solvent with similar viscosity, density and refractive indices but differing greatly in the bulk permittivity values. (Ref Table 3.1). This perhaps constitute a "quasi-perfect" mixture with the possibility of varying the dielectric constant values in a bigger window compared to the former. The ε and the n_D values were parameterized (ref ulf thesis) using the method described earlier and the parameterized equations are given as follows.

$$\varepsilon_s\left(x_{DMSO}\right) = 5.82\exp\left(x_{DMSO}/0.479\right) + 0.067 \tag{3.10}$$

$$n_D\left(x_{DMSO}\right) = 1.502 - 0.0123x_{DMSO} + 0.0017x_{DMSO}^2 + 0.0124x_{DMSO}^3 \tag{3.11}$$

Toluene/Dimethylsulfoxide

The mixture of Toluene and DMSO provide a perfect condition for producing a medium with heterogeneous fluctuations mediated by the solvent dipoles of DMSO. The large difference in the dielectric constant values of the two components and the dissimilarity in their other macroscopic solvent properties like viscosity, refractive index further add to the heterogeneity of the medium. We have parameterized the bulk dielectric constant of the solvent mixture using the method described above and the parameterized equation is as follows.

$$\varepsilon_{s,mix} = 62.5\exp\left(-x_{TOL}/0.78\right) - 15.6 \tag{3.12}$$

The above is an exponential fit. We have also fitted the plot with a Polynomial, but the results of both the fit were tested to be equally good. The Polynomial fit is represented by the following equation, but for all practical purposes, the exponential fit was used.

$$\varepsilon_{s,mix} = 46.5 - 73.1x_{TOL} + 28.8x_{TOL}^2 \tag{3.13}$$

Propylene Carbonate/Toluene

In order to check whether the medium simulated by the solvent pair TOL/DMSO really exerts any special effect w.r.t. dielectric polarization and concentration fluctuations, or whether any special effect is exerted by the dipoles of the soft sulfur molecules in DMSO, a similar solvent pair TOL/PC was devised for comparison. In this solvent mixture too, the dielectric constants of the two components differ to a great extent, and all the other properties which modify electron transfer phenomenon like the viscosity and the refractive indices are also dissimilar. The dielectric constant of the mixture was parameterized as per the following equations (here also both exponential and polynomial fit were done, both equations equally good, but for practical purposes the exponential one was always used).

$$\varepsilon_{s,mix} = 95.3\exp\left(-1.64x_{TOL}\right) - 15.9 \tag{3.14}$$

$$\varepsilon_{s,mix} = 76.2 - 127.0x_{TOL} + 53.0x_{TOL}^2 \tag{3.15}$$

3.9 Calibration for Temperature Dependent Studies

The task of performing temperature dependent studies under maximum insulation and minimal heat loss is quite challenging. We tried to circumvent the problem of heat loss from the sample holder between the poles of the magnet by sticking thin layers or cork on all the faces of the cuvette holder. The plastic pipes, carrying water to and from the thermostat were tightly packed inside foam sheets and were sealed from outside. Inspite of all these arrangements, some heat loss was inevitable, which resulted in a small difference in temperature between the bath and the solution inside the cuvette. To account for this we did a calibration on the temperature inside the cell with respect to the temperature inside the bath. Using distilled water as the calibrating fluid and measuring the temperature inside the cell using a thermo-couple, we calibrated the temperature from 15^0C to 85^0C by first moving up in steps of about ten degrees and then coming down to the starting value in similar fashion. The calibration curve obtained by such a procedure is given in figure *3.9*. The linear regression which describes this dependence was found out to be

$$T_{cell}(K) = 0,83T_{bath}(K) + 54.2 \qquad (3.16)$$

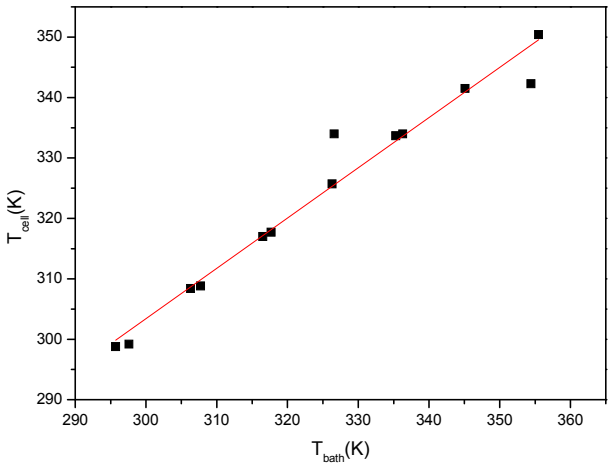

Figure 3.9: Calibration curve for the temperature dependent studies

Equation Chapter 4 Section 1

4 Results

4.1 Photochemistry

Our discussion of the results starts with the discussion of the photochemistry of the compounds under investigation. The photochemical investigations mainly involve the following:

- The absorption and excitation spectra of the compounds studied. This step is indispensable not only for requiring a good understanding of the basic photophysical characteristics of the compounds under investigation, but also to select the excitation and the observation wavelengths used in MARY spectroscopy.
- To determine the possibility of static quenching and ground state complex formation of the donor /acceptor pair, through absorption and emission spectrum of the donor/acceptor pair.
- To determine the possibility of dimerization in the excited state (excimer formation) .
- To elucidate the mechanism of the MARY spectrum.

Before we discuss the above points, we will first introduce the structures of the compounds under investigation.

The structures of the compounds are as follows:

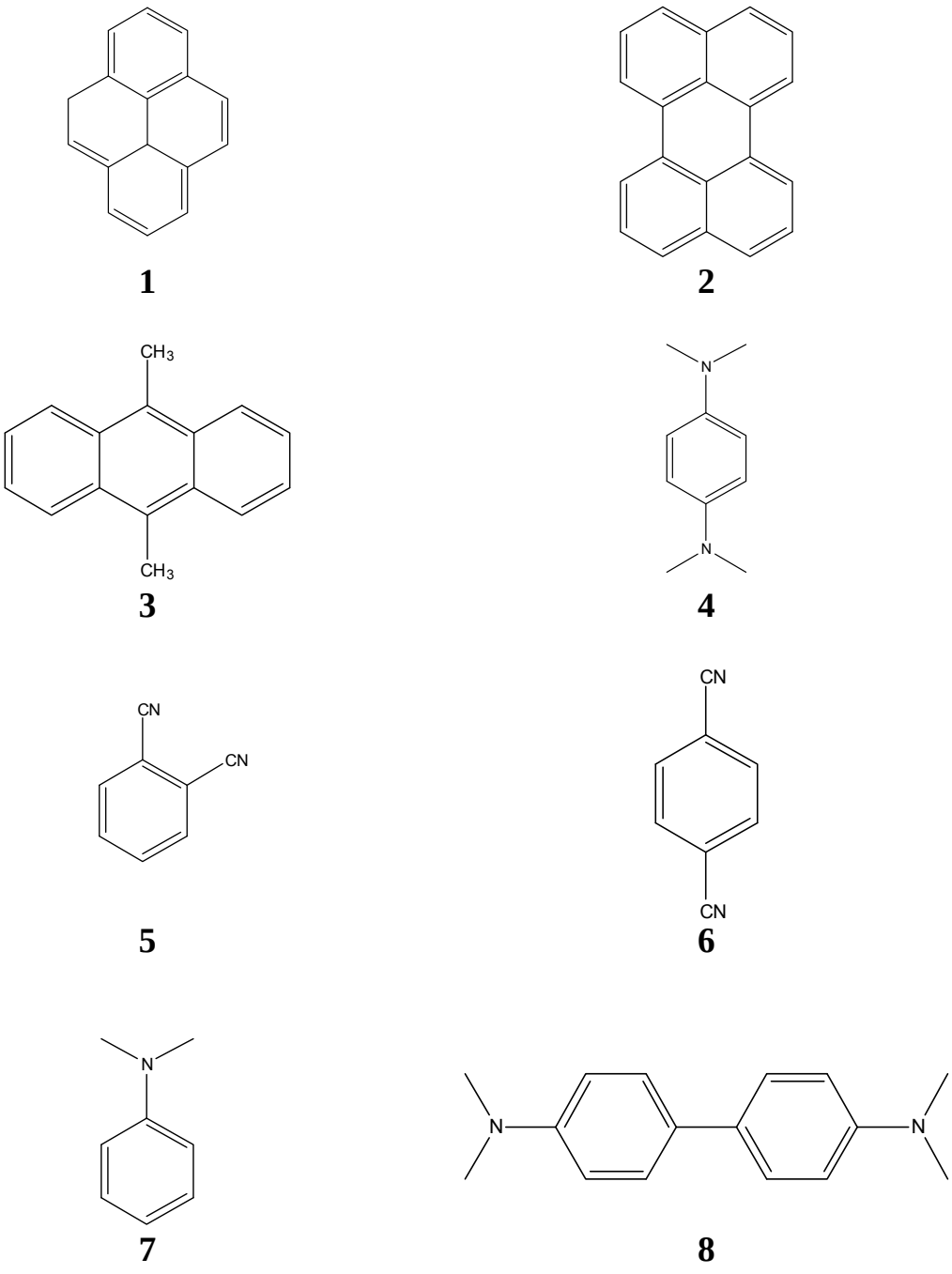

Figure 4.1:The structures of the substances investigated. **1** Pyrene, **2** Perylene, **3** 9,10 dimethylanthracene, **4** N,N,N',N'-tetramethyl-1,4-phenylendiamine (TMPPD), **5** 1,2-dicyanobenzene, **6** 1,4-dicyanobenzene, **7** N,N'-dimethylaniline **8** 4,4'-Bis(dimethylamino)diphenylmethane

Henceforth a compilation in the values of the oxidation and the reduction potentials of the of the fluorophore and quenchers used, the $E_{1/2}^{ox}$ and the $E_{1/2}^{red}$ values and their function in ET is compiled.

Table 4-1:Compilation of the $E_{1/2}^{ox}$ and $E_{1/2}^{red}$ values of the used substances

Substance	Function in ET process	$E_{1/2}^{ox}$ vs. SCE (volt)	$E_{1/2}^{red}$ vs. SCE (volt)
Pyrene	D/A	1.16	-2.1
Perylene	D	0.85	-1.66
TMPPD		0.13	-
DMAnt	D	0.95	-1.98
1,2-dicyanobenzene	A		-1.70
1,4-dicyanobenzene	A		
DMA	A	0.81	-
DMDPM	A		

The excitation and the emission spectrum which is of the primary importance to us is the one of 9,10-dimethylanthracene with or without the quencher DMA and DMDPM. The plots below show the spectrum from which the wavelength of excitation has been chosen at 378 nm, and the wavelength of observation has been chosen at 515nm, a region where the exciplex emission is around the maximum value, and the fluorophore emission is almost negligible.

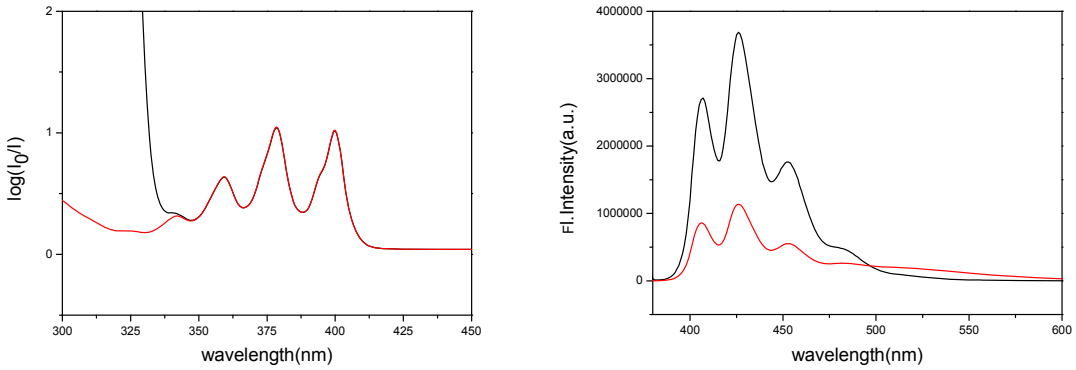

Figure 4.2 (Left) The absorption spectrum of 9,10-dimethylanthracene ($1x10^{-4}$ M) in red and with N,N'-dimethyaniline ($5x10^{-2}$M) in black. (Right) Fluorescence spectrum of 9,10-dimethylanthracene ($1x10^{-4}$ M) in black and with N,N'-dimethyaniline ($5x10^{-2}$M) in red.

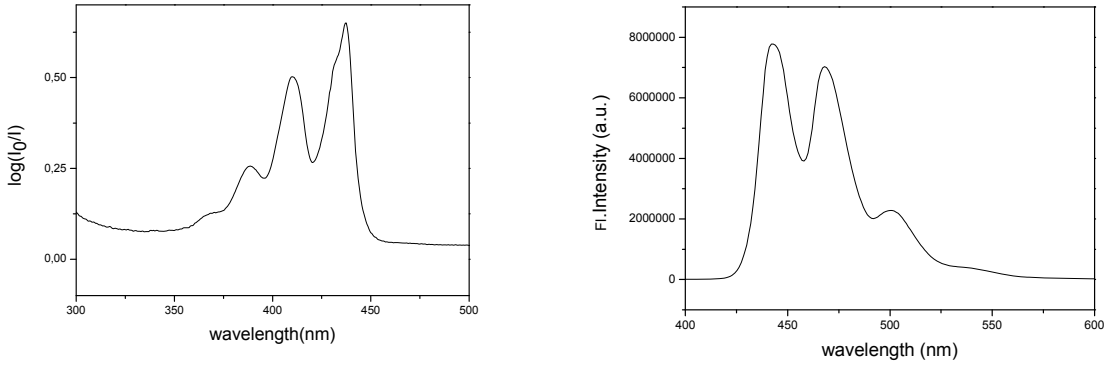

Fig: (Left) The absorption spectrum of $4x10^{-5}$M Perylene (PER) in 1:4 DMF/THF mixture and (right) the emission spectrum of the same .

4.2 Temperature Dependent Measurements using MARY Spectroscopy

4.2.1 Introduction and Scope of Study

As has been outlined in the theoretical section, the linewidth effect in MARY spectroscopy and its intrinsic dependence on the concentration of the neutral molecule [Q] and the exchange rate constant (equation *4.1*) allows one to perform temperature dependent studies on the degenerate exchange reaction in a spin-correlated radical-ion pair. A plot of the exchange rate constant (k_{ex}) against 1/T allows one to extract out the activation energies out of these reactions. So much so for the pros side, on the cons lies the extreme difficulty of finding a suitable system that is responsive to temperature changes, finding solvents (or solvent blends) that is stable in the window of the accessible temperature range (generally 15-80 degree Celsius using a water thermostat), encompassing the problem of solvation at certain concentration of the quencher when it is in solid form, insulating the system to ensure minimal heat loss and moisture precipitation effect and last but not the least extracting out meaningful values of the activation energy from a convolution of other potential temperature dependent factors. Not much report of temperature dependent studies on the magnetic field effecting PET reaction in condensed media are to be found in literature except some sporadic ones[47] where the microenvironment within the reverse micelles Triton-100 in cyclohexane are studied using the magnetosensitive probe Pyrene/N,N' dimethyaniline from absolute field effects. While all these factors will be discussed in due course, we would start the section by pointing out the fact that temperature dependent studies of this sort has been undertaken for the first time which could throw light on the dynamics of electron transfer using MARY spectroscopy as a tool.

4.2.2 Systems under investigation

The following systems were investigated to probe the temperature dependent effect:

1. Pyrene/1,2 dicyanobenzene (in Tetrahydrofuran (THF) as solvent)

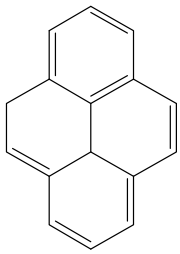

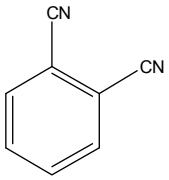

2. Pyrene/ 1,4 dicyanobenzene (in THF and Propyl acetate/Butyronitrile mixture in weight ratio 62:38)

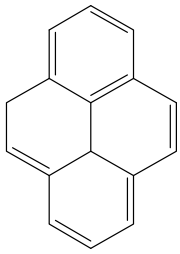

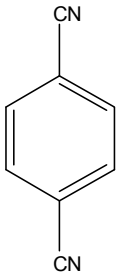

3. N,N,N',N'-tetramethyl-p-phenylenediamine (TMPPD) photoionization in Toluene/DMSO (60/40 mixture by volume)

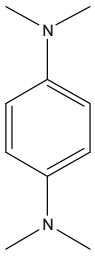

4.2.3 Our Systems

Our system under investigation is mainly focused on TMPPD photolysis in Toluene/DMSO (60/40 by vol.). TMPPD photo-ionization is widely studied phenomenon in photo and radiation chemistry perhaps due to its broad absorption band, low ionization potential and electron affinity. TMPPD photo-ionizes at room temperature to generate free radicals, a complex photochemical process in this case, which has attracted considerable attention not only in theoretical and experimental[48-50] studies but also due to its potential applications in the field of solar cells, photorefractivity and electroluminescence. In the past years considerable volume of research have included the photo-ionization mechanism of TMPPD which generates free radicals/radical ion pairs from across various parts of the world using various probes and techniques. Some of this include flourescnece studies in various alkanes[51], (ref) photo-reaction in alcohols using laser excited TR-ESR studies, (ref) temperature dependent single-photon ionization quantum yields in various alcohols, (ref)TR-photoconductivity measurements in liquid alcohol under the presence of a magnetic field and many others. But from the point of view of magnetic field effect phenomenon, an important report (ref) on the discovery of the magnetic field effect (MARY Spectroscopy) on the TMPPD photo-ionization in Toluene/DMSO (ref) and a later report (ref) which tries to throw light on the identity of the radical ion-pair generated by TMPPD in Toluene/DMSO as the solvent using magnetic field effect and magnetic isotope effect have motivated us to utilize this system, which produces a MARY spectrum with good S/N ratio for the study of the photo-ionization mechanism and other facets of electron transfer mechanism using temperature dependent magnetic field effect. The boiling point of the solvents (table *3.1*) also allows us to vary the temperature in a much larger window from 15 to 80 degree Celsius. The concentration of TMPPD was always kept at $6x10^{-3}$ M and Toluene/DMSO was in volume ratio 60/40.

The other system under consideration is the system of pyrene/1,2 DCB and pyrene/1,4 DCB. As is widely known in the world of photochemists, pyrene with its long lifetime is one of the most widely studied substances in photochemistry.

4.2.3.1 Scheme of work/Working Equation

As has also been discussed in the theoretical section, the scheme of the temperature dependent MARY measurements is as follows.

- Keeping the quencher concentration and other external parameters same (viz. modulation amplitude, modulation frequency and scan rate etc) and taking MARY spectra at different temperatures.
- Analyzing the different spectra to extract out the $B_{1/2}$ values at different T(K).
- Finding the $B_{1/2}(0)$ values by plotting the $B_{1/2}$ vs. [Q] values and extrapolating the data to find $B_{1/2}(0)$, the $B_{1/2}$ value at concentration tending to zero.
- Using the equation below, to find out k_{ex} values at different T(K)

$$B_{1/2}([Q]) = B_{1/2}([Q] \to 0) + \frac{\hbar}{g\mu_B} k_{ex}[Q] \tag{4.1}$$

- Plot the ln(k_{ex}) values against 1/T and extract the activation energy data from the plot.

4.2.3.2 Experimental Results

We performed the temperature dependent measurements on the systems listed above, and the MARY spectrum at different temperatures for the pertinent systems are shown below. It might be referred here that, as shall be seen in the respective table for the $B_{1/2}$ variation with T(K), the pyrene/1,2 dicyanobenzene and pyrene/1,4 dicyanobenzene are quite insensitive towards any change in temperature. Although work has been done on the concentration dependence of the MARY linewidth values (ref Martin papers) of these systems, the response to temperature changes on this system is far from perceivable and therefore no further analysis of the spectral data has been performed (The spectra obtained and the linewidth values are although shown, see Appendix). The only system

under consideration is the system of TMPPD in Tol/DMSO (60/40 vol), which has some response to temperature variation. The experiment on this system was performed a multiple number of times, and the best data available is reported here. The repetition of the experiments was done to see the reproducibility of the line-width values especially.

At this point it might be worthwhile to write a few words on the limitations on the temperature dependence of the linewidth values in general. As it has been also pointed out earlier, the scope of the experimentalist is limited in performing temperature dependent measurements not only for the choice of systems and solvents, but also due to the temperature window in which one can measure and general difficulty to obtain a sufficient spread in the linewidth data. The fact is that even for concentration dependence of the linewidth data, where one has the option to vary the concentration in a much larger range (usually 2 orders of magnitude) , the changes in the $B_{1/2}$ values from one extreme to the other are in the range of 2-5 G. So in the temperature dependent measurements where one can only vary only between 15-80 degrees, the changes in the linewidth values are evident to be even narrower, with experimental errors adding to the effect. This argument is supported from[52] where the changes in the linewidth values with concentration for the pyrene/dicyanobenzenes are shown below.

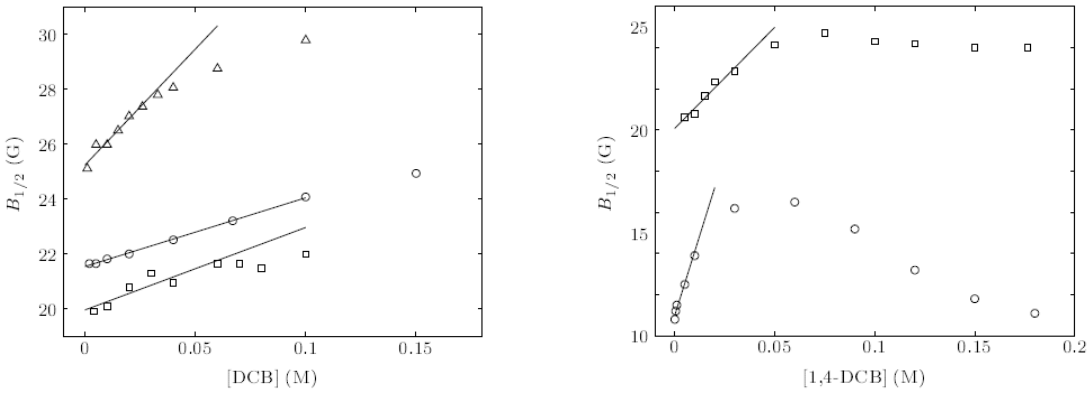

Figure 4.3: $B_{1/2}$ vs. concentration of the quencher plot for pyrene with (right) 1,2 DCB and (left) 1,4 DCB[52].

As is evident from the plots, that the changes of the linewidth with concentration is also not that prominent, with changes as indicated earlier varying between 2-5 G in the linear range. The matter is further complicated by the fact that the change in the linewidth or the $B_{1/2}$ values necessarily need not stay in the linear range. As is known from the self-exchange kinetics, the variation is linear only in the limit of the slow exchange. Under the limit of the fast exchange especially when the quencher concentration becomes high, the linear behavior is no longer found. However in order to extract the activation energies out of Arrhenius-type plot, a linear behavior is necessary. All these factors complicate the effect, and the temperature dependent effect is hard to realize in practice.

The following table gives the results of our measurements.

Table 4-2:Temperature dependent MARY of TMPPD ($6x10^{-3}$ M) in Toluene/DMSO at different temperatures and the associated spectral parameters with modulation amplitude at 5G, modulation frequency at 225 Hz, λ_{obs}=420nm, λ_{ex}=372 nm.

Serial Number	T_{cell} (K)	$1/T_{cell}(K^{-1})$ $x10^{-3}$	ΔB_{pp}(G)	$B_{1/2}$(G)
1	303.1	3.29	57.77	50.0
2	307.5	3.25	58.26	50.5
3	321.2	3.11	58.53	50.5
4	325.2	3.07	59.76	50.75
5	333.2	3.00	59.86	51.85
6	341.7	2.92	59.12	51.2
7	349.8	2.85	60.81	52.7

4.2.3.3 Analysis of the Results

The results above in the table (***) are treated as follows. First, as indicated earlier, plotting the $B_{1/2}$ vs. [Q] values and extrapolating the data to find $B_{1/2}(0)$, the $B_{1/2}$ value at concentration tending to zero. This has been done in the graph below, the extrapolated value being 51.9 G.

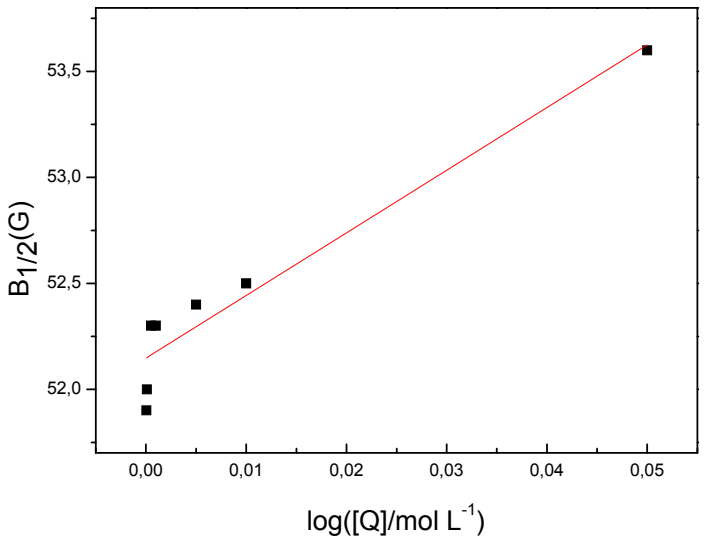

But from this point onwards, the analysis becomes difficult owing to the nature of the system under investigation. The system undergoes photo-ionization and yields a MARY spectrum without any quencher. The solvated electron most probably does the function of the quencher. But, for the given system the value of $B_{1/2}(0)$ is 51.9 G. Using this value to find k_{ex} will give negative values of the rate constant. Henceforth no further analysis has been done and our search is on for other suitable system showing good temperature dependent MARY effect. The spectral data is however shown below. The results for the other system are shown in the appendix.

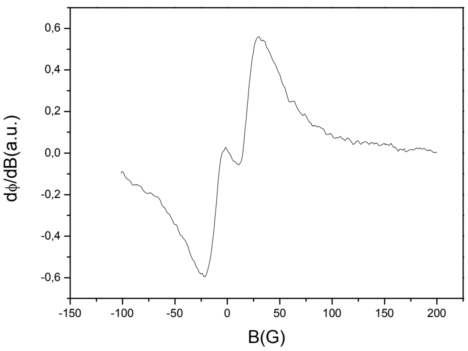
dϕ/dB(a.u.)
B(G)

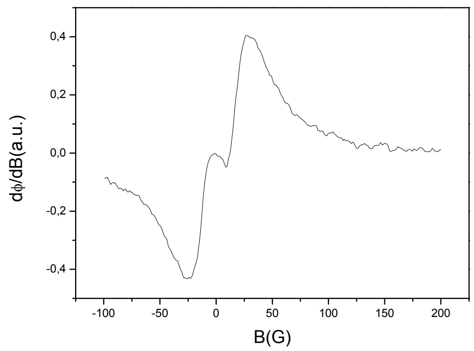
dϕ/dB(a.u.)
B(G)

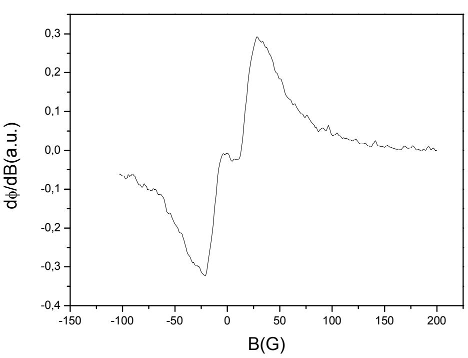
dϕ/dB(a.u.)
B(G)

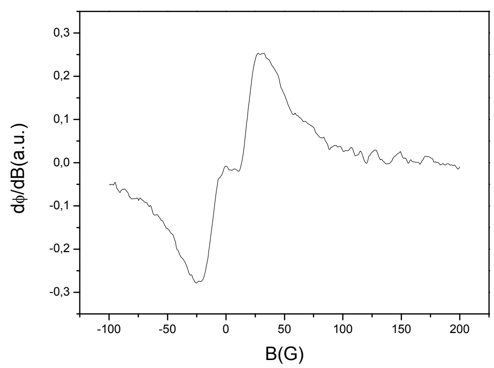
dϕ/dB(a.u.)
B(G)

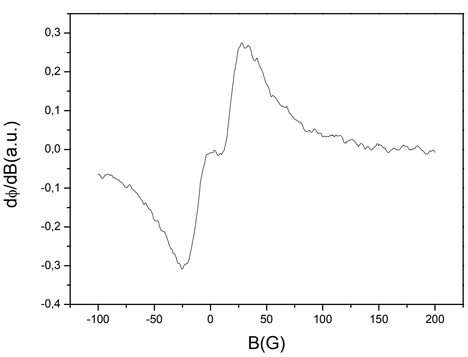
dϕ/dB(a.u.)
B(G)

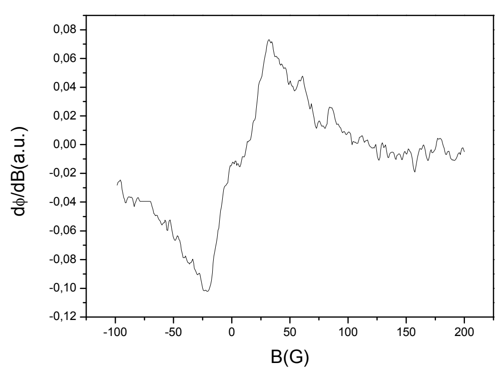
dϕ/dB(a.u.)
B(G)

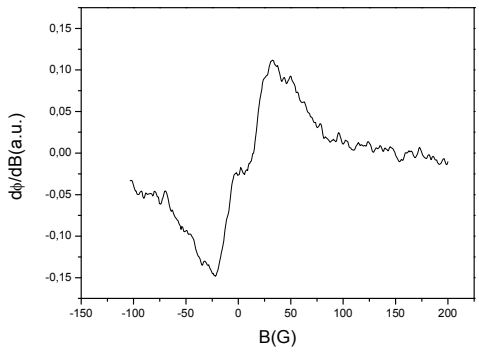

Figure 4.4: MARY spectra of TMPPD ($6x10^{-3}$ M) in Toluene/DMSO at different temperatures

4.3 Solvatochromic Effect in Binary Solvent Mixtures studied by Fluorescence Spectroscopy

Introduction- From this section onwards, we will be discussing the most important part of our Magnetic Field Effect studies. Here we aim at the study of the effect of "preferential solvation", devising four solvent mixtures referred to in the experimental chapter and exclusively on the system of 9,10 dimethylanthracene (DMAnt) as fluorophore and N,N' dimethylaniline (DMA) as quencher. Some studies with the fluorophore mentioned above and the quencher DMDPM (4, 4'-Bis(dimethylamino) diphenylmethane) are also listed, but as they are presently incomplete and not reproduced, discussion on their results is deferred till future studies. As we will be also talking about later, for the first time the MARY spectrum of the DMAnt/DMA system in so many solvent systems have been taken and extensively studied. Past studies (ref) have been done in this area of course, but till date no studies on the effect of the linewidth of the MARY spectrum with varying dielectric constants in different solvent mixtures have been done so far. Our solvents mixtures as referred to earlier are also one of the newest blends to be applied to this end, although some past studies (ref) have utilized these mixtures. Our discussion of the subsequent sections is based on the following plan.

- Investigation of the Solvatochromic data for all the systems
- Tabulation of the linewidth data and the absolute magnetic field effect values as a function of solvent dielectric constant are done for the four solvent pairs.
- Hence forth the justification of the trends in the linewidth and absolute values are attempted in qualitative (and quantitative) terms with respect to different models.

4.3.1 Solvatochromic Effects

Solvatochromism refers to the shift in the emission or absorption bands of the flourophore with the polarity of the solvent. In general the solvatochromism is classified as negative (blue shift of the spectrum with the increasing solvent polarity) and positive (with the spectrum showing red shift with the solvent polarity). The origin of solvatochromic effect is based on the solvent relaxation properties in the excited state and could be explained on the basis of Lippert equation[43].

The main reason to look at the solvatochromic data in the field of magnetic field effect involving binary solvent effect is to find the possibility and initial indications of preferential solvation effect involving binary solvent mixtures. Although we have taken the emission spectrum of all the systems studied at various dielectric constant scans, what interests us in this respect is the differences in solvatochromic data of the various systems studied with respect to neat solvent. We have chosen tetrahydrofuran (THF) as the neat solvent of our reference, and have compared how the solvatochromic properties in the system under study have deviated from the reference system in THF. A positive or negative shift in solvatochromic values at polarity of the binary system comparable to THF is a clear of the differential stabilization of the excited state by the solvent dipoles of the binary system compared to a neat solvent. This information, although does not really lead to some definitive conclusion, is however a nice photochemical bit of information on the system studied. The solvatochromic data in THF is given below.

Position of Peak (1)/nm	Position of Peak (2)/nm	Position of Peak (3)/nm	Position of Peak (4)/nm	Position of Peak (5)/nm (Exciplex)
406.36	426.52	451.5	478.7	--
406.15	426.5	451.81	482.76	501.93

4.3.2 Solvatochromic Effect in Binary Solvent Mixture

The following tables indicate the solvatochromic properties of the 9,10-dimethylanthracene($1x10^{-4}$ M)/N,N'-dimethyaniline ($5x10^{-2}$M) system in different solvents. The solvent is referred to at the top of each table. The entity (F) refer to the emission spectrum of the fluorophore alone and the entity (F+Q) to the emission spectrum of the fluorophore and the quencher. The spectrum is fitted with multiple peaks using a Gaussian function and the peak values are reported. The recorded spectra are shown below

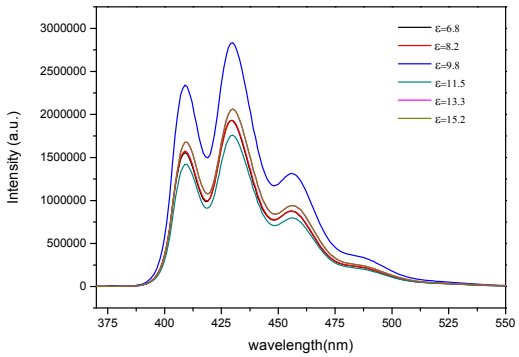

Figure 4.5:Fluorescence Spectra of 9,10 dimethylanthracene ($1x10^{4}$ M) in TOL/DMSO at 'ε_s' values of 6.8, 8.2, 9.8, 11.5, 13.2, 15.2

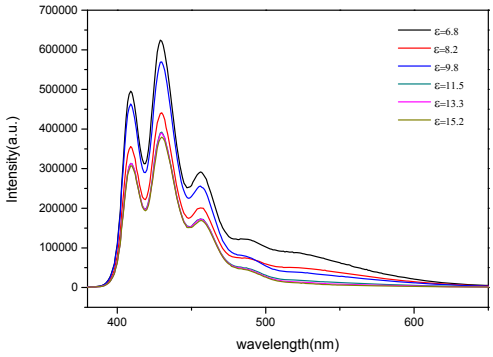

Figure 4.6: Fluorescence Spectra of 9,10 dimethylanthracene ($1x10^{-4}$ M) and N,N'-dimethyaniline ($5x10^{-2}$M) in TOL/DMSO at 'ε_s' values of 6.8, 8.2, 9.8, 11.5, 13.2, 15.2

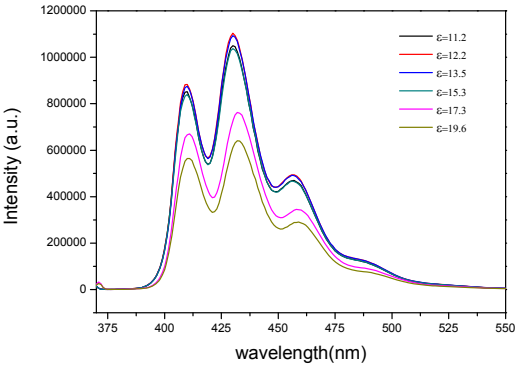

Figure 4.7:Fluorescence Spectra of 9,10 dimethylanthracene ($1x10^{4}$ M) in BA/DMSO at 'ε_s' values of 11.2, 12.2, 13.5, 15.3, 17.3, 19.6

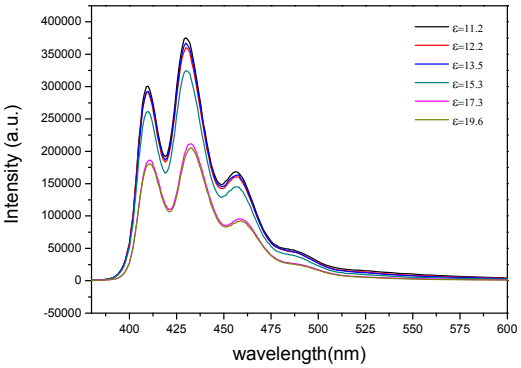

Figure 4.8:Fluorescence Spectra of 9,10 dimethylanthracene ($1x10^{-4}$ M) and N,N'-dimethyaniline ($5x10^{-2}$M) in BA/DMSO at 'ε_s' values of 11.2, 12.2, 13.5, 15.3, 17.3, 19.6

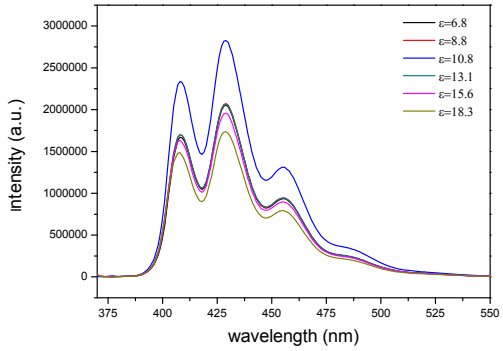

Figure 4.9:Fluorescence Spectra of 9,10 dimethylanthracene ($1x10^{4}$ M) in PC/TOL at 'ε_s' values of 6.8, 8.8, 10.8, 13.1, 15.6, 18.3

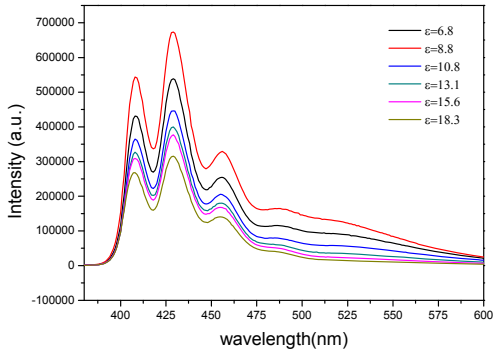

Figure 4.10:Fluorescence Spectra of 9,10 dimethylanthracene ($1x10^{-4}$ M) and N,N'-dimethyaniline ($5x10^{-2}$M) in PC/TOL at 'ε_s' values of 6.8, 8.8, 10.8, 13.1, 15.6, 18.3

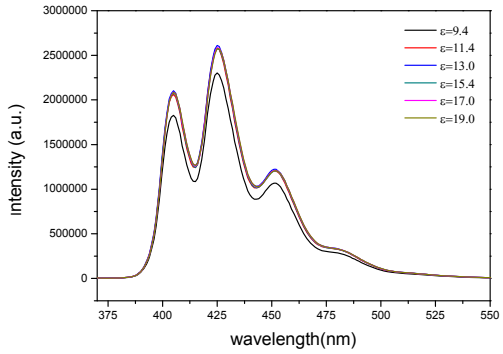

Figure 4.11: Fluorescence Spectra of 9,10 dimethylanthracene ($1x10^{4}$ M) in PA/BN at 'ε_s' values of 9.4, 11.4, 13.0, 15.35, 17.0, 19.0

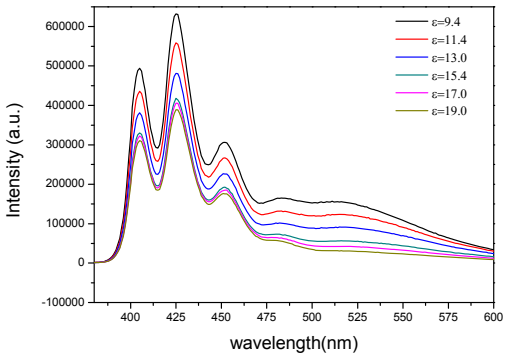

Figure 4.12: Fluorescence Spectra of 9,10 dimethylanthracene ($1x10^{-4}$ M) and N,N'-dimethyaniline ($5x10^{-2}$M) in PA/BN at 'ε_s' values of9.4, 11.4, 13.0, 15.35, 17.0, 19.0

The position of the peak and the exciplex humps are found out using a fitting function, and the values are reported in the upcoming tables. The dielectric constants of the solvent against which the spectra are recorded correspond to the values used for the actual MARY measurements. The order of the tables of the spectral data in different solvents follow the same order in which the spectra are reported.

Table 4-3: Table showing the position of the peaks for the emission spectrum of the fluorophore (marked as 'F' in parenthesis) and the fluorophore and quencher together (marked as 'F+Q' in parenthesis) in Toluene/DMSO binary solvent mixture. The fluorophore is 9,10 dimethylanthracene($1x10^{-4}$ M) and the quencher N,N'-dimethyaniline ($5x10^{-2}$M).

Dielectric Constant of Mixture/Composition	Mole fraction of DMSO	Position of Peak (1)/nm	Position of Peak (2)/nm	Position of Peak (3)/nm	Position of Peak (4)/nm	Position of Peak (5)/nm (Exciplex)
6.8 (F)	0.20	408.82	429.81	454.90	477.26	
6.8 (F+Q)	0.20	408.96	429.76	455.54	486.37	508.614
8.2 (F)	0.25	408.85	429.97	455.08	476.67	
8.2(F+Q)	0.25	408.97	429.89	455.68	486.43	511.33
9.8(F)	0.30	408.82	430.02	455.69	462.47	
9.8 (F+Q)	0.30	408.97	429.94	455.67	486.18	509.73
11.5 (F)	0.35	409.12	430.16	455.34	473.58	
11.5 (F+Q)	0.35	409.25	430.25	455.89	486.75	499.50
13.3(F)	0.40	409.17	430.24	455.89	462.28	
13.3(F+Q)	0.40	409.30	430.17	455.94	486.52	492.22
15.2(F)	0.45	409.24	430.34	456.0	462.46	
15.2(F+Q)	0.45	409.33	430.27	456.07	486.47	485.20

As can be seen from the solvatochromic data, that this system shows a positive solvatochromic shift compared to the system in THF, both at comparable and higher permittivity values.

Table 4-4: Table showing the position of the peaks for the emission spectrum of the fluorophore (marked as 'F' in parenthesis) and the fluorophore and quencher together (marked as 'F+Q' in parenthesis) in Benzylacetate/DMSO binary solvent mixture. The fluorophore is 9,10 dimethylanthracene($1x10^{-4}$ M) and the quencher N,N'-dimethyaniline ($5x10^{-2}$M).

Dielectric Constant of Mixture/Composition	Mole fraction of DMSO	Position of Peak (1)/nm	Position of Peak (2)/nm	Position of Peak (3)/nm	Position of Peak (4)/nm	Position of Peak (5)/nm (Exciplex)
11.2 (F)	0.31	409.42	430.45	456.08	462.09	
11.2 (F+Q)	0.31	409.48	430.39	456.24	462.36	540.64
12.15 (F)	0.35	409.42	430.45	456.08	462.09	
12.15(F+Q)	0.35	409.48	430.49	456.10	468.58	543.45
13.5 (F)	0.39	409.53	430.51	456.12	461.81	
13.5 (F+Q)	0.39	409.56	430.54	456.14	466.85	546.41
15.3 (F)	0.46	409.47	430.63	456.21	462.48	
15.3 (F+Q)	0.46	409.54	430.63	456.17	465.58	---
17.3(F)	0.52	410.63	432.72	458.02	476.68	
17.3(F+Q)	0.52	410.67	432.70	458.25	469.89	---
19.6(F)	0.58	410.58	432.76	458.09	476.13	
19.6(F+Q)	0.58	410.66	432.74	458.23	471.11	---

As can be seen from the solvatochromic data, that this system shows a positive solvatochromic shift compared to the system in THF, both at comparable and higher permittivity values.

Table 4-5: Table showing the position of the peaks for the emission spectrum of the fluorophore (marked as 'F' in parenthesis) and the fluorophore and quencher together (marked as 'F+Q' in parenthesis) in Toluene/Propylenecarbonate binary solvent mixture. The fluorophore is 9,10 dimethylanthracene($1x10^{-4}$ M) and the quencher N,N'-dimethyaniline ($5x10^{-2}$M).

Dielectric Constant of Mixture/Composition	Mole fraction of PC	Position of Peak (1)/nm	Position of Peak (2)/nm	Position of Peak (3)/nm	Position of Peak (4)/nm	Position of Peak (5)/nm (Exciplex)
6.8 (F)	0.125	408.25	429.32	454.32	476.34	
6.8(F+Q)	0.125	408.32	429.21	454.89	485.9	508.61
8.8 (F)	0.175	408.14	429.30	454.30	475.95	
8.8(F+Q)	0.175	408.27	429.25	454.92	486.02	506.05
10.8 (F)	0.225	408.09	429.27	454.39	474.37	
10.8 (F+Q)	0.225	408.28	429.23	454.90	485.74	509.52
13.1 (F)	0.275	408.06	429.25	454.26	475.21	
13.1F+Q)	0.275	408.18	429.18	454.85	485.49	504.87
15.6(F)	0.325	407.87	429.20	454.23	473.71	
15.6(F+Q)	0.325	408.01	429.13	454.78	485.45	499.17
18.3(F)	0.375	407.56	429.14	454.16	474.03	
18.3(F+Q)	0.375	407.69	429.09	454.77	491.30	491.30

As can be seen from the solvatochromic data, that this system shows a positive solvatochromic shift compared to the system in THF, both at comparable and higher permittivity values.

Table 4-6: Table showing the position of the peaks for the emission spectrum of the fluorophore (marked as 'F' in parenthesis) and the fluorophore and quencher together (marked as 'F+Q' in parenthesis) in Propylacetate/Butyronitrile binary solvent mixture. The fluorophore is 9,10-dimethylanthracene($1x10^{-4}$ M) and the quencher N,N'-dimethyaniline ($5x10^{-2}$M).

Dielectric Constant of Mixture/Composition	Weight fraction of BN	Position of Peak (1)/nm	Position of Peak (2)/nm	Position of Peak (3)/nm	Position of Peak (4)/nm	Position of Peak (5) /nm (Exciplex)
9.4 (F)	0.18	404.75	425.52	450.04	475.40	
9.4 (F+Q)	0.18	404.85	425.50	450.60	481.48	509.41
11.4 (F)	0.29	404.78	425.60	450.08	473.60	
11.4 (F+Q)	0.29	404.95	425.56	450.58	481.48	512.04
13.0 (F)	0.375	404.81	425.70	450.20	472.83	
13.0 (F+Q)	0.375	404.93	425.64	450.71	481.47	513.39
15.35 (F)	0.5	404.89	425.79	450.31	473.72	
15.35 (F+Q)	0.5	405.0	425.72	450.87	481.42	513.78
17.0(F)	0.59	404.96	425.85	450.37	473.73	
17.0(F+Q)	0.59	405.09	425.75	450.88	481.56	512.29
19.0(F)	0.70	405.0	425.94	458.49	471.82	
19.0(F+Q)	0.70	405.15	425.84	451.00	481.60	508.95

As can be seen from the solvatochromic data, that this system shows a slight negative solvatochromic shift compared to the system in THF, both at comparable and higher permittivity values.

4.4 Linewidth and Absolute Magnetic Field Effect in Binary Solvent Systems

The topic of the effect of the solvent parameters on the absolute magnetic effect is not new. Much work has been done on the subject by various groups in the world (ref). The principle of the dependence of absolute magnetic effect values on solvent properties, especially the dielectric constant provides a very powerful tool to probe the solvent dynamical properties using magnetic field effect on photo-induced electron transfer phenomenon as a probe method. But what distinguishes our method from the research done so far is the following. First of all the solvent mixture that we have chosen (please refer to section *3.8*) for the purpose provide unique experimental conditions. For example, the solvent propylacetate/butyronitrile allows us to scan the dielectric constant at constant viscosity. Needless to say here that the implicit dependence of the magnetic field effect on both viscosity and dielectric constant calls for solvent blends in which either of the property could be tuned keeping the other constant. To this end the ebove mixture serves this purpose. The mixture of benzylacetate/dimethylsulfoxide also serves a similar purpose, except that the overall viscosity of this mixture is higher than the former. The other two mixtures employed by us, although not serving the purpose of performing a dielectric constant scan at constant viscosity, but on the other hand provides perfect heterogeneous medium with viscosities which are in the "low-limit" as to facilitate smooth magnetic field dependent phenomenon and also at the same time the overall viscosities not changing much with the composition of the mixture. But the most important feature of our work lies in studying the solvent mixture composition (with varying dielectric constant) dependence of the linewidth or alternatively $B_{1/2}$ parameter of the MARY spectrum, which in our knowledge has not been undertaken yet.

4.4.1 The system of 9,10 dimethylanthracene/ N,N'-dimethylaniniline in Toluene/DMSO

The system gives a good spectrum with high S/N ratio across the whole range of dielectric constant scan performed. (The actual spectra are shown later). The modulation amplitude applied was 8G and the modulation frequency was kept fixed at 230 Hz. The scan was performed from -70 G to 420 G, where the saturation values of the magnetic field effect is reached. The concentration of the fluorophore 9,10 dimethylanthracene was maintained at $1x10^{-4}$ M and the quencher N,N'-dimethyaniline at $5x10^{-2}$M. The temperature of the system was fixed at 25^0C. In the following table the obtained $B_{1/2}$ values and the absolute magnetic field effect values using the process described in section *3.4.2* and *3.4.3*) are reported. In should be noted that both the linewidth data and the absolute magnetic field effect values are reported as an average of at least three scans with usually very little spread in the values. The errors in the experiment are indiacted through error bars in the relevant plots. The same set of conditions apply for the other systems to be discussed subsequently as well, and therefore will not be referred to anymore unless there is any exception.

Table 4-7: Tabulation of the MARY measurements on the 9,10 dimethylanthracene/N,N'-dimethyaniline system in Toluene/DMSO binary solvent mixture with dielectric constants described by the parametric equation $\varepsilon_{mix} = 62.5\exp\left(-x_{TOL}/0.78\right) - 15.6$. The trends in the $B_{1/2}(G)$ values and the absolute field effect are given as a function of the dielectric constant of the solvent mixture.

Sl.No.	Dielectric Constant of Mixture	Mole fraction of DMSO	$B_{1/2}(G)$	Magnetic Field Effect (%age)
1	6.8	0.20	69.9	1.37
2	8.2	0.25	65.2	6.07
3	9.8	0.30	63.3	9.15
4	11.5	0.35	61.3	7.93
5	13.3	0.40	59.8	7.38
6	15.2	0.45	58.9	5.76

The salient features of the dielectric constant dependence of magnetic filed effect phenomenon in Toluene/DMSO as the solvent are as follows:

- As one can see, the onset of the magnetic field effect phenomenon takes off when the mole fraction of the polar component is even lower than 0.20. This observation is quite significant as compared to the other systems. The onset value of the bulk dielectric constant in producing perceivable magnetic field values is an important marker in showing the possible effect of preferential solvation and related concentration fluctuation effect on the fluorescence detected magnetic field effect phenomenon. The rule of thumb might be stated as, lower is the value of the mole-fraction of the polar component in inducing magnetic field effect values, more probable are the effects of binary solvent effects on the fluorescence detected magnetic field effect values. In this context, it is also worthwhile to look at the values of the bulk dielectric constant as well, from wherein the field effects are more or less starting. Any value around 1% is taken as a standard reference value for the onset of the magnetic field effects, given the fact, that in the system studied the signal to noise ratio permits only effects more that 1% to be studied conveniently without much error and that the highest values of the magnetic field effects can reach upto 10% in certain systems (as will be seen later). So yet

another rule of thumb could be formulated regarding the onset value with respect to bulk dielectric constant as, lower is the value of the bulk dielectric constant, from where magnetic field effects take off, more probable is the effect of binary solvent effects on the fluorescence detected magnetic field effect values. This rule of thumb is however only a corollary of the rule stated before regarding the onset value with respect to. mole-fraction in giving magnetic field effect, given the fact that the bulk dielectric constants are sole functions of the mole-fraction of the components at a give temperature. However for the purpose of better understanding of the system, the rule has been stated. But in a qualitative way, we can of course justify the relevance of the rules stated above as follows. Going by the mechanism and the effect of the solvent on the of the magnetic field effect phenomenon as discussed in theoretical section, the magnetic field effect does not operate at very low values of the dielectric constant (where the diffusional excursion of the incipient RIP is impeded by strong coloumbic interaction) and neither at very high values of the dielectric constant (where the escape of correlated RIP's from the geminate cage is dominant over the recombination process) but rather in a dielectric window of around 10-20. So any phenomenon which can bring down the lower limit of the window, must have somewhat affected the diffusional dynamics of the RIP-evolution and imposed spatial restrictions on the RIP such that the lower limit of the window has been brought down and this value deserves a further look. In all probability, this apparent "quenching" in the onset values of the bulk dielectric constant fingers at the involvement of concentration fluctuation effects in magnetic field effect phenomenon. But is it really so?

- The other important trends in the table which deserves a closer look as far as absolute magnetic field effects are concerned is the fashion of the transition in the values of the absolute field effect from one end of the dielectric constant scan to the other, the position of the maxima in the plot (both in the effect vs. dielectric constant and also effect vs. mole fraction of the polar component plot) and the trends of saturation. As can be seen in the table and the plot (fig ….) , the

maximum in the absolute field effect values reaches a maximum value of 9.15% at dielectric constant values of around 10 and molefraction of DMSO (polar component) at around 0.30. Hereafter with further increase in the DMSO content of the mixture, the field effect falls off slowly to around 5.8% at $\varepsilon_s = 15.2, x_{DMSO} = 0.45$. The data has not been further recorded, but the values are obvious to fall off slowly to lower values with increasing mole fraction of DMSO. But the most interesting feature in the trend of the absolute field effect values with increasing DMSO concentration is the sudden jump in the values from 1.4% to 6.1% from going to 0.05 notches jump in the molefraction of DMSO in the mixture. The DMSO molefraction have been systematically varied in steps of 0.05, but no where else in the region has the field effect had taken such sharp jump on going from one step to the next. This feature probably deserves better look and will be taken up later.

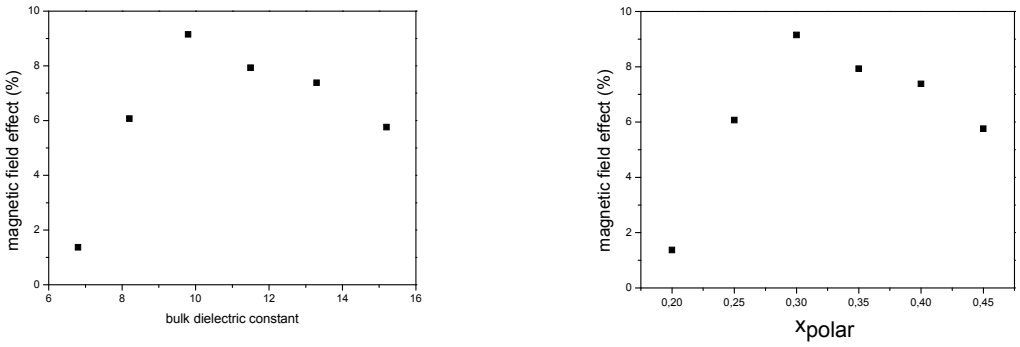

Figure 4.13: Plots of magnetic field effect (%) vs. bulk dielectric constant of solvent mixture (left) and magnetic field effect (%) vs. x_{polar} (the molefraction of the polar component)on right in TOL/DMSO

- The next important trend, which in our knowledge has not been studied before (and therefore might be difficult to understand), is the trend in the $B_{1/2}$ values. No previous studies on the variation of the $B_{1/2}$ values and linewidth values with dielectric constant scan have been studied so far, and this work tries to rationalize this dependence on quantitative and qualitative ways. MARY spectroscopy of

course has been used as a tool. The parameter $B_{1/2}$ is the field, at which there is half saturation of the magnetic field effect. This quantity is characteristic for a particular system showing magnetic field dependent behavior, and differs among various systems. However the variation of this property within a particular system with changes in the external factors which perturb magnetic field effect value, especially the solvent dynamical factors like the dielectric constant and the viscosity signals some physico-chemical effect brought in by the perturbing factors. In particular, if any spatial restriction in the RIP dynamics is imposed by the perturbing factors, which in turn can modify the interplay of diffusion and spin dynamics of the RIP, the $B_{1/2}$ values are certain to show a concomitant change. In general, however not much dependence of the $B_{1/2}$ values with solvent dynamical properties have been reported in literature, but in the systems we have studied, with some solvent mixtures an unprecedented magnitude of change in the $B_{1/2}$ values has been found on scanning the dielectric constant values across a certain range. In this system of TOL/DMSO, the $B_{1/2}$ shows a major change across a dielectric constant scan from 6.8-15.2. The overall change in the $B_{1/2}$ value is more than 11 G, in a rather decreasing fashion, starting from about 70 G to 59 G. It could have probably decreased further on further increase of dielectric constant of the mixture, but the S/N ratio of the spectrum does not practically allow further scans with higher dielectric constant values. But one thing is worth noting in the trend of the change in the $B_{1/2}$ values is that, after the onset of the field effect, the values decreases suddenly by 5 G (with only an increase of 0.05 notches in the mole fraction of DMSO), and with further increase of the polarity of the mixture, the change takes in a gradual fashion to further lower values. This big leap after the onset in the $B_{1/2}$ values also corresponds to the region where the absolute field effect takes a sharp upward turn. (For the trends in $B_{1/2}$ changes with the dielectric constant and the molefraction of the polar component (x_{polar}) please see figure *4.21*)

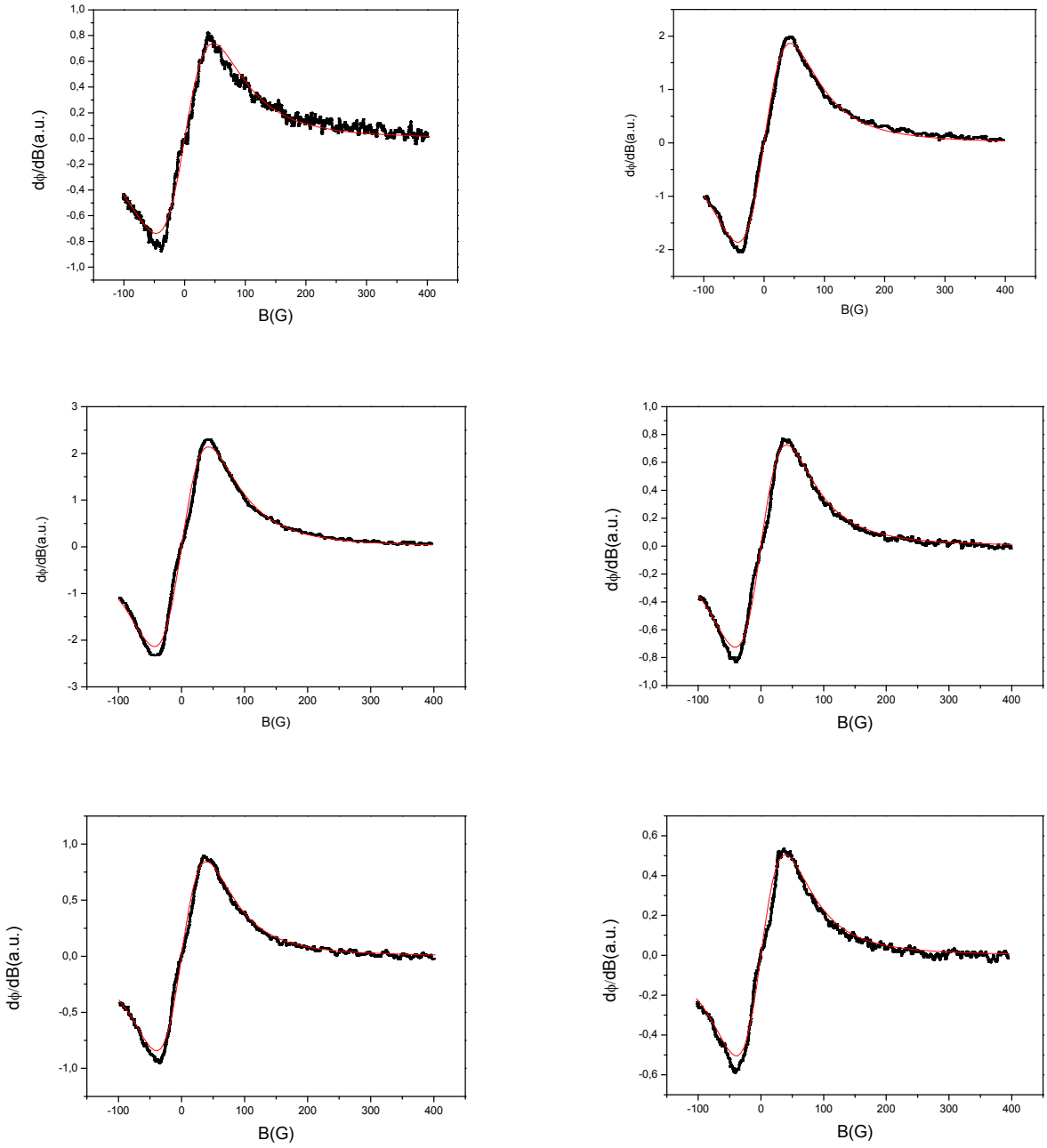

Figure 4.14: Experimental MARY spectra of 9,10 dimethylanthracene ($1x10^{-4}$M)/ DMA ($5x10^{-2}$M) in Toluene/DMSO and corresponding simulations with Lorentzian derivative fit (the smooth lines). The bulk dielectric constant of the mixture and the mole fraction of the polar component increase from top to bottom. Left, from top to bottom: $\varepsilon_{s,mix}$=6.8, 9.8, 13.3; x_{polar}=0.2, 0.3, 0,4; Right, from top to bottom: $\varepsilon_{s,mix}$=8.2, 11.5, 15.2; x_{polar} = 0.25, 0.35, 0.45. Modulation Amplitude= 8G, Modulation frequency= 230 Hz, Temp= 25^0C.

4.4.2 The system of 9,10 dimethylanthracene/ N,N'-dimethylaniniline in Benzylacetate/DMSO

Table 4-8: Tabulation of the MARY measurements on the 9,10 dimethylanthracene/N,N'-dimethyaniline system in Benzylacetate(BA)/DMSO binary solvent mixture with dielectric constants described by the parametric equation $\varepsilon_s\left(x_{DMSO}\right)=5.82\exp\left(x_{DMSO}/0.479\right)+0.067$. The trends in the $B_{1/2}\left(G\right)$ values and the absolute field effect are given as a function of the dielectric constant of the solvent mixture.

Sl.No.	Dielectric Constant of Mixture	Mole fraction of DMSO	$B_{1/2}\left(G\right)$	Magnetic Field Effect (%age)
1	11.2	0.31	62.8	1.25
2	12.15	0.35	62.76	2.14
3	13.5	0.40	61.32	1.96
4	15.3	0.46	58.91	2.51
5	17.3	0.52	57.73	1.64

The salient features of the dielectric constant dependence of magnetic filed effect phenomenon in BA/DMSO as the solvent are as follows. It is worthwhile to notice that the viscosity of both the solvents are quite high and so are the possible of preferential solvation (as is evident from the solvatochromic data). In this light, the features of the system will be discussed.

- Although solvatochromic data point at high chances of preferential salvation and concentration fluctuation effects, the onset of the magnetic field effect phenomenon requires comparatively higher values of both the molefraction of the

polar component and the bulk dielectric constant of the mixture. While the value of the molefraction of the polar component required to induce magnetic field effect is around 0.30 , the value of the bulk dielectric constant where this happens is 11.2. Both these values are much higher compared to the Toluene/DMSO system, although chances of preferential solvation is not diminished in this mixture as well (the value of the bulk dielectric constant of BA is 5.7, while that of TOL is 2.4; the other component in the mixture is same for both), the issues of higher viscosity of the mixture has to be taken into account. But at the same time it is also surprising enough, that this mixture, inspite of its high viscosity produces magnetic field after all, because many pure solvents with lower viscosity (like various alcohols) and comparable dielectric constants do not give any perceivable magnetic field effect. This might indicate the fact binary solvent effect could in fact dominate the impeding effects of high viscosity of the solvent. But this aspect needs a closer and detailed look, and any conclusion at this stage might be premature.

- The other important features (similar to the system above) which we discern from the table about the magnetosensitive behavior of the system are with respect to the fashion of the transition absolute field effect values from one end of the dielectric constant scan to the other, the position of the maxima in the plot (both in the effect vs. dielectric constant and also effect vs. mole fraction of the polar component plot) and the trends of saturation. The trends in the aforementioned categories are by far much different from the system of Toluene/DMSO. The field effect values do not show prominent maxima, although the dielectric constant values are increasing in that direction. It is more or less a constant curve, with possibly a hump at $\varepsilon_s = 15.3, x_{DMSO} = 0.46$. But by far there is not any satisfactory conclusion about the transition trend (more or less flat), the position of maxima referred to above possibly needs to be reconsidered. The trends in the saturation are also not clear.

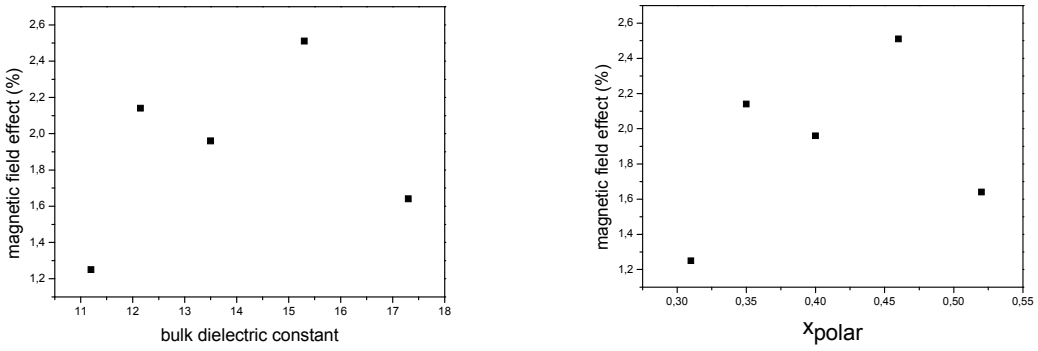

Figure 4.15: Plots of magnetic field effect (%) vs. bulk dielectric constant of solvent mixture (left) and magnetic field effect (%) vs. x_{polar} (the molefraction of the polar component) on right in BA/DMSO

- The trends in $B_{1/2}$ values in this system are as follows. The maximum value of this parameter reached in this system is only 62.8 G, unlike the system of TOL/DMSO or PC/TOL where higher values of this parameter is reached. This is a bit surprising on the basis of the chances of preferential salvation (also detected from solvatochromic shifts) which are quite also for this mixture as well. However, it should be remembered that this solvent is highly viscous, compared to the other solvent. Whether the viscosity of the mixture has any prominent role in the $B_{1/2}$ values need to be seen in detail. Also, the overall shift in the $B_{1/2}$ values from going from one end of the dielectric constant scan to the other is only about 5 G, that too also brought about in a gradual manner across the scan. (For the trends in $B_{1/2}$ changes with the dielectric constant and the molefraction of the polar component (x_{polar}) please see figure *4.21*)

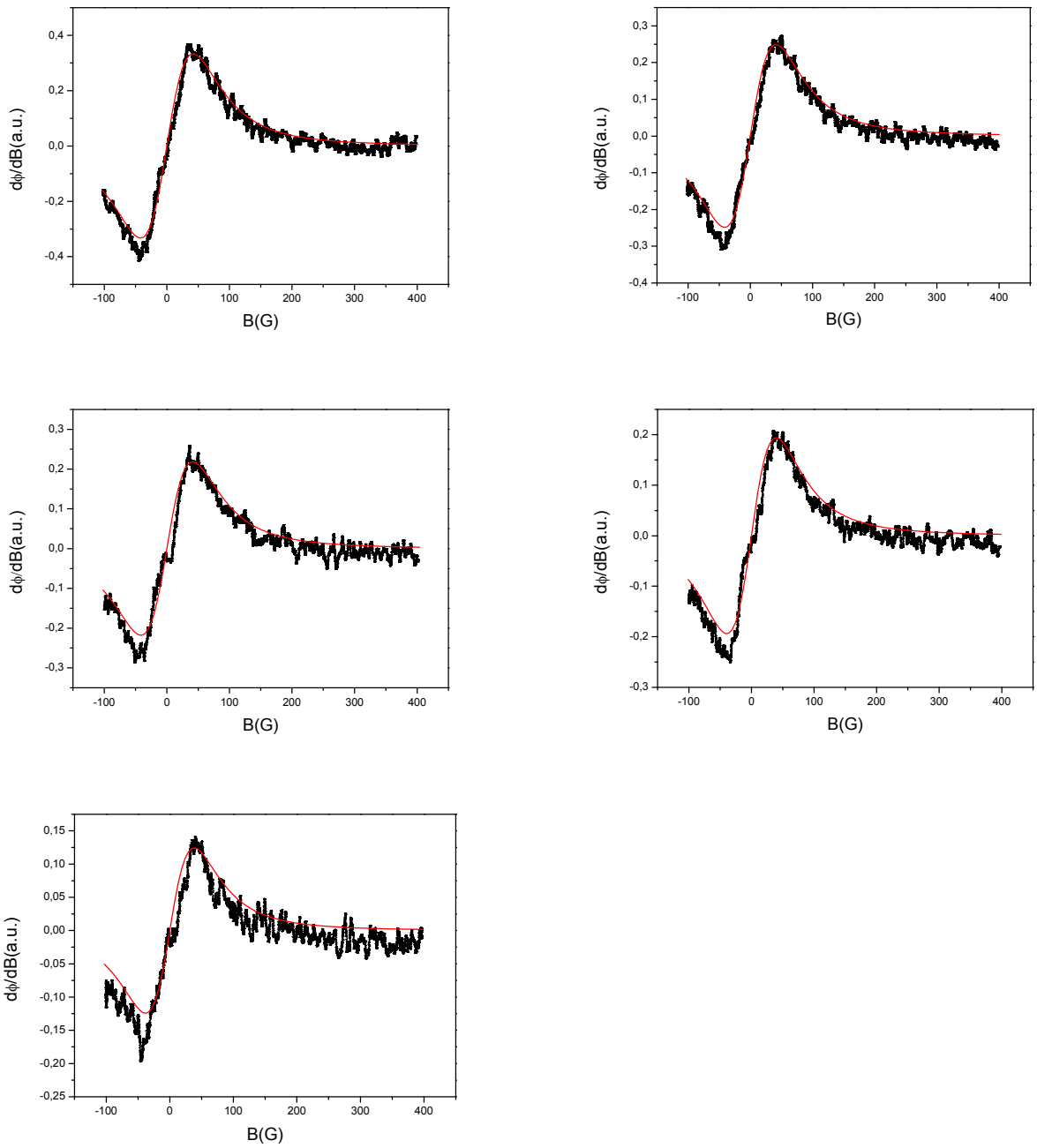

Figure 4.16:Experimental MARY spectra of 9,10-dimethylanthracene ($1x10^{-4}$M)/ DMA ($5x10^{-2}$M) in BA/DMSO and corresponding simulations with Lorentzian derivative fit (the smooth lines). The bulk dielectric constant of the mixture and the mole fraction of the polar component increase from top to bottom. Left, from top to bottom: $\varepsilon_{s,mix}$=11.2, 13.5, 17.3; x_{polar}=0.31, 0.4, 0,52; Right, from top to bottom: $\varepsilon_{s,mix}$=12.715, 15.3; x_{polar} = 0.35, 0.46. Modulation Amplitude= 8G, Modulation frequency= 230 Hz, Temp= 25^0C.

4.4.3 The system of 9,10 dimethylanthracene/ N,N'-dimethylaniniline in Propylenecarbonate/Toluene

Table 4-9: Tabulation of the MARY measurements on the 9,10-dimethylanthracene/N,N'-dimethylaniline system in Propylenecarbonate(PC)/Toluene(TOL) binary solvent mixture with dielectric constants described by the parametric equation $\varepsilon_{s,mix} = 95.3\exp(-1.64x_{TOL}) - 15.9$. The trends in the $B_{1/2}(G)$ values and the absolute field effect are given as a function of the dielectric constant of the solvent mixture.

Sl.No.	Dielectric Constant of Mixture	Mole fraction of PC	$B_{1/2}(G)$	Magnetic Field Effect (%age)
1	6.8	0.125	70.55	1.14
2	8.75	0.175	65.21	4.47
3	10.85	0.225	63.21	8.95
4	13.1	0.275	62.73	9.75
5	15.6	0.325	61.9	8.75
6	18.3	0.375	59.23	7.19

The salient features of the dielectric constant dependence of magnetic filed effect phenomenon in PC/TOL as the solvent are as follows. Here it might be told that the past studies on binary solvent effect using magnetic field dependent fluorescent phenomenon has invariably included Benzene/DMSO as one the blends. While at present we have substituted benzene with toluene for its carcinogenic effects, the mixture of Toluene/DMSO is by means no different from the former. However special observations were made in the past (ref) about the Benzene/DMSO systems with respect to binary solvent effects. To this end its was desirable to devise a solvent like TOL/DMSO, similar in other macroscopic properties and most importantly whose components are very widely separated with respect to the bulk dielectric constant values so that the magnetic field

effect phenomenon in this mixture could be compared vis-à-vis TOL/DMSO. The reader is referred to table *3.1*, where the macroscopic properties of the solvents used are appended, and one can easily notice that being more or less similar to DMSO in other respects, it provides even higher difference in bulk dielectric constant to the non-polar component compared to DMSO. So the effects of preferential salvation are expected to be similar to that in TOL/DMSO. It might also be referred at this point that this very mixture has never been employed in the past to do studies related to photochemistry. Now coming to the features of the system:

- The onset of the magnetic field effect phenomenon start at a very early value of the bulk dielectric constant of the mixture at 6.8 or even before. But when one looks at the value of the mole fraction of the polar component when the magnetic field effect start, for this mixture this is only 0.125. This is the lowest value of the mole fraction of the polar component where the magnetic field effect start among the four solvent pairs being employed. This value even surpasses the one for the TOL/DMSO pair, and evidently this solvent mixture might be referred to as the "most heterogeneous" among all the solvent mixture from the view point that its components are most widely separated in their bulk dielectric constant values. Does this therefore confirm the common notion of the concentration fluctuations on magnetic field effects? Well this requires closer look.

- Yet coming to our second point, the characteristics of the transition of absolute field effect values from one end of the dielectric constant scan to the other, the position of the maxima in the plot (both in the effect vs. dielectric constant and also effect vs. mole fraction of the polar component plot) and the trends of saturation, we see the following. The magnetic effect increases rapidly with increasing dielectric constant of the mixture until the maxima is reached at around 10%. This value of the absolute field effect is highest to be achieved among the four systems studied. The corresponding values of the dielectric constant and the molefraction of the polar component where this maxima is reached are 13.1 and 0.275 respectively. The following plot of the data shows these figures.

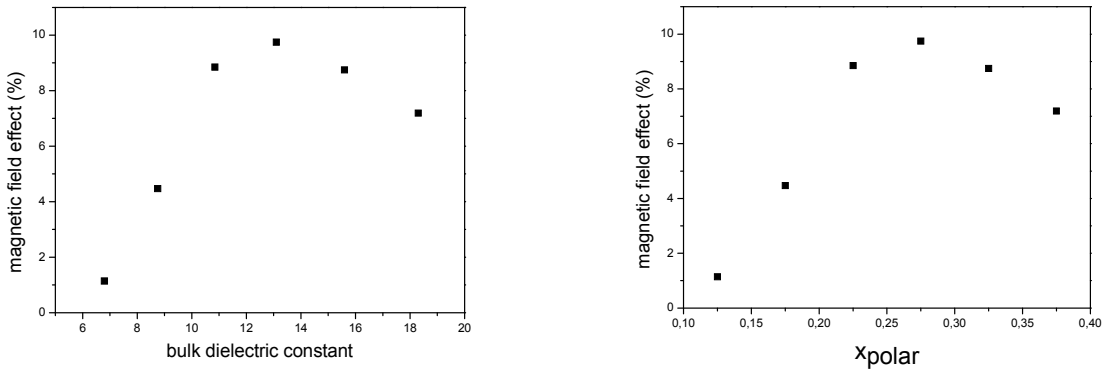

Figure 4.17: Plots of magnetic field effect (%) vs. bulk dielectric constant of solvent mixture (left) and magnetic field effect (%) vs. x_{polar} (the molefraction of the polar component) on right in PC/TOL

- This system, like the TOL/DMSO also registers a large change in the $B_{1/2}$ values from one end to the other end of the dielectric constant scan. It starts as 70.5 G , decreases sharply to 65.2 G with 0.05 notches change in the molefraction of DMSO, and further plunges gradually to 59.2 G. A more than 11 G of change in detected. This system also registers the highest value of $B_{1/2}$, corresponding to the onset of magnetic field effects. (For the trends in $B_{1/2}$ changes with the dielectric constant and the molefraction of the polar component (x_{polar}) please see figure *4.21*)

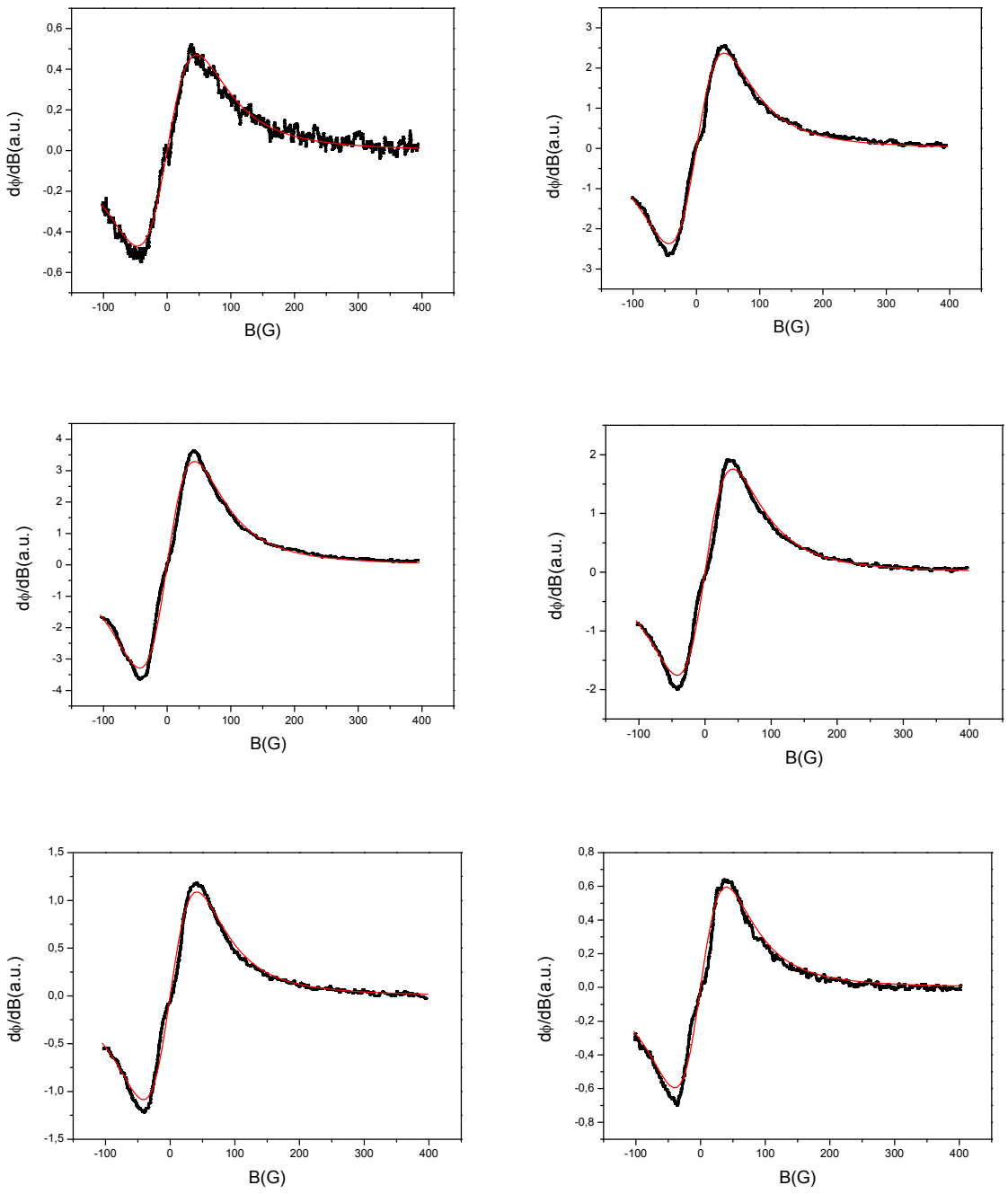

Figure 4.18: Experimental MARY spectra of 9,10 dimethylanthracene ($1x10^{-4}$M)/ DMA ($5x10^{-2}$M) in PC/TOL and corresponding simulations with Lorentzian derivative fit (the smooth lines). The bulk dielectric constant of the mixture and the mole fraction of the polar component increase from top to bottom. Left, from top to bottom: $\varepsilon_{s,mix}$=6.8, 10.85, 15.6; x_{polar}=0.12, 0.225, 0,325; Right, from top to bottom: $\varepsilon_{s,mix}$=8.75, 13.1, 18.3; x_{polar} = 0.175, 0.275, 0.375. Modulation Amplitude= 8G, Modulation frequency= 230 Hz,Temp= 25^0C.

4.4.4 The system of 9,10 dimethylanthracene/ N,N'-dimethylaniniline in Propylacetate/Butyronitrile

Table 4-10: Tabulation of the MARY measurements on the 9,10 dimethylanthracene/N,N'-dimethylaniline system in Propylacetate/Butyronitrile binary solvent mixture with dielectric constants described by the parametric equation $\varepsilon_s(w_1) = w_1\varepsilon_1 + (1-w_1)\varepsilon_2$. The trends in the $B_{1/2}(G)$ values and the absolute field effect are given as a function of the dielectric constant of the solvent mixture.

Sl.No.	Dielectric Constant of Mixture	Mole fraction of BN	$B_{1/2}(G)$	Magnetic Field Effect (%age)
1	9.4	0.24	62.02	<1
2	11.4	0.37	63.63	2.48
3	13.0	0.46	63.10	5.33
4	15.35	0.59	63.54	7.22
5	17.0	0.68	63.55	7.88
6	19.1	0.77	63.75	7.72

From the fit of the equation $\varepsilon_s(w_1) = w_1\varepsilon_1 + (1-w_1)\varepsilon_2$, which parameterizes the dielectric constant of the mixture, one can understand the specialty of the mixture employed. This is a quasi-perfect mixture in the sense that it stands as a "foil" to the other mixture employed and allows us to contrast directly the results from the other mixture that we have employed. This mixture which is composed from two components having equal viscosity and refractive index, is like a pure solvent, although still with the provision of varying the dielectric constant owing to the difference in bulk permittivity values of the

components (the difference is not no large as the other mixtures although), but at the same time behaving like a homogenous system. The results obtained in this mixture are also different in all ways, and contrasted with the other system surely point to multiple number of phenomenon in play that might possibly contribute to those effect. The salient features of this system are:

- The onset of the magnetic field effect phenomenon occurs at relatively higher value of the dielectric constant of the mixture (around 10 where the value of field effect is around 1%), and also at relatively higher values of the molefraction of the polar component (at around 0.24 by the molefraction of butyronitrile). All these values are higher compared to the other system.

- Coming to next point, the characteristics of the transition of absolute field effect values from one end of the dielectric constant scan to the other, the position of the maxima in the plot (both in the effect vs. dielectric constant and also effect vs. mole fraction of the polar component plot) and the trends of saturation, we see the following. The absolute magnetic field effect values rise slowly and reach a maximum of 7.9% with corresponding values of the dielectric constant and the molefraction of the polar component at maxima being 17.0 and 0.68 respectively. It might be surprising to note the value of the molefraction of the polar component where this maxima is reached, compared to the other systems where he maxima is reached at much lower values of this parameter. A very "relaxed" tendency of the solvent blend is noted in sustaining higher values absolute field effect even at higher values of the x_{polar}. The trend in the values of the field effect after the maxima is reached also apparently takes a gentle downturn, with x_{polar} values of 0.77 still sustaining field effect of 7.7%, only slightly lesser than the maximum. It seems quite obvious that perceivable magnetic field effects will still remain with $x_{polar} \to 1$, contrary to the other systems where the field effect values fall of much rapidly with x_{polar} values after the maxima is reached. The following plot of the data shows these figures.

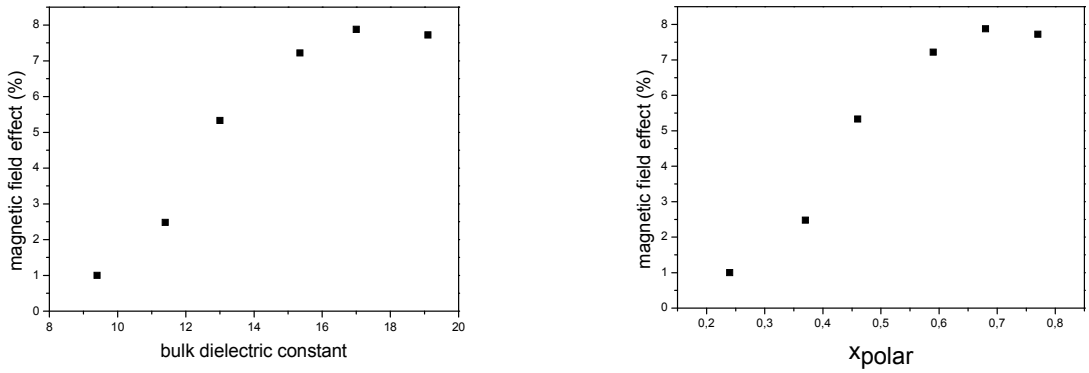

Figure 4.19: Plots of magnetic field effect (%) vs. bulk dielectric constant of solvent mixture (left) and magnetic field effect (%) vs. x_{polar} (the molefraction of the polar component) on right in PA/BN solvent mixture

- The trends in the $B_{1/2}$ values of this system, which involves a solvent mixture which behaves almost like an ideal mixture, are worth noting. Expected to show different behavior than the other systems, the system lives upto that. After the initial onset value at roughly 62 G, the $B_{1/2}$ values, unlike other systems *increases* slightly on increase of 0.13 notches in the molefraction of the polar component. Thereafter the $B_{1/2}$ values remains almost constant around 63.5 G (mean value) with further increase in the dielectric constant of the mixture. The absolute magnetic field effect values, however donot remain constant and changes accordingly with the polarity of the mixture, but the $B_{1/2}$ values stagnates for this system. The initial increase is also a strange observation. (For the trends in $B_{1/2}$ changes with the dielectric constant and the molefraction of the polar component (x_{polar}) please see figure *4.21*)

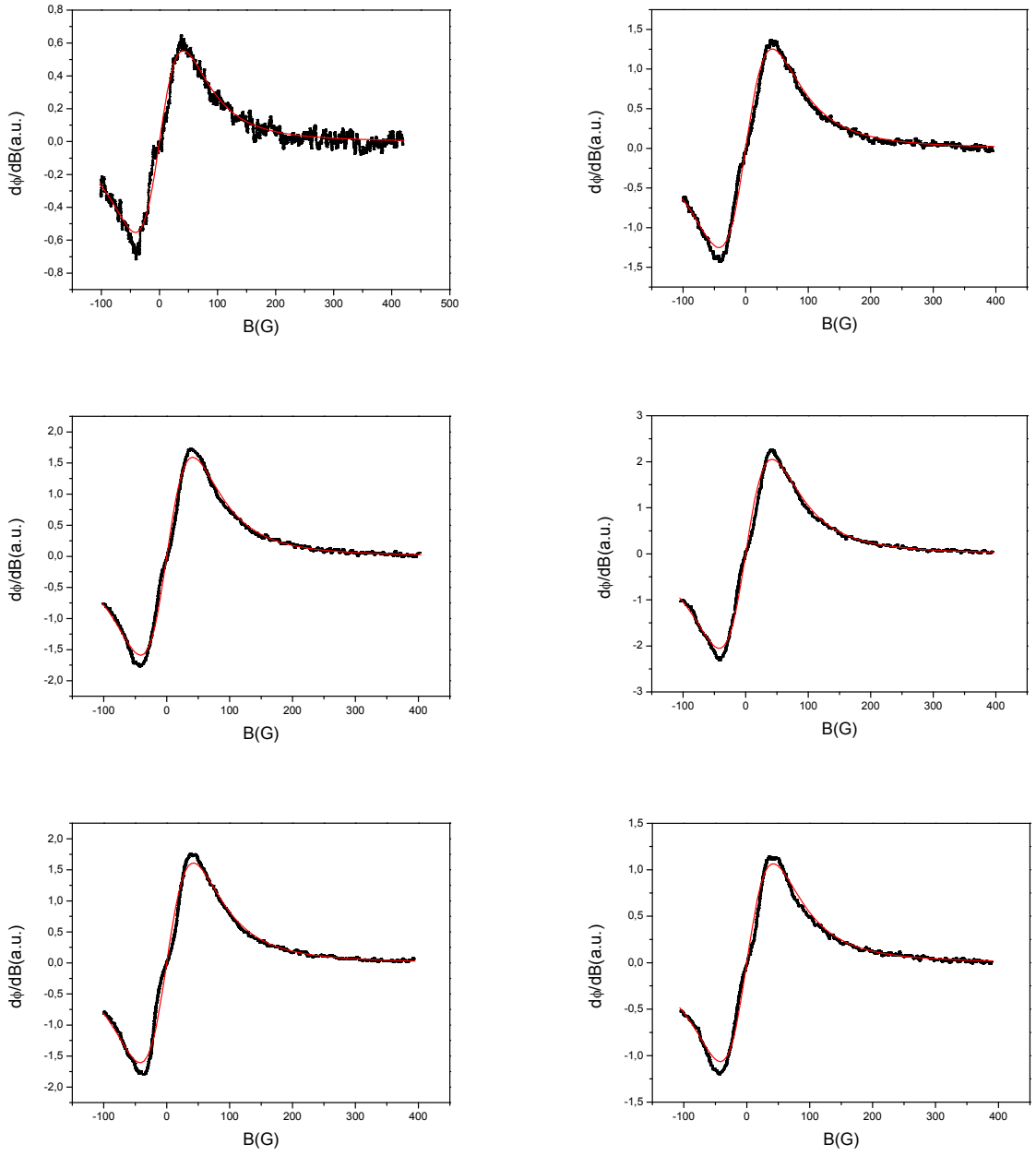

Figure 4.20: Experimental MARY spectra of 9,10 dimethylanthracene ($1x10^{-4}$M)/ DMA ($5x10^{-2}$M) in PA/BN and corresponding simulations with Lorentzian derivative fit (the smooth lines). The bulk dielectric constant of the mixture and the mole fraction of the polar component increase from top to bottom. Left, from top to bottom: $\varepsilon_{s,mix}$=9.4, 13.0, 17.0; x_{polar}=0.24, 0.46, 0,68; Right, from top to bottom: $\varepsilon_{s,mix}$=11.4, 15.35, 19.1; x_{polar} = 0.37, 0.59, 0.77. Modulation Amplitude= 8G, Modulation frequency= 230 Hz, Temp= 25^0C.

4.4.5 Qualitative Explanation of the Magnetic Field Effect values

Before attempting any possible explanation of the trends in the magnetic field effect parameters, let us first make a vis-à-vis comparison of all the four system under consideration. The following table compiling the trends in the plots is done with respect to all the systems under consideration.

Table 4-11: Trends in Magnetic Field Affected Parameters in all Systems

Property /System	$\varepsilon_{s,onset}$	x_{onset}	$\varepsilon_{s,\max}$	$x_{\max}$	$B_{1/2}^{\max}$ (G)	$\Delta B_{1/2}$	$\chi_{\max}$ (%)
DMAnt /DMA in TOL/DMSO	6.8	0.2	9.8	0.30	69.9	11	9.15
DMAnt /DMA in TOL/PC	6.8	0.125	13.1	0.275	70.6	11	9.75
DMAnt /DMA in BA/DMSO	11.2	0.31	--	--	62.8	5	--
DMAnt /DMA in PA/BN	9.4	0.24	17.0	0.68	63.7	1.7	7.9

$\varepsilon_{s,onset}$ =Dielectric constant value marking onset of field effect , x_{onset} =Mole fraction of polar component value marking onset of field effect, $\varepsilon_{s,\max}$ =Dielectric constant value marking maximum field effect, $x_{\max}$ = Mole fraction of polar component marking maximum of field effect, $B_{1/2}^{\max}$ =Highest $B_{1/2}$ value obtained (G), $\Delta B_{1/2}$ =Change in $B_{1/2}$ values across the dielectric constant scan (G), $\chi_{\max}$ =Maximum Value of field effect (%)

The discussion of the above table is done in the following line of argument:

- **The $\varepsilon_{s,onset}$ and x_{onset} values**: As told earlier, the $\varepsilon_{s,onset}$ value are the preliminary signs of preferential salvation effects, lower the value of this higher are the chances of preferential salvation effects perturbing the MFE phenomenon. In this respect, the system of TOL/DMSO and PC/TOL shows the lowest value of $\varepsilon_{s,onset}$. This could be taken as an indirect indication of the preferential salvation effects on MFE, an effect which is lesser in quasi-homogenous solvent mixture like PA/BN (the $\varepsilon_{s,onset}$ value in this mixture being 9.4). It is difficult to comment on the BA/DMSO mixture, that why in spite of high chances of preferential salvation, the $\varepsilon_{s,onset}$ value is still pegged at 11.2, even higher than PA/BN mixture. The apparent effect of high viscosity is still to be confirmed. Further confirmation of this effect is seen in the x_{onset} values among the four mixtures, the lowest being the one in PC/TOL at 0.125 molefraction of PC. In contrast, for the PA/BN quasi-homogenous mixture, the value of this parameter is twice as much for the onset to take place.

- **The $\varepsilon_{s,\max}$ and $x_{\max}$ values**: "Cage effect", as described in the theoretical section and geminate recombination effects are the controlling factors in deciding the extent (or magnitude) of the absolute field effect. For example in systems where the bulk dissociation could be fully eliminated by using systems in which the magnetic field effect is taking place from a intramolecular chain-linked species (ref) or in micellar medium (ref) where the geminate recombination could also be manifold enhanced, show unusually high values of MFE. It is although clear from our data, that the effect of heterogeneity of the medium plays an important role in the MFE phenomenon, but the exact characteristics of the heterogeneous solvent effect are the subject of our study. In this respect, the values of $\varepsilon_{s,\max}$ and $x_{\max}$ might also throw light on the exact nature of the effect in the following way. For each solvent pair studied, we have scanned the dielectric constant from the

point of onset to some higher values where they start gradually falling off. Now how fast the point, which corresponds to the maximization of the field effect is reached after the initial onset is reflected by the $\varepsilon_{s,\max}$ and $x_{\max}$ values. The composition of the solvent mixture at the this point, where the maximum field effect is reached and its comparison to other systems might also throw light on the intrinsic difference in the process in which preferential salvation effect operates in each system. Alternatively, structural analysis at these values might bring into light the micro-environment and its characteristics at the peak positions. Among the systems studied, the in the system TOL/DMSO, the $\varepsilon_{s,\max}$ value is reached faster than any other system, at 9.8, with the initial onset at 6.8. The TOL/PC system, similar to the TOL/DMSO system, has however the $\varepsilon_{s,\max}$ value at 13.1, after an initial onset also at 6.8. The $x_{\max}$ value for both these system however occur around 0.30 molefraction of the polar component. But worth noting is the difference of the PA/BN system with these above systems, in that $\varepsilon_{s,\max}$ for this system occurs at 17, with a corresponding $x_{\max}$ at 0.68 in the molefraction of the polar component! The absolute field effect values does not also start falling sharply after $\varepsilon_{s,\max}$ and $x_{\max}$ values are passed. This is in quite contrast to the other systems (more on this in the next point). The system BA/DMSO is an exception, with no prominent maxima marking the system. The exact physical interpretation of these observations still awaits future studies.

- **The $\chi_{\max}$ value**: The $\chi_{\max}$ value, the value of the highest absolute field effect is a direct indication of the corresponding "cage effect" and geminate recombination probabilities, provided some other factors do not interfere with the magnetic field effect phenomenon realized by the RIP mechanism. In this respect, the highest $\chi_{\max}$ value occur for the system of TOL/PC, pegged at around 10%. The other systems all register lower values of $\chi_{\max}$. Whether this indicates the maximum cage effect exerted by this solvent mixture is yet to be seen.

- **The $B_{1/2}^{max}$ and $\Delta B_{1/2}$ values:** The studies of dependence of the $B_{1/2}$ values on some variable parameter like concentration, viscosity, dielectric constant are rather rare in literature. Justinek *et al* (ref) have used MARY spectroscopy to study the concentration dependence of the line-width data of the self-exchange reactions involving RIP's and extracted the rate constant of the self exchange reactions using MARY spectroscopy as a tool. The physical basis of the variation of the line-width of the MARY spectrum with the concentration of the quencher, as explained in the theoretical section is based on the mechanism of the quencher concentration modulating the life-time of the RIP, which turn changes the S or T recombination yield thereby also modulating the $B_{1/2}$ values. However, the scope of the experiment allows one to generally vary the quencher concentration in the range of two to three orders in magnitude, and thereby depending on the system, a somewhat good change in the $B_{1/2}$ values could be expected. But the highest values in the overall change of $B_{1/2}$ were as low as only 2G in pyrene/dicyanobenzene system, and as high as 5G in the carbazole systems. But in our work, where the quencher concentration remains constant throughout, a change in the $B_{1/2}$ values across the dielectric constant scan($\Delta B_{1/2}$ **)** was found to be as high as 11G (please refer to the plots below for a overall comparison) . This value, which could have probably increased further, if the S/N ratio of the spectra permitted scans beyond the highest value of the dielectric constant measured, is large keeping in mind the usual ranges of line-width effect changes obtained not only in MARY but also in ESR measurements. In general, a prominent change in the $B_{1/2}$ value in this scenario with constant quencher concentration indicates some phenomenon at molecular level which imposes spatial restrictions on the RIP evolution dynamics. The system in PC/TOL registers the maximum in the $B_{1/2}$ value at 70.6, corresponding roughly to the onset value of the MFE. The system of TOL/DMSO has almost comparable value, but other systems have lower values of $B_{1/2}$. The explanation is attempted in the subsequent sections.

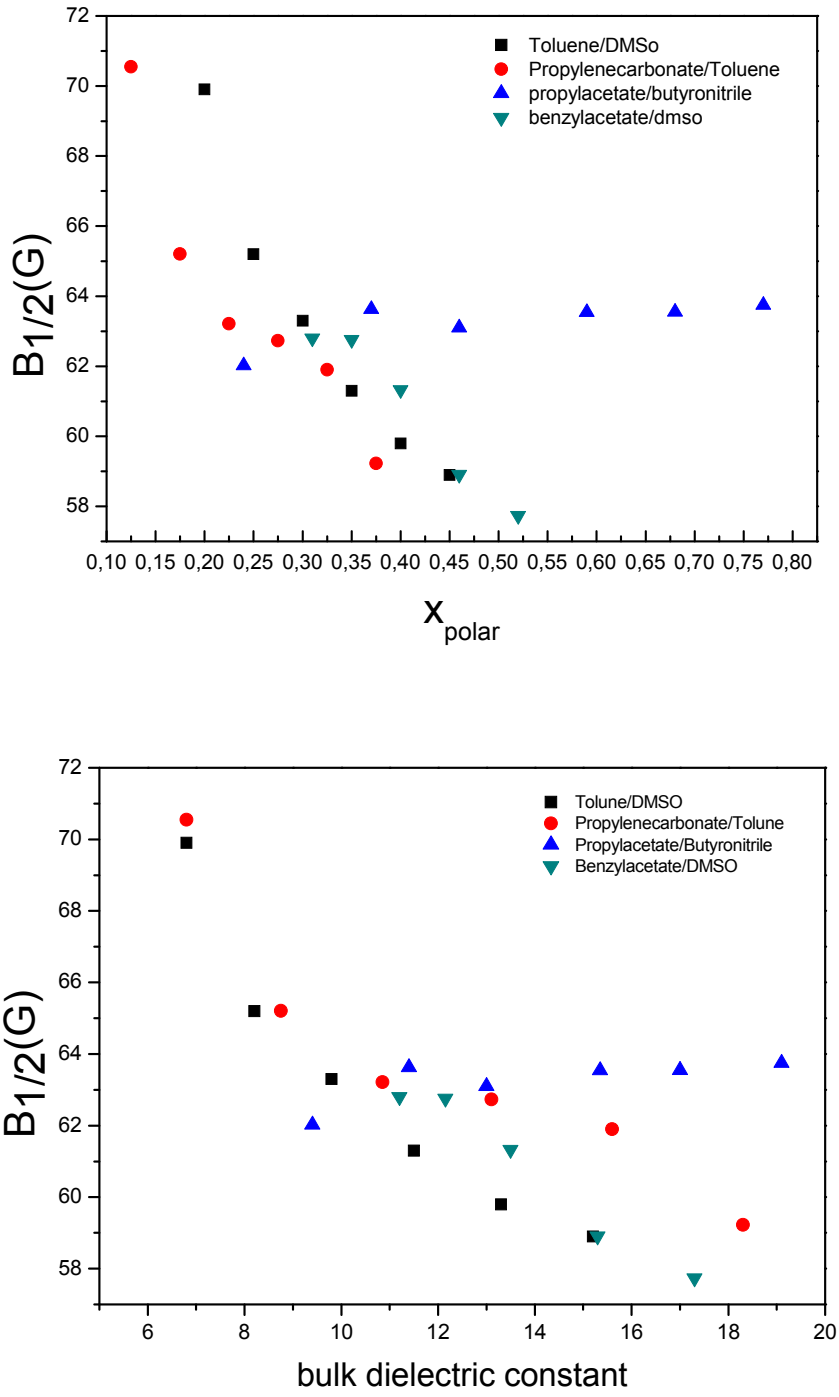

Figure 4.21: Graph showing the variation of $B_{1/2}$ values with the polar component of the solvent mixture (above) and the variation of $B_{1/2}$ values with the bulk dielectric constant of the mixture (below) for all the systems studied.

4.4.6 Interpretation of the MFE features

Having seen and compared the magnetic field effect phenomenon in four binary mixtures, let us now turn at interpreting the data. In the present scope, it is only possible to interpret the data in a qualitative way, the theoretical interpretation is expected to be done in very near future. The direction of our interpretation is based primarily on the work of Petrov *et al* and Chowdhury *et al.*

4.4.6.1 The Concentration Fluctuation Effect

As also has been highlighted in the theoretical section, the concentration fluctuations have the capacity to influence the events of the electron transfer reaction in its geminate stage and therefore will also contribute to the magnetic field effects. In this respect, it might be said that in multicomponent system, where preferential solvation effect take place, one or all the components of the mixture can form unstable aggregates at the interface of the solute and the solvent. The unstable aggregates, whose formation has been confirmed by various experiments, is formed due to the concentration fluctuation of the solvent molecule in the solvation shell. The solvation shell around the solute is therefore a layer, whose composition is changing continuously. The time scale of the concentration fluctuation, being in the picosecond-femtosecond range, compared to the usually nanosecond lifetime of the RIP can therefore affect the fate of the RIP, if somehow possible. But how are the concentration fluctuations generally able to affect the dynamics of the RIP?

The physical picture of the solvation effect involving the binary solvent effect through a modified Onsager model, as explained in the theoretical section is a sheath of solvent shell around the solute/fluorophore molecule, the layer being composed of both the solvent molecules. Now in this model the obvious physical picture is the competition of the solvent molecules among each other to find a place in the solvation shell. It is this competition of the solvent shell among each other that the RIP evolution under the effect of a magnetic field might become dependent on the composition of the solvent in the

respect that the ability of a certain component in the solvent mixture to stabilize or destabilize the RIP will accordingly influence the magnetic field effect parameters described before. With this information let us now take a look at the solvent pairs employed and the results obtained. As has been seen, the two solvent pairs Tol/DMSO and PC/TOL, whose components differ the greatest in their permittivity values, bring about fully different changes than the solvent mixture PA/BN. The most striking difference lies in the magnitude of the $B_{1/2}$ values and the absolute field effect also. As can be seen, the $B_{1/2}$ values in TOL/DMSO and TOL/PC are much larger compared to the $B_{1/2}$ values obtained in PA/BN. This larger magnitude of the $B_{1/2}$ values in these solvents point to some spatial restriction in the RIP evolution dynamics brought about by these two solvents whose component differ strongly in their polarities. We can think of the stabilization of the RIP in this case by formation of energy-minimizing ion-dipole and dipole-dipole interaction from the strongly polar component of the mixture in this case. This stabilization enhances the geminate recombination and impedes the immediate dissociation of the RIP into ions. The result is obvious, the restriction brought about in the journey of the RIP from the contact ion pair (CIP) to the solvent separated ion pair (SSIP) allows more scope for the spin evolution to take place and hence saturation at higher fields (reflecting a higher $B_{1/2}$ in these systems) compared to the system in PA/BN. The effect also possibly explains the other properties of earlier onset of MFE in these systems, the maximum field effect of 10% obtained in PC/TOL etc. However the hypothesis requires further theoretical backing. Please refer to the figure below for a better representation of the effect.

4.4.6.2 The Saturation of the Preferential Solvation Effect

The preferential solvation effect, which starts with the introduction of the polar component in the non-polar bulk, do not increase linearly with the increasing molefraction values of the polar component. The physical phenomenon of accumulation of the polar component near the solute in excess compared to the non-polar component saturates after a certain molefraction of the polar component is surpassed. The effect is

strong at the lower values x_{polar} and saturates with a certain value, making further increase of the polar component virtually ineffective to the preferential solvation effects. This phenomenon perhaps also has influence in the changes in $B_{1/2}$ values with varying dielectric constant. As could be recalled from the previous sections, that the $B_{1/2}$ values shows a sharp decrease in the system like TOL/DMSO or PC/TOL around the region of the onset of MFE, and later with further increase in x_{polar}, the values fall more slowly. The effect the maximization of preferential solvation effect and the saturation might play a role here. During the onset, when x_{polar} values are low, any changes in its value is expected to strongly influence the preferential solvation and the $B_{1/2}$ values, hence the strong plunge and thereafter gradual changes. The system where preferential salvation effects are negligible like in PA/BN shows practically no changes in the $B_{1/2}$ values with changes in x_{polar}. In the system of BA/DMSO, the role if any of the high viscosity of the medium is still to be understood.

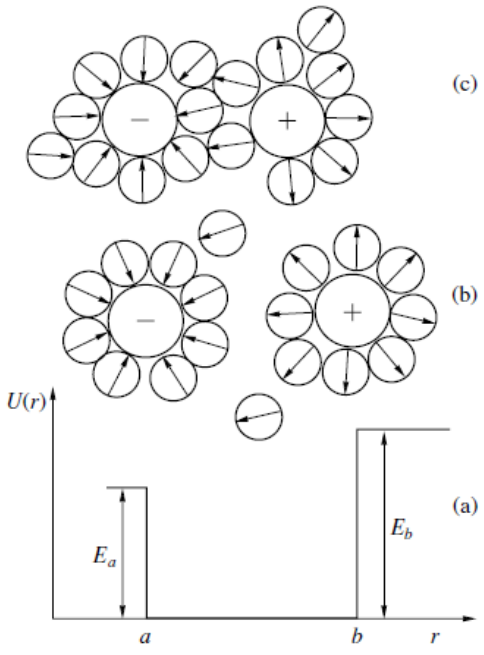

Figure 4.22:Schematic representation of the preferential solvation effect depicting the a) the potential energy of interaction of radical ions, b) RIP's with separated solvation shell (strong electrostatic interaction), and c) solvent separated RIP with a commom polar salvation shell (weak electrostatic interaction)

4.4.6.3 Interpretation on the basis of Hildebrand Theory of Solubility

Previous research on the area have attempted to interpret the maximum values of absolute magnetic field obtained against the parameter $V_{mP}\left(\delta_P - \delta_N\right)^2$ (please see section *2.6.3*), a factor which appears in the Hildebrand theory of solubility. The parameter referred to above signifies the work required the formation of a cluster from molecules of the polar component of the mixture. On this line we have also tried to plot our data points with respect to this parameter and see if there is any correlation to be found. The following table shows the Hildebrand parameters of the solvents used, their molar volumes at 25^0C and their dielectric constants.

Table 4-12: Hildebrand parameters for the solvents used

Solvent[a]	ε_s	$V_m / cm^{-3}mol$ (25^0C)	$\delta / cal^{-1/2}cm^{3/2}$
DMSO	50.0	71.33	12.0
PA	6.0	115.56	8.8
BN	24.7	87.86	10.5
BA	5.7	142.82	15.5
TOL	2.4	115.51	8.9
PC	64.9	85.42	13.3
THF	7.6	81.7	9.1

[a] Used acronyms : dimethylsulfoxide (DMSO), propylacetate (PA), butyronitrile (BN), benzylacetate (BA), toluene (TOL), propylenecarbonate (PC), tetrahydrofuran (THF).

Now plotting a graph against the maximum magnetic field obtained for the four systems and the $V_{mP}\left(\delta_P - \delta_N\right)^2$ values calculated from the table is as follows.

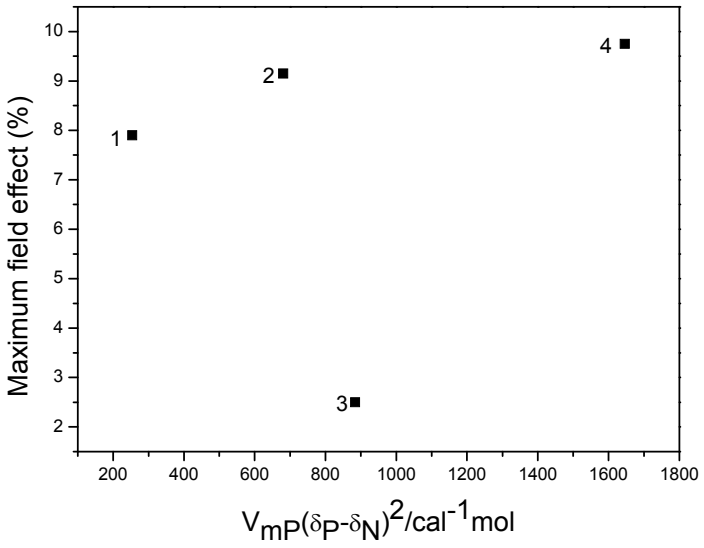

Figure 4.23: The plot of the $V_{mP}\left(\delta_P - \delta_N\right)^2$ values vs. maximum in absolute field effect in (1) PA/BN, (2) Toluene/DMSO, (3) BA/DMSO, (4) PC/Toluene for 9,10 dimethylanthracene ($1x10^{-4}$M)/ DMA ($5x10^{-2}$M).

According to their hypothesis, the size of the polar cluster, formed as a result of concentration fluctuation in solvents with at room temperature with solvents mixtures having $\varepsilon_s = 50, \mu = 4D$, should lead to values of *r*, the characteristic length of the ion-dipole interaction at around 3 angstroms. At such constraints, there should be large enhancement in the $B_{1/2}$ values. However the $B_{1/2}$ values for the system studied by them in almost all binary solvent mixture are more or less the same with a very little spread in the value. They have tried to rationalize the fact on the basis of polar cluster formation and doing a same $V_{mP}\left(\delta_P - \delta_N\right)^2$ vs. maximum field effect plot. For most of the solvent mixtures studied by them, the maximum values in the field effect lies in the narrow range of 500-600 cal/mol of the above parameter, while the energy of thermal motion is also 600cal/mol. The correlation is attempted with the argument that the formation of cluster, optimal for the maximization of the MFE can take place where the work of the cluster formation equals the thermal energy. With this work being lower than the thermal energy, the cluster formation is hindered as the mixture starts behaving like a homogenous

system. On the other hand, when this work is very high, the thermodynamic probability of cluster formation decreases significantly.

But our results stand quite contrary to their findings! As can be see from the plot above, there can be no correlation found between a certain window of the $V_{mP}\left(\delta_P - \delta_N\right)^2$ values and the maximum field effect. The mixture PA/BN which is almost as good as a one-component neat solvent exhibits comparable MFE values to systems which do not have such behavior and with higher values of $V_{mP}\left(\delta_P - \delta_N\right)^2$. On the other hand, a system with $V_{mP}\left(\delta_P - \delta_N\right)^2$ values around 800 cal/mol, exhibits very low MFE values. This feature of our system is quite intriguing and a look is required to make sure if at all the mechanism of cluster formation and the associated phenomenon is at all responsible for the magnetic field effect phenomenon in binary solvent mixture, or some totally different mechanism is at play.

Moreover, their system shows $B_{1/2}$ values which are quite close to neat solvents. Our system has $B_{1/2}$ values which are quite higher to neat solvents or alternatively solvent mixtures which behave like homogenous systems. The explanation to this could have entirely different roots. It is perhaps the very simplistic approach in the Hildebrand solubility theory that oversimplifies matter and a more realistic model of salvation needs to be applied for the interpretation.

4.4.6.4 Fitting our data

Although in our work, the obtained trend in the magnetic field effect has not been fitted yet with some function depicting a certain model of the geminate recombination and further theoretical inputs are still awaited, yet the model proposed by Nath *et al*(ref) seems quite promising which relies on the analytical solution of the classical Smoluchowski equation under certain boundary conditions and with the assumption that

the formation of the RIP takes place at a distance greater than the reaction distance R (a long range electron transfer) and that the minimum inter-radical distance R_B , characterized by $\omega_{HFI} = V_{ST}(R_B)$ is required for the spin evolution to take place.

The classical Smoluchowski equation represented as

$$\frac{d\rho}{dt} = \nabla\left\{D\left(\nabla\rho + \frac{\rho}{kT}\nabla F\right)\right\} \tag{4.2}$$

where ρ is the probability per unit volume for finding the two radicals at a relative distance r at a time t; D is the mutual diffusivity of the two radicals, k is the Boltzmann constant, T is the absolute temperature and F, the potential over the surface governing the radical motion could be applied under boundary conditions pertaining to the systems viz.

$$\begin{aligned} &t = 0; \rho \to \frac{\delta\left(r - r_g\right)}{4\pi r_g^2} \\ &r \to \infty; \rho \to 0 \\ &r \to R; D\left(\frac{\delta\rho}{\delta r} + \frac{\rho}{kT}\frac{\delta F}{\delta r}\right) \to h\rho \end{aligned} \tag{4.3}$$

to yield analytical expression for the enhancement of the magnetic field as a function of the dielectric constant of the medium is given by a complex expression as

$$\frac{\Delta\phi}{\phi} = \frac{2}{3} \times C \times \frac{r_c}{1 - \exp\left(-r_c / r_g\right)} \times \left[\frac{\left(\overline{\alpha} r_c / R^2 - 1\right)\exp\left(-r_c / R\right) + \exp\left(-r_c / r_g\right)}{1 + \left(\overline{\alpha} r_c / R^2 - 1\right)\exp\left(-r_c / R\right)}\right] \tag{4.4}$$

where the Onsager radius $r_c = e^2 / \varepsilon kT$ is expressed as function of the permittivity, C is a constant, $\overline{\alpha} = \left(D/h\right) \times 10^8; h = \kappa U_0 / 4$, where D is the diffusion coefficient, and h is the

adjustable parameter composed of , κ, the transmission coefficient and U_0, the effective velocity at which the potential barrier is crossed. R is the reaction distance and r_g is the distance at which the RIP is formed.

Our data was test fitted with the above analytical expression, but although the fit is not very exact. The above expression is also takes involves alcoholic mixtures as well, and we are not very sure at this stage, until further theoretical study the exact form of the fit of our data. The fit for the permittivity dependence of the $B_{1/2}$ values which has not been attempted in the past, we are trying to find out a suitable theory to fit the data.

Equation Chapter 5 Section 1

5 Conclusion

This work aims at understanding the various facets of electron transfer reaction using MARY spectroscopy as the tool. Given the fact that electron transfer reactions can undergo an exciplex mediated process, the events of which could be modulated by an external magnetic field opens new vistas for understanding the various complex features of this type of reaction using the magnetic field modulation of the exciplex luminescence method. To this end we have employed this effect in understanding the electron transfer reaction from the following approaches. In the first place, the electron transfer reaction is associated with the vital activation energy parameters, the latter being a complex function of solvent dynamical effects. We have tried to employ temperature dependent MARY spectroscopy to extract knowledge about the activation energy parameters of self-exchange reactions and thereby disentangle the effects of the dynamic solvation effects upon the activation energy parameters. Secondly and more importantly which constitutes the bulk of our studies include employing this form of spectroscopy in understanding the effect of preferential solvation in binary solvents in modulating the fate of electron transfer reactions compared to neat solvents. Apart from this magnetic field effect on other systems has also been discovered for the first time. Having said so we will categorically point out new insights and directions the work has tried to achieve in its limited scope.

The major achievements of this work are summarized as follows:

- MARY spectroscopy on a number of systems has been recorded and reported which has not been previously done. This primarily includes the system of Perylene/DMA which has been found to show magnetic field effect for the first time. Apart from that the modulated MARY spectra of 9,10-dimethylanthracene with DMA and especially with DMDPM has been reported for the first time.

- The other striking feature of the work includes studying MARY spectroscopy in solvent mixtures which has either been rarely used or used for the first time. The solvent mixture of PC/Toluene has been employed for the first time while the other solvent mixtures reported like PA/BN or BA/DMSO has been used in MARY spectroscopy for the first time, although they have been used in magnetic field effect studies using other related techniques.

- The other major striking features which has been an achievement not only in realization of an effect using MARY spectroscopy, but also in developing the necessary instrumental infrastructure for converting the theory into reality of experiment is the TEMPERATURE DEPENDENT MARY SPECTROSCOPY. This type of study has been attempted for the first time on various systems and although not really very successful with the response of common organic systems to temperature changes on the linewidth effect, an attempt has although been made on one of the systems which is somewhat responsive to temperature changes to extract out activation energy parameters . Unfortunately, the behavior of the $B_{1/2}$ values with concentration of TMPPD does not permit us to do further calculation.

- The next major achievement in the same respect as above is studying the binary solvation effect using MARY spectroscopy as a tool. For the first time a systematic study of a relatively less used system, which otherwise yields MARY spectra with very good S/N ratio has been done. The specialty of our study lies in the fact that although in past, the binary solvent dependence of absolute field effect has been studied, the study regarding the linewidth dependence of binary solvent effect has been studied for the first time. And more interestingly large changes in the MARY linewidth or alternatively the $B_{1/2}$ values has been achieved with permittivity changes in various solvents, something which contradicts to certain extent the earlier studies in this field, which involved although not MARY spectroscopy, but similar magnetic field dependence of exciplex luminescence techniques.

We would like to stress hereby that, the binary solvent effect studies, which forms the major chunk of our studies, confirm the imperative effect of the heterogeneity and homogeneity of the solvent medium on the fate of electron transfer reaction, especially from the aspect of the events in the geminate cage and geminate cage reaction. Any process which helps in the enhancement of the geminate lifetime of the RIP will thereby have an influence on the absolute field effect. The more heterogeneous solvent mixture is certain to increase this effect, as hypothesized in earlier published theories through the formation of dipole-ion bridges to stabilize the RIP is hereby also confirmed in our studies. The justification in the changes of the $B_{1/2}$ values with the permittivity of the medium is also attributed to the restrictions brought about in the RIP evolution dynamics by the concentration fluctuation effects. The concentration fluctuation effect possibly leads to the formation of the dipole-ion or dipole-dipole stabilized structures, the effect of concentration fluctuation maximizing at lower values of the molefraction of the polar component and falling off gradually with increasing concentration of the polar component. The possibility of explanation of the events of the process, especially during the early stages has been highlighted by the use of the Smoluchowski equation with the Noolandi approach.

Although this work aims at studying electron transfer reactions with a approach which has not been done in past, the outcome of the study calls for further improvisation and development of explicit and elaborate theoretical models to understand the process in further detail. In this respect it is worthwhile to mention the following points, the respects in which our study requires further refinement and search for better systems. First, our study requires theoretical interpretation using plausible models of the preferential solvation phenomenon. This task of devising a suitable model of solvation is quite challenging keeping in mind the general complexity involved in taking into account the interplay of various factors like solvent dynamical effects, polarization effects operating in the condensed medium, in this case a medium composed of two different solvents. Secondly, using the models of preferential solvation, fit the experimental curves and the observed trends in the absolute magnetic field effect values. The involvement of viscosity

on the preferential salvation effects also need to be verified with respect to the results obtained for the BA/DMSO system. With respect to the temperature dependent measurements, since most of the systems investigated do not really produce prominent changes with temperature in the magnetic field dependent measurements, we are given the task of finding a suitable system which might show a large change in the line-width values with temperature. Or otherwise it might also be an option to instrument our apparatus to allow for temperature dependent studies at sub-zero temperatures as well and thereby increase the window of the temperature range.

The method of MARY spectroscopy in general is a powerful tool to study the short lived RIP's *in vivo*. The other established techniques of studying the RIP's or radical pairs(RP), especially the CW-ESR, ENDOR, CIDEP in general depend on production of stabilized RIP's or RP's (at times under very sensitive conditions) with lifetime generally around 100ms. This prerequisites, which are often difficult to meet with due the difficulty in the sysnthesis of the RIP/ and or its stabilization is waived-off in MARY spectroscopy. As pointed out earlier, this technique relies on *in vivo* production of RIP's using photo-excitation (in some cases excitation using x-rays or gamma radiation) with the required RIP's lifetime sufficient around few nano-seconds. This method therefore has the capability to probe processes occurring at much faster timescale than the other methods. But like every other method, this method also suffers from its natural drawbacks as well. The greatest limitation of using the process lies in the fact that the system studied should undergo the steps of the electron transfer reaction (both in the forward and reverse direction) involving an emissive exciplex. It is the exciplex/delayed exciplex emission that is magnetic field modulated, but as it is known many photochemical systems do not show exciplex emission but could be interesting to study are not the candidates for MARY spectroscopy. But when the exciplex is formed, even a weak one, the technique is sensitive enough to detect the magnetic field dependence, if any of that system. Further limitation is imposed on the choice of the solvent used in the spectral technique, given that using solvents whose permittivity gives only very low magnetic field values, the spectra accordingly also suffers from poor S/N ratios. The poor S/N ratio of the spectra in certain solvents compared to other often leads to an error in the analysis of the spectral

parameters and difficulties in comparing various systems. Nevertheless, this is a very powerful technique indeed to probe electron transfer reaction under the effect of a magnetic field.

Suggested Future Experiments

"Sung songs are sweet, unsung songs are sweeter"

Our present work opens the possibility of future work, both in experimental and theoretical perspective in the following directions.

- One of the powerful tools to probe magnetic field effects in binary solvents and examine how the solvent shell rearranges in my doing time-resolved fluorescence experiments. Work could be done using time-resolved MARY therefore to gain deeper insight into the process using suitable reference functions.

- To perform life-time studies on the systems in various solvents, the lifetime data having some correlation with the $B_{1/2}$ values obtained in MARY experiments.

- Extend the study to other systems and other quenchers. For example such systematic studies involving the Pyrene/DMA system with respect to linewidth studies could be a good example. Further solvent mixture could also be devised to study the effect.

- Work might also be done in micellar and other bio-mimicking environment for comparision

- Needless to say, development in the theory of the process in a plausible form is perhaps the most challenging task of the day. As pointed out earlier, the theory

need to take into account the experimental curves, the rationalization of the changes in $B_{1/2}$ values and the complex salvation phenomenon.

It is our hope that we will be soon able to make all ends meet to produce plausible interpretation of this complex phenomenon.

Equation Chapter 6 Section 1

6 Appendix

6.1 Tables and Calculational Tools

6.1.1 Constants and Conversions

Fundamental constants used in the work are appended below in the table

Table: Fundamental constants (ref 22 M)

Quantity	Symbol	Value	Units
Bohr Magneton	μ_B	$9.2740154 \times 10^{-24}$	JT^{-1}
		$9.2740154 \times 10^{-28}$	JG^{-1}
Nuclear Magneton	μ_n	$5.0507866 \times 10^{-27}$	JT^{-1}
		$5.0507866 \times 10^{-31}$	JG^{-1}
Electron g-factor	g_e	2.0023193	
Proton g-factor	$g_{n,H}$	5.5856948	
Planck constant	h	$6.6260755 \times 10^{-34}$	Js
Reduced Planck's constant	$\hbar = h/2\pi$	$1.0545727 \times 10^{-34}$	Js

Apart from these constants, the other useful information regarding some conversion equation used in the work are the one involving the conversion of the magnetic field strength B from the usual one in gauss to one in frequency ν or the angular frequency ω unit. The equation connecting these two is represented as follows.

$$\omega = \frac{g_e \mu_B}{\hbar} B \tag{6.1}$$

where the symbols has already been explained in the earlier table. The angular frequency is in turn connected to the frequency through the equation

$$\omega = 2\pi\nu \tag{6.2}$$

The table below gives the conversion factors between the various units of the magnetic field, and the interconversion factors between various units.

Table: Conversion factors between various units of magnetic field.

	G	mT	10^6 rad/s	MHz
1G	1	0.1	17.6085	2.80249
1mT	10	1	176.085	28.0249
10^6 rad/s	0.0567907	0.00567907	1	0.159155
1MHz	0.356826	0.0356826	6.62319	1

6.1.2 List of Abbreviations

Abbreviation	Full Expression
AC	Alternating current
BA	Benzylacetate
BN	Benzonitrile
CIDEP	Chemically Induced Dynamic Electron Polarisation
CIDNP	Chemically Induced Dynamic Nuclear Polarisation
CIP	Contact Ion Pair
DC	Direct Current
DCB	Dicyanobenzene
DMA	N,N'-dimethylaniline
DMAnt	9,10-dimethylanthracene
DMDPM	4,4'-bis(diphenylamino) dimethylenebenzene
DMF	Dimethylformamide
DMSO	Dimethylsulfoxide
ESR	Electron Spin Resonance
FIS	Free Ions
HF	Hyperfine
HFC	Hyperfine Coupling
HFI	Hyperfine Interaction
MARY	Magnetic field effect on Reaction Yield
MFE	Magnetic Field Effect
NMR	Nuclear Magnetic Resonance
PA	Propylacetate
PC	Propylenecarbonate
PER	Perylene
PY	Pyrene
PMT	Photo-Multiplier Tube
RIP	Radical Ion Pair
RP	Radical Pair

S	Singlet
S/N	Signal-to-Noise
SSIP	Solvent Separated Ion Pair
T	Triplet
THF	Tetrahydrofuran
TMPPD	N,N,N’,N’-tetramethyl-para-phenylenediamine
TOL	Toluene

6.2 Miscellaneous Studies and Results

6.2.1 MARY Spectrum of Perylene/ N,N'-Dimethylaniline

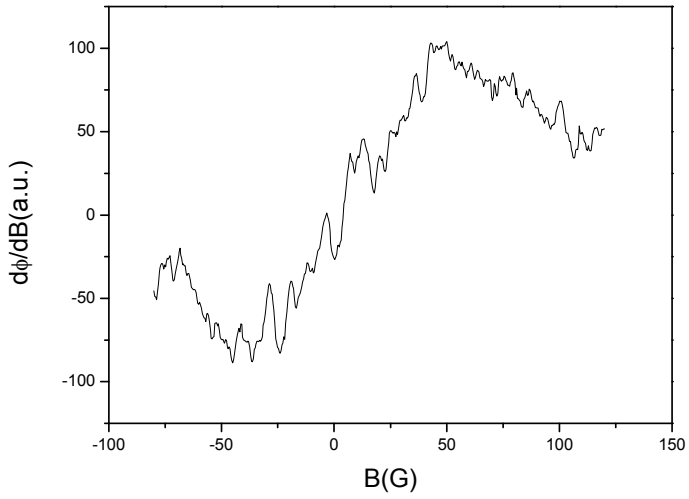

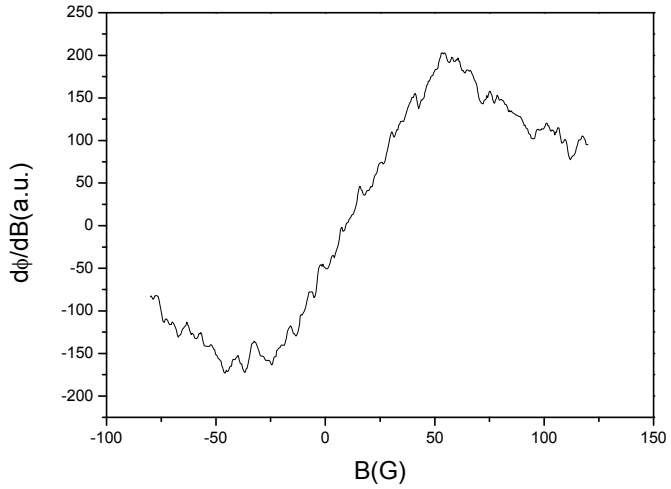

Figure 6.1: MARY spectrum of Perylene($4x10^{-5}M$) with DMA ($5x10^{-2}M$) in 1:4 DMF/THF with modulation amplitude 5G (above) and 10 G (below).

6.2.2 The System of Pyrene/ 1,2-Dicyanobenzene

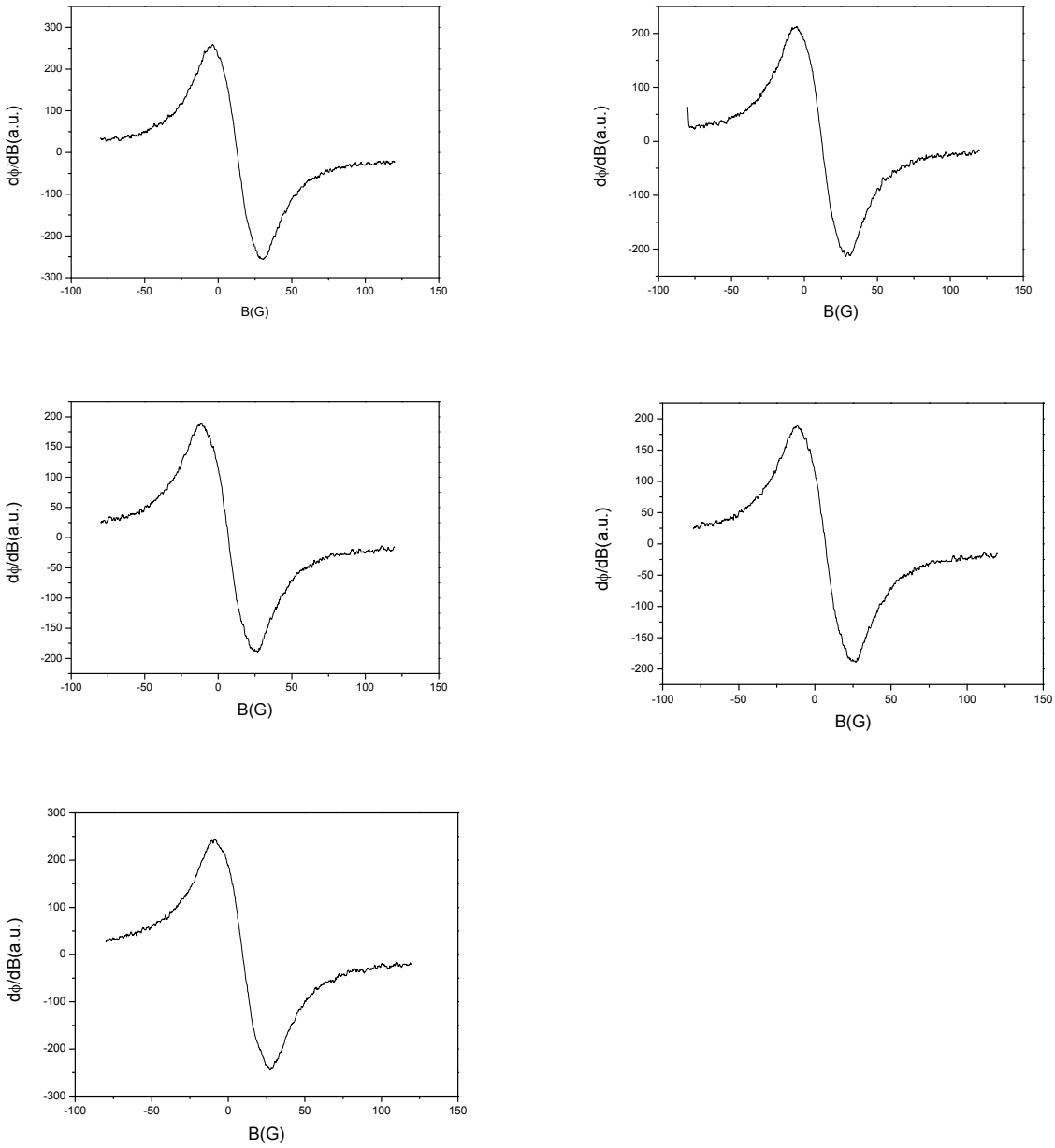

Figure 6.2: MARY spectrum of Pyrene ($1x10^{-4}$M)/DMA(0.05 M) in THF at different temperatures. From top to bottom (right) at 21.6 ^{0}C, 42.2 ^{0}C, 60.7 ^{0}C and from top to bottom (left) at 32.0 ^{0}C, 51.4 ^{0}C.

References:

(1) Salikov, K. M.; Sagdeev, R. Z.; Molin, Y. N.; Buchachenko, A. L. *Spin Polarization and magnetic effects in radical reactions* Elsevier: Amsterdam, 1984.

(2) Atkins, P. W. *Chem.Br.* **1976**, 214.

(3) Atkins, P. W.; Lambert, T. P. *Annu. Rep. Chem. Soc* **1975**, *A72*, 67.

(4) Buchachenko, A. L. *Russ. Chem. Rev* **1976**, *45*, 761.

(5) Gould, I. R.; N.J.Turro; M.B.Zimmt *Advances in Physical Organic Chemistry* **1984**, *20*, 1.

(6) Sagdeev, R. Z.; Salikov, K. M.; Molin, Y. N. *Russ. Chem. Rev* **1977**, *46*, 297.

(7) Steiner, U. E.; Ulrich, T. *Chem.Rev* **1989**, *89*, 51.

(8) Bhattacharyya, K.; Chowdhury, M. *Chem.Rev.* **1993**, *93*, 507.

(9) Sen, K.; Bandyopadhyay, S.; Bhattacharya, D.; Basu, S. *J.Phys. Chem. A* **2001**, *105*, 9077.

(10) S.Aich; S.Basu *J.Phys. Chem. A* **1998**, *102*, 722.

(11) Krissinel, E. B.; Burshtein, A. I.; Lukzen, N. N.; Steiner, U. E. *Mol.Phys.* **1999**, *96*.

(12) Justinek, M.; Grampp, G.; Landgraf, S. *Phys. Chem.Chem.Phys* **2002**, *4*.

(13) Bhatnagar, S. S.; Mathur, R. N.; Kapur, R. N. *Philos.Mag* **1929**, *8*, 457.

(14) Kavarnos, G. J.; Turro, N. J. *Chem.Rev* **1986**, *86*, 401.

(15) Staerk, H.; Kühnle, W.; Treichel, R.; Weller, A. *Chem. Phys.Lett* **1985**, *118*, 19.

(16) C.A.Hamilton; J.P.Hewitt; K.A.McLauchlan *Mol.Phys.* **1988**, *65*, 423.

(17) Weller, A.; Nolting, F.; Staerk, H. *Chem. Phys. Lett* **1983**, *96*, 24.

(18) Bolton, J. R.; Archer, M. D. *Electron Transfer in Inorganic, Organic and Biological Systems*; American Chemical Society: Washington, 1991; Vol. 228.

(19) Weaver, M. J. *Chem.Rev* **1992**, *92*, 463.

(20) G.Grampp *Spectrochim. Acta* **1998**, *54*, 2349.

(21) M.Eigen *Z.Phys.Chem.Neue Folge* **1954**, *1*, 176.

(22) M.Fuoss *J.Am.Chem.Soc.* **1958**, *80*, 5059.

(23) N.Sutin *Prog.Inorg.Chem.* **1983**, *30*, 441.

(24) Marcus, R. A.; N.Sutin *Biochim.Biophys.Acta* **1985**, *811*, 265.

(25) Wilford, J. H. *J.Phys. Chem,* **1985**, *89*, 5395.

(26) R.A.Marcus *J.Chem.Phys* **1956**, *24*, 966.

(27) R.D.Cannon *Chem. Phys.Lett* **1977**, *49*, 299.

(28) G.Grampp; W.Jaenicke *Ber.Bunsenges.Phys.Chem* **1991**, *95*, 904.

(29) Atherton, N. M. *Principles of Electron Spin Resonance*; Ellis Horwood: New York, 1993.

(30) Kaplan, J. I.; Fraenkel, G. *J.Am.Chem.Soc.* **1972**, *94*, 2907.

(31) Alexander, S. *J.Chem.Phys* **1962**, *37*, 974.

(32) K.Schulten; Wolynes, P. J. *J.Chem.Phys* **1978**, *68*, 3292.

(33) Knapp, E. K.; K.Schulten *J.Chem.Phys* **1979**, *71*, 1878.

(34) Basilevsky, M.; Odikonov, A.; Nikitina, E.; Gregorev, F.; Petrov, N.; Alfinov, M. *J.Phys. Chem,* **2009**, *130*, 024505.

(35) Basilevsky, M.; Odikonov, A.; Nikitina, E.; Grigoriev, F.; Petrov, N.; Alfinov, M. *J.Phys. Chem,* **2009**, *130*, 024504.

(36) Suppan, P. *J. Chem Soc. Faraday Trans.* **1987**, *83*, 495.

(37) Rosenthal, S. J.; Jimenez, R.; Fleming, G. R.; Kumer, P. V.; Maroncelli, M. *J.Mol.Liq.* **1994**, *60*, 25.

(38) Petrov, N. K.; Wiessner, A.; Staerk, H. *J.Chem.Phys* **1998**, *108*, 2326.

(39) Petrov, N. K.; Borisenko, V. N.; Starostin, A. V.; Alfinov, M. V. *Izv. Akad. Nauk SSSR, Ser. Khim.* **1991**, *11*, 2456.

(40) Vukus, M. F. *Rasseyanie sveta v gazakh, zhidkostei* Leningr.Gos.Univ: Leningrad, 1977.

(41) Petrov, N. K. *J. Chem Soc. Faraday Trans.* **1994**, *90*, 109.

(42) Petrov, N. K. *J.Phys. Chem. A* **1998**, *102*, 7878.

(43) Lakowicz, J. R. *Principles of Fluorescence Spectroscopy*; Plenum Publishers: New York, 1999.

(44)

(45) Weil, J. A.; Bolton, J. R.; Wertz, J. E. *Electron Paramagnetic Resonance: Elementary Theory and Practical Applications*; John Wiley & Sons: New York, 1994.

(46) Bonilla, A.; Vassos, B. *J.Chem.Educ.* **1977**, *54*, 130.

(47) Das, D.; Nath, D. N. *Journal of Physical Chemistry B* **2007**, *111*, 11009.

(48) Schulten, Z.; Schulten, K. *The Journal of Chemical Physics* **1977**, *66*, 4616.

(49) Werner, H. J.; Schulten, Z.; Schulten, K. *The Journal of Chemical Physics* **1977**, *67*, 646.

(50) Noolandi, J.; Hong, K. M. *The Journal of Chemical Physics* **1979**, *70*, 3230.

(51) Wu K., L. S. *J.Chem.Phys* **1977**, *66*.

(52) Justinek, M. *Magnetic Field Effects Used for the Determination of Electron Self-Exchange Kinetics*; Technische Universität Graz: Graz, 2003.